UNIVERSIDADE FEDERAL DE LAVRAS

JOHN JAIRO AREVALO HERNANDEZ

MACRO AND MICROPLASTICS IN THE SOIL: ABUNDANCE, CHARACTERIZATION, IDENTIFICATION, AND INTERACTIONS UNDER DIFFERENT LAND USES IN AN AGRICULTURAL SUB-BASIN

LAVRAS – MG
2025

JOHN JAIRO AREVALO HERNANDEZ

MACRO AND MICROPLASTICS IN THE SOIL: ABUNDANCE, CHARACTERIZATION, IDENTIFICATION, AND INTERACTIONS UNDER DIFFERENT LAND USES IN AN AGRICULTURAL SUB-BASIN

Tese apresentada à universidade federal de lavras, como parte das exigências do programa de pós-graduação em Ciência do Solo, área de concentração em Recursos Ambientais e Uso da Terra, para obtenção do título de Doutor.

Prof. Dr. Marx Leandro Naves Silva
Orientador

Prof. Dra. Angela Dayana Barrera de Brito
Coorientadora

LAVRAS – MG
2025

Ficha catalográfica elaborada pelo Sistema de Geração de Ficha Catalográfica da Biblioteca Universitária da UFLA, com dados informados pelo(a) próprio(a) autor(a).

Arévalo-Hernández, John Jairo.
Macro and microplastics in the soil: abundance, characterization, identification, and interactions under different land uses in an agricultural sub-basin / John Jairo Arévalo-Hernández. - 2025.
131 p. : il.

Orientador(a): Marx Leandro Naves Silva.
Coorientador(a): Angela Dayana Barrera de Brito
Tese (doutorado) - Universidade Federal de Lavras, 2025.
Bibliografia.

1. Diffuse pollution. 2. Polymer. 3. Land use. 4. Spatial distribution. 5. Soil tropical. I. Silva, Max Leandro Naves. II. Brito, Angela Dayana Barrera de. III. Título.

Ficha elaborada por André Felipe Calsavara (CRB6/3137)

JOHN JAIRO AREVALO HERNANDEZ

MACRO E MICROPLÁSTICO NO SOLO: ABUNDÂNCIA, CARACTERIZAÇÃO, IDENTIFICAÇÃO E INTERAÇÕES SOB DIFERENTES USOS DO SOLO EM UMA SUB-BASIA AGRÍCOLA

MACRO AND MICROPLASTICS IN THE SOIL: ABUNDANCE, CHARACTERIZATION, IDENTIFICATION, AND INTERACTIONS UNDER DIFFERENT LAND USES IN AN AGRICULTURAL SUB-BASIN

Tese apresentada à universidade federal de lavras, como parte das exigências do programa de pós-graduação em Ciência do Solo, área de concentração em Recursos Ambientais e Uso da Terra, para obtenção do título de Doutor.

APROVADA em 15 de abril de 2025

Profa. Dra. Eloana Janice Bonfleur	UFPR
Profa. Dra. Alessandra Angélica de Pádua Bueno	UFLA/DEC
Prof. Dr. Junior Cesar Avanzi	UFLA/DCS
Prof. Dr. Yuri Lopes Zinn	UFLA/DCS

Prof. Dr. Marx Leandro Naves Silva
Orientador

Prof. Dra. Angela Dayana Barrera de Brito
Coorientadora

LAVRAS – MG
2025

À Deus.

À minha esposa e filha, pelo amor incondicional.

À meus pais e irmãos, pelo apoio inabalável.

Dedico

AGRADECIMENTOS

A realização deste doutorado foi uma jornada desafiadora e enriquecedora, e muitas pessoas e instituições foram fundamentais para sua concretização.

Expresso minha profunda gratidão à Universidade Federal de Lavras (UFLA), especialmente ao Departamento de Ciência do Solo (DCS), pelo suporte acadêmico e infraestrutura disponibilizada para o desenvolvimento desta pesquisa. Da mesma forma, agradeço à Universidad Surcolombiana pelo apoio institucional ao longo deste percurso.

Um agradecimento especial ao meu orientador, Prof. Dr. Marx Leandro Naves Silva, e à minha coorientadora, Prof. Dra. Angela Dayana Barrera de Brito, pela orientação, dedicação e incentivo em todas as etapas deste trabalho. Sua expertise e apoio foram essenciais para meu crescimento acadêmico e profissional.

Agradeço também a todos os professores que contribuíram para minha formação ao longo desses quatro anos, transmitindo conhecimento e guiando-me com dedicação. Meu reconhecimento especial ao pessoal dos laboratórios de Física de Solos, Manejo e Conservação do Solo e Água e laboratório de ótica do departamento da Física, que me apoiaram durante a execução da pesquisa, oferecendo auxílio técnico e compartilhando sua experiência.

O presente trabalho foi realizado com apoio da Coordenação de Aperfeiçoamento de Pessoal de Nível Superior – Brasil (CAPES) – Código de Financiamento 001.

Um agradecimento especial a Eduardo Medeiros Severo e sua esposa Gabi Medeiros Hermógenes, por suas amizades, apoio e incentivo ao longo dessa jornada.

Aos membros da banca, por aceitarem o convite e toda contribuição.

A todos que, de alguma forma, contribuíram para a realização deste trabalho, meu muito obrigado!

RESUMO

Os resíduos plásticos representam um grave problema para o meio ambiente. Além disso, a gestão inadequada dos resíduos na produção agrícola tem contribuído significativamente para o aumento da poluição do solo, gerando grandes impactos nos agroecossistemas. Esses resíduos incluem macroplásticos (MaP, >25 mm), mesoplásticos (MeP, 5–25 mm) e microplásticos (MP, <5 mm), cujas concentrações e características variam conforme o uso do solo e a região, o que justifica a necessidade de pesquisas detalhadas em solos tropicais. Quatro estudos foram realizados em uma sub-bacia hidrográfica do alto Rio Grande, em Lavras Minas Gerais, Brasil, para avaliar a abundância, morfologia e identificação dos MaP, MeP e MP em solos de uso agrícola, pastagem e florestal, além de relacioná-los com atributos físicos e químicos do solo, atributos do terreno e o Índice de Vegetação por Diferença Normalizada (NDVI). No primeiro estudo, foi avaliada a eficiência de recuperação de MP usando a metodologia de separação por densidade com três soluções extratoras em solos tropicais brasileiros, obtendo taxas de recuperação de 81,0%–98,8% para polietileno de baixa densidade (LDBD) e 59,7%–75,2% para policloreto de vinila (PVC). O segundo estudo realizou um levantamento georreferenciado de MaP e MeP, identificando polímeros como polipropileno (40,94%), polietileno (30,20%) e policloreto de vinila (11,41%), com abundância variando de $0{,}509 \times 10^3$ a 104×10^3 peças ha^{-1} e massa de 0,039 a 405 kg ha^{-1}. Esses detritos plásticos apresentaram correlação com a declividade, o fator LS e a cobertura vegetal. No terceiro estudo analisou-se a presença de MP na camada de 0–20 cm do solo, identificando majoritariamente partículas de polipropileno, polietileno, politereftalato de etileno e policloreto de vinila, na forma de filmes e fragmentos. A abundância média de microplasticos em solos agrícolas, florestais e de pastagem foi de 3.406, 3.826 e 2.553 peças kg^{-1}, respectivamente. A abundância de MP correlacionou-se negativamente com matéria orgânica, argila e porosidade e positivamente com atributos topográficos. Por fim, no quarto estudo, realizou-se uma análise geoestatística da poluição plástica para prever a distribuição espacial dos MP, revelando forte dependência espacial, seguindo o modelo gaussiano. O mapa de krigagem indicou concentrações de MP que variam entre 600 e 7.400 peças kg^{-1}, com maior acúmulo em áreas agrícolas e florestais. A variabilidade espacial de MaP, MeP e MP em solos tropicais é influenciada pelo uso da terra, topografia e propriedades do solo. A identificação de diferentes tipos de polímeros e morfologias de partículas evidencia a complexidade da contaminação plástica nos agroecossistemas. Esta distribuição espacial dos MP permite identificar pontos críticos de poluição plástica na área de estudo, apresentando padrões relacionados às características da paisagem. Essas descobertas ressaltam a necessidade de estratégias de gestão mais eficazes para mitigar o acúmulo de resíduos plásticos em ambientes agrícolas e naturais.

Palavras-Chaves: atributos do solo; distribuição espacial; polímeros; poluição difusa; solo tropical; uso do solo.

ABSTRACT

Plastic waste represents a serious environmental problem. Additionally, inadequate waste management in agricultural production has significantly contributed to increased soil pollution, causing major impacts on agroecosystems. This waste includes macroplastics (MaP, >25 mm), mesoplastics (MeP, 5–25 mm), and microplastics (MP, <5 mm), whose concentrations and characteristics vary according to land use and region, highlighting the need for detailed research in tropical soils. Four studies were conducted in a sub-basin of the Upper Rio Grande in Lavras, Minas Gerais, Brazil, to assess the abundance, morphology, and identification of MaP, MeP, and MP in agricultural, pasture, and forest soils, as well as to relate them to the physical and chemical attributes of the soil, terrain characteristics, and the Normalized Difference Vegetation Index (NDVI). In the first study, the efficiency of MP recovery was evaluated using the density separation methodology with three extracting solutions in Brazilian tropical soils, obtaining recovery rates of 81.0%–98.8% for low-density polyethylene (LDPE) and 59.7%–75.2% for polyvinyl chloride (PVC). The second study conducted a georeferenced survey of MaP and MeP, identifying polymers such as polypropylene (40.94%), polyethylene (30.20%), and polyvinyl chloride (11.41%), with abundance ranging from 0.509×10^3 to 104×10^3 pieces ha^{-1} and mass from 0.039 to 405 kg ha^{-1}. These plastic debris showed a correlation with slope, the LS factor, and vegetation cover. These plastic debris showed a correlation with slope, the LS factor, and vegetation cover. In the third study, the presence of MP in the 0–20 cm soil layer was analyzed, identifying mainly polypropylene, polyethylene, polyethylene terephthalate, and polyvinyl chloride particles in the form of films and fragments. The average abundance of microplastics in agricultural, forest, and pasture soils was 3,406, 3,826, and 2,553 pieces kg^{-1}, respectively. The abundance of MP correlated negatively with organic matter, clay, and porosity, and positively with topographic attributes. Finally, in the fourth study, a geostatistical analysis of plastic pollution was conducted to predict the spatial distribution of MP, revealing strong spatial dependence following the Gaussian model. The kriging map indicated MP concentrations ranging from 600 to 7,400 pieces kg^{-1}, with higher accumulation in agricultural and forest areas. The spatial variability of MaP, MeP, and MP in tropical soils is influenced by land use, topography, and soil properties. The identification of different polymer types and particle morphologies highlights the complexity of plastic contamination in agroecosystems. This spatial distribution of MP allows for the identification of critical plastic pollution hotspots in the study area, revealing patterns related to landscape characteristics. These findings emphasize the need for more effective management strategies to mitigate the accumulation of plastic waste in agricultural and natural environments.

Keywords: soil attributes; spatial distribution; polymers; diffuse pollution; soil tropical; land use.

INDICADORES DE IMPACTO

O presente trabalho teve como objetivo investigar a presença e distribuição de resíduos plásticos como são, macroplásticos (MaP), mesoplásticos (MeP) e microplásticos (MP), em solos tropicais de diferentes usos na sub-bacia hidrográfica do alto Rio Grande, em Lavras, Minas Gerais, Brasil. Considerando suas correlações com atributos físicos, químicos e topográficos do solo. Os resultados obtidos evidenciam impactos ambientais relevantes destacando-se que a análise demonstrou que a gestão inadequada de resíduos na produção agrícola contribui significativamente para a poluição do solo, com implicações diretas sobre a saúde dos agroecossistemas e, indiretamente, sobre a segurança alimentar e o bem-estar das comunidades rurais. A eficiência de métodos de extração de microplásticos foi validada, com taxas de recuperação variando de 59,7% a 98,8% dependendo do tipo de polímero e solução utilizada, representando um avanço metodológico relevante para estudos futuros. A quantificação de MaP e MeP revelou uma ampla variação na abundância ($0,509 \times 10^3$ a 104×10^3 peças ha^{-1}) e massa (0,039 a 405 kg ha^{-1}), com predominância de polipropileno, polietileno e PVC, cujas distribuições mostraram relação direta com características da paisagem, como declividade e cobertura vegetal. A presença de MP na camada superficial do solo (0–20 cm) foi observada em todos os tipos de uso do solo, com abundâncias médias de 3.406 peças kg^{-1} em áreas agrícolas, 3.826 peças kg^{-1} em áreas florestais e 2.553 peças kg^{-1} em pastagens, evidenciando que mesmo ambientes menos antropizados estão sendo impactados. Os dados indicam que a poluição plástica nos solos é um fenômeno complexo, associado tanto a atividades humanas quanto a processos naturais de transporte e redistribuição, exigindo intervenções articuladas entre produtores rurais, gestores públicos e a sociedade civil. Os impactos tecnológicos incluem o desenvolvimento de protocolos mais precisos para quantificação e mapeamento da poluição, enquanto os impactos sociais e culturais abrangem a conscientização sobre os riscos ambientais e a promoção de práticas agrícolas mais sustentáveis. Os impactos estão diretamente relacionados a diversos Objetivos de Desenvolvimento Sustentável (ODS) da Agenda 2030 da ONU, como o ODS 2 (Fome Zero e Agricultura Sustentável), ODS 6 (Água Potável e Saneamento), ODS 12 (Consumo e Produção Responsáveis), ODS 13 (Ação Contra a Mudança Global do Clima) e ODS 15 (Vida Terrestre), demonstrando a relevância do tema para o cumprimento dos compromissos globais assumidos pelo Brasil.

IMPACT INDICATORS

The present study aimed to investigate the presence and distribution of plastic debris—namely macroplastics (MaP), mesoplastics (MeP), and microplastics (MP)—in tropical soils under different land uses within the sub-basin of the Upper Rio Grande, in Lavras, Minas Gerais, Brazil, considering their correlations with physical, chemical, and topographic soil attributes. The results highlight significant environmental impacts, showing that inadequate waste management in agricultural production contributes substantially to soil pollution, with direct implications for agroecosystem health and indirect consequences for food security and the well-being of rural communities. The efficiency of MP extraction methods was validated, with recovery rates ranging from 59.7% to 98.8%, depending on the type of polymer and the solution used, representing a relevant methodological advancement for future studies. The quantification of MaP and MeP revealed wide variations in abundance (0.509×10^3 to 104×10^3 pieces ha^{-1}) and mass (0.039 to 405 kg ha^{-1}), with a predominance of polypropylene, polyethylene, and PVC, whose distributions showed a direct relationship with landscape features such as slope and vegetation cover. MP were detected in the surface soil layer (0–20 cm) across all land use types, with average abundances of 3,406 pieces kg^{-1} in agricultural areas, 3,826 pieces kg^{-1} in forest areas, and 2,553 pieces kg^{-1} in pastures, indicating that even less anthropized environments are being affected. The data suggest that plastic pollution in soils is a complex phenomenon, linked both to human activities and to natural processes of transport and redistribution, requiring coordinated action among farmers, public managers, and civil society. Technological impacts include the development of more accurate protocols for quantifying and mapping pollution, while social and cultural impacts involve raising awareness of environmental risks and promoting more sustainable agricultural practices. These impacts are directly related to several Sustainable Development Goals (SDGs) of the UN 2030 Agenda, such as SDG 2 (Zero Hunger and Sustainable Agriculture), SDG 6 (Clean Water and Sanitation), SDG 12 (Responsible Consumption and Production), SDG 13 (Climate Action), and SDG 15 (Life on Land), demonstrating the relevance of the topic to the fulfillment of global commitments undertaken by Brazil.

SUMMARY

FIRST PART

GENERAL INTRODUCTION

Plastic waste of various sizes, colors, shapes, and polymer types is found in all terrestrial environments. Its widespread presence is primarily attributed to excessive use in everyday products, inadequate recycling, and high resistance to degradation (Hu et al., 2022). Consequently, it is considered a persistent and ubiquitous emerging pollutant (Akca et al., 2024). Their occurrence is linked to using plastic products in agriculture, atmospheric deposition, and improper recycling (Bläsing; Amelung, 2018; Fernandes et al., 2022).

The first studies on plastic residues were conducted in aquatic environments (Sierra et al., 2020). However, current research has expanded to other settings, including river and lake sediments (Gerolin et al., 2020), beaches and mangroves (Garcés-Ordóñez et al., 2019), terrestrial environments (Qi et al., 2020), the atmosphere (Liu et al., 2023), and even within organisms such as small crustaceans, fish, and plants (Huang et al., 2022), soil biota (Adhikari et al., 2023), and the human body (Yang et al., 2022).

These plastic residues include macroplastics (MaP), larger than 25 mm; mesoplastics (MeP), ranging from 5 to 25 mm; and microplastics (MP), smaller than 5 mm (Kumar et al., 2021; Li et al., 2020). MP are small polymer particles classified by their origin into primary and secondary microplastics. Primary MP are intentionally manufactured for industrial applications (Thompson et al., 2004). Secondary MP results from the fragmentation or degradation of larger plastic products (Guo et al., 2023). This degradation is driven by various environmental factors, including moisture, heat, oxygen, radiation, light exposure, mechanical friction, and biodegradation by microorganisms (Gui et al., 2021; Yan et al., 2022).

In the initial phase of plastic waste studies in soil, implementing quality assurance and control practices is essential to prevent sample contamination and ensure reliable data (Fernandes et al., 2022; Maddela et al., 2023). In the second phase, various methodologies are used for plastic waste separation and extraction from soil. Currently, no standardized methodology exists for these procedures (Radford et al., 2021), For MaP and MeP separation, using a 5 mm sieve, along with cleaning and visual identification procedures, facilitates the accurate collection of data on the presence and characteristics of plastics in agricultural environments (Cesarini; Scalici, 2022; Meng et al., 2020).

On the other hand, for MP embedded in the soil matrix, the extraction process must begin with the digestion of organic matter to prevent overestimation or underestimation of their concentration (Grause et al., 2022; Radford et al., 2021). Subsequently, density separation is performed using solutions of different densities (Liu et al., 2019; Quinn; Murphy; Ewins, 2016), followed by filtration, which isolates the MP onto filter paper (Li et al., 2020; Thomas et al., 2020).

The quantification and characterization of MP are conducted using stereoscopic microscopy, where particles are counted and classified based on color, size, and shape, with the support of specialized image analysis software (Samanta et al., 2022; Zhang; Liu, 2018). Finally, the polymer composition of plastic residues is identified through non-destructive techniques such as Fourier Transform Infrared Spectroscopy (FTIR) and Raman Spectroscopy (Munno et al., 2020; Souza Machado et al., 2019; Thomas et al., 2020).

Several studies have linked the concentration of plastic residues to land use (Zhang; Yang; Zhang, 2024), the application of organic fertilizers (Corradini et al., 2019), proximity to urban areas (Wang et al., 2021), and industrial centers (Zhou et al., 2023), as well as natural processes such as rainfall, wind, vegetation type and density, microfauna, and erosion (Hu et al., 2022; Li et al., 2021). These factors can contribute to migrating MP in the soil, both horizontally and vertically (Pérez et al., 2022). However, most authors indicate that human activities, such as agriculture (Dogra et al., 2024), irrigation (Liu et al., 2023b), and recreation (ZHOU et al., 2021), are the main contributors to the concentration of plastic residues in the soil (Feng; Lu; Yao, 2023; Liu et al., 2023).

Plastic residues in terrestrial environments can pose significant environmental risks (He et al., 2018). The ingestion of microplastics can affect various soil organisms, including earthworms, nematodes, and springtails, compromising their health and ecological functions (Souza Machado et al., 2018; Tian et al., 2022). Additionally, microplastics can interfere with crop root growth (Wang et al., 2022), cause severe harm to soil organisms (Bonnevie et al., 2021), alter water infiltration rates (Souza Machado et al., 2019), increase carbon dioxide and nitrogen loss, reduce soil fertility (Li et al., 2022), and consequently decrease agricultural production (Nizzetto; Futter; Langaas, 2016).

However, many impacts of microplastic pollution on agroecosystems remain unknown (La et al., 2024). Therefore, studies on the presence of macroplastic (MaP), mesoplastic (MeP), and microplastic (MP) residues in tropical soils, as well as their potential ecological risks, are relevant (Zhou et al., 2020; He et al., 2018) to better understand their occurrence, characteristics, and potential ecological risks. This is particularly important for Brazilian agricultural soils, where research on microplastics within the soil matrix is still in its early stages (Paes et al., 2022; Sarti et al., 2022).

Therefore, in this study, we examined factors influencing the concentration and spatial distribution of plastic particles, including terrain morphology, vegetation type, and land use. In addition to determining the abundance of plastic waste and identifying the most representative polymer types in the soil samples, we analyzed the spatial distribution of MP. This analysis permits the identification of critical points of plastic pollution in the study area, revealing patterns related to landscape characteristics. These findings underscore the need for more effective management strategies to mitigate plastic waste accumulation in agricultural and natural environments.

OBJECTIVES AND THESIS STRUCTURE

The general objective of this thesis was to assess the abundance of plastic residues in tropical soils, characterize and identify these residues, and analyze their interactions with land use in an agricultural sub-basin. The specific objectives of this study were: i) To develop and evaluate a method for extracting and analyzing LDPE and PVC microplastics in four representative types of tropical agricultural soils in Southeastern Brazil. ii) To quantify and characterize the abundance, mass, and polymer composition of macroplastics, mesoplastics, and coarse microplastics in tropical agricultural soils, identifying their sources of contamination. Additionally, it will describe and analyze their spatial distribution and relationship with topographic features such as slope, LS factor, and vegetation cover, considering parameters such as quantity, mass, area, diameter, and perimeter to identify patterns and potential accumulation hotspots. iii) To assess the presence of microplastics in the 0–20 cm soil layer and examine their relationship with soil physical and chemical properties, terrain attributes, and the Normalized Difference Vegetation Index (NDVI). iv) To determine the abundance of microplastics in the soil and predict their spatial distribution within a sub-watershed, using geostatistical methods for three land use types: forest, grassland, and agricultural land.

This thesis is structured into four scientific papers to achieve its research objectives. The first paper evaluates a methodology for extracting and identifying microplastics in four tropical agricultural soils, as well as quantifying and characterizing the microplastics present. The second paper utilizes geostatistical tools and satellite data to generate distribution maps of plastic residues on the soil surface, employing *ImageJ* software to determine their dimensions and abundance. A multiple-factor analysis is conducted to assess the relationship between these variables and terrain characteristics, as well as vegetation cover, to identify accumulation patterns. The third paper investigates the physical and chemical properties of the soil and their relationship with microplastics extracted from the 0–20 cm soil profile, incorporating data from the SAGA-GIS basic terrain analysis in QGIS software. This analysis considers variables such as slope, valley depth, distance to the channel network, channel network base level, planar curvature, profile curvature, convergence index, topographic wetness index, relative slope position, and LS factor, which are extracted to the sampling grid using the *Point Sampling Tool* with bilinear interpolation. Finally, the fourth paper applies geostatistical analysis using the R computational system, along with the *Gstat* and *GeoR* libraries, to predict the spatial distribution of microplastic abundance identified in the third paper, with interpolation performed using the ordinary kriging predictor.

REFERENCES

ADHIKARI, K. et al. Earthworms Exposed to Polyethylene and Biodegradable Microplastics in Soil : Microplastic Characterization and Microbial Community Analysis. **ACS Agric. Sci. Technol.**, v. 3, p. 340–349, 2023.

AKCA, H. et al. An evaluation on microplastic accumulations in Turkish soils under different land uses. **Science of the Total Environment**, v. 911, n. September 2023, 2024.

BLÄSING, M.; AMELUNG, W. Plastics in soil: Analytical methods and possible sources. **Science of the Total Environment**, v. 612, p. 422–435, 2018.

BONNEVIE, J. et al. Macroplastic in soil and peat. A case study from the remote islands of Mausund and Froan landscape conservation area, Norway; implications for coastal cleanups and biodiversity. **Science of the Total Environment**, v. 787, p. 0–8, 2021.

CESARINI, G.; SCALICI, M. Riparian vegetation as a trap for plastic litter. **Environmental Pollution**, v. 292, n. October 2021, p. 118410, 2022.

CORRADINI, F. et al. Evidence of microplastic accumulation in agricultural soils from sewage sludge disposal. **Science of the Total Environment**, v. 671, p. 411–420, 2019.

DOGRA, K. et al. Traversing the prevalence of microplastics in soil-agro ecosystems: Origin, occurrence, and pollutants synergies. **Journal of Contaminant Hydrology**, v. 266, n. July, 2024.

FENG, S.; LU, H.; YAO, T. Effects of multiple environmental factors and land use patterns on microplastic distribution in the topsoil of the Qinghai and Sichuan provinces of China. **Journal of Environmental Chemical Engineering**, v. 11, n. 3, p. 109657, 2023.

FERNANDES, A. N. et al. Microplastics in Latin America Ecosystems: A Critical Review of the Current Stage and Research Needs. **Journal of the Brazilian Chemical Society**, v. 33, n. 4, p. 303–326, 2022.

GARCÉS-ORDÓÑEZ, O. et al. Marine litter and microplastic pollution on mangrove soils of the Ciénaga Grande de Santa Marta, Colombian Caribbean. **Marine Pollution Bulletin**, v. 145, n. 2, p. 455–462, 2019.

GEROLIN, R. C. et al. Microplastics in sediments from Amazon rivers, Brazil. **Science of the Total Environment**, v. 749, n. 141604, p. 2016–2021, 2020.

GRAUSE, G. et al. Separation of microplastic from soil by centrifugation and its application to agricultural soil. **Chemosphere**, v. 288, n. September 2021, p. 132654, fev. 2022.

GUI, J. et al. Microplastics in composting of rural domestic waste: abundance, characteristics, and release from the surface of macroplastics. **Environmental Pollution**, v. 274, p. 116553, 2021.

GUO, S. et al. Organic fertilizer and irrigation water are the primary sources of microplastics in the facility soil, Beijing. **Science of the Total Environment**, v. 895, n. June, p. 165005, 2023.

HE, D. et al. Microplastics in soils: Analytical methods, pollution characteristics, and ecological risks. **TrAC Trends in Analytical Chemistry**, v. 109, p. 163–172, dez. 2018.

HU, J. et al. National-scale distribution of micro (meso) plastics in farmland soils across China: Implications for environmental impacts. **Journal of Hazardous Materials**, v. 424, n. April 2021, p.

127283, 2022.

HUANG, D. et al. Research progress of microplastics in soil-plant system: Ecological effects and potential risks. **Science of the Total Environment**, v. 812, n. 151487, 2022.

KUMAR, P. et al. Micro- and nano-plastic pollution: Behavior, microbial ecology, and remediation technologies. **Journal of Cleaner Production**, v. 291, n. 125240, p. 1–22, 2021.

LA, Y. et al. The microplastics distribution characteristics and their impact on soil physicochemical properties and bacterial communities in food legumes farmland in northern China. **Journal of Hazardous Materials**, v. 471, n. January, p. 134282, 2024.

LI, H. et al. Vertical migration of microplastics along soil profile under different crop root systems. **Environmental Pollution**, v. 278, 2021.

LI, P. et al. Analytical methods and environmental processes of nanoplastics. **Journal of Environmental Sciences (China)**, v. 94, p. 88–99, 2020.

LI, R. et al. Spatiotemporal heterogeneous effects of microplastics input on soil dissolved organic matter (DOM) under field conditions. **Science of the Total Environment**, v. 847, n. July, 2022.

LIU, M. et al. A method for extracting soil microplastics through circulation of sodium bromide solutions. **Science of the Total Environment**, v. 691, p. 341–347, 2019.

LIU, S. et al. Spatial distribution, source apportionment, and potential ecological risk assessment of suspended atmosphere microplastics in different underlying surfaces in Harbin. **Science of the Total Environment**, v. 901, n. 1, p. 166040, 2023.

LIU, Y. et al. Effects of irrigation on the fate of microplastics in typical agricultural soil and freshwater environments in the upper irrigation area of the Yellow River. **Journal of Hazardous Materials**, v. 447, n. November 2022, p. 130766, 2023.

MADDELA, N. R. et al. Do Microplastics and Nanoplastics Pose Risks to Biota in Agricultural Ecosystems? **Soil systems**, v. 7, n. 1, p. 1–29, 2023.

MENG, F. et al. Effects of plastic mulching on the accumulation and distribution of macro and microplastics in soils of two farming systems in Northwest China. **PeerJ**, v. 8, p. 1–20, 2020.

MUNNO, K. et al. Increasing the accessibility for characterizing microplastics: introducing new application-based and spectral libraries of plastic particles (SLoPP and SLoPP-E). **Analytical chemistry**, v. 92, n. 3, p. 2443–2451, 2020.

NIZZETTO, LUABNT, 2022CA; FUTTER, M.; LANGAAS, S. Are Agricultural Soils Dumps for Microplastics of Urban Origin? **Environmental Science & Technology**, v. 50, n. 20, p. 10777–10779, 2016.

PAES, E. DA S. et al. Widespread microplastic pollution in mangrove soils of Todos os Santos Bay, northern Brazil. **Environmental Research**, v. 210, n. February, 2022.

PÉREZ, R. R. et al. Microplastics in Agricultural Systems: Analytical Methodologies and Effects on Soil Quality and Crop Yield. **Agriculture**, v. 12, n. 8, p. 1162, 2022.

QI, Y. et al. Impact of plastic mulch fi lm debris on soil physicochemical and hydrological properties. **Environmental Pollution**, v. 266, p. 115097, 2020.

QUINN, B.; MURPHY, F.; EWINS, C. Validation of density separation for the rapid recovery of microplastics from sediment. **Analytical Methods**, v. 9, p. 1491–1498, 2016.

RADFORD, F. et al. Developing a systematic method for extraction of microplastics in soils. **Analytical Methods**, v. 13, n. 14, p. 1695–1705, 2021.

SAMANTA, P. et al. An insight on sampling, identification, quantification, and characteristics of microplastics in solid wastes. **Trends in Environmental Analytical Chemistry**, v. 36, n. September, 2022.

SARTI, F. M. E. et al. Municipal Park Grounds and Microplastics Contamination. **Journal of Polymers and the Environment**, v. 30, p. 5202–5210, 2022.

SIERRA, I. et al. Identification of microplastics in wastewater samples by means of polarized light optical microscopy. **Environmental Science and Pollution Research**, v. 27, n. 7, p. 7409–7419, 2020.

SOUZA MACHADO et al. Impacts of Microplastics on the Soil Biophysical Environment. **Environmental Science & Technology**, v. 52, n. 17, p. 9656–9665, 2018.

SOUZA MACHADO et al. Microplastics Can Change Soil Properties and Affect Plant Performance. **Environmental Science & Technology**, v. 53, n. 10, p. 6044–6052, 2019.

THOMAS, D. et al. Sample Preparation Techniques for the Analysis of Microplastics in soil. A Review. **Sustainability**, v. 12, p. 9074, 2020.

THOMPSON, R. C. et al. Lost at Sea : Where Is All the Plastic ? **Science**, v. 304, p. 838, 2004.

TIAN, L. et al. Microplastics in agricultural soils: sources, effects, and their fate. **Environmental Science & Health**, v. 25:100311, n. Edited by Haibo Zhang and Ajit Sarmah, p. 1–8, 2022.

WANG, J. et al. Distinct microplastic distributions in soils of different land-use types : A case study of Chinese farmlands. **Environmental Pollution**, v. 269, p. 116199, 2021.

WANG, S. et al. Occurrence of macroplastic debris in the long-term plastic fi lm-mulched agricultural soil: A case study of Northwest China. **Science of the Total Environment**, v. 831, p. 154881, 2022.

YAN, P. et al. Field management changes the distribution of mesoplastic and macroplastic in Mollisols of Northeast China. **Chemosphere**, v. 308, n. August, 2022.

YANG, X. et al. Environmental health impacts of microplastics exposure on structural organization levels in the human body. **Science of the Total Environment**, v. 825, p. 154025, 2022.

ZHANG, F.; YANG, X.; ZHANG, Z. Effects of soil properties and land use patterns on the distribution of microplastics: A case study in southwest China. **Journal of Environmental Management**, v. 356, n. February, p. 120598, 2024.

ZHANG, G. S.; LIU, Y. F. The distribution of microplastics in soil aggregate fractions in southwestern China. **Science of the Total Environment**, v. 642, p. 12–20, 2018.

ZHOU, J. et al. The microplastisphere: Biodegradable microplastics addition alters soil microbial community structure and function. **Soil Biology and Biochemistry**, v. 156, n. March, 2021.

ZHOU, Y. et al. Microplastics in soils: A review of methods, occurrence, fate, transport, ecological and environmental risks. **Science of the Total Environment**, v. 748, p. 141368, 2020.

ZHOU, Y. et al. Trends in the occurrence and accumulation of microplastics in urban soil of Nanjing and their policy implications. **Science of the Total Environment**, v. 903, n. June, 2023.

SECOND PART - PAPERS

This paper was submitted and is under review in the journal Soil Systems.

PAPER 1 - A METHOD FOR THE EXTRACTION AND ANALYSIS OF MICROPLASTICS FROM TROPICAL AGRICULTURAL SOILS IN SOUTHEASTERN BRAZIL

ABSTRACT

Microplastics (MP) are widespread pollutants that pose a risk to soil ecosystems globally, especially in agricultural soils. This study introduces a method to extract and identify MP in Brazilian tropical soils, targeting low-density polyethylene (LDPE) and polyvinyl chloride (PVC) polymers, commonly present in agricultural settings. The method involves removing organic matter and extracting MP using density separation with three flotation solutions: distilled water, NaCl, and $ZnCl_2$. Extracted MP are then analyzed through optical microscopy and Fourier transform infrared spectroscopy. Recovery rates for LDPE ranged from 81.0% to 98.8%, while PVC samples showed a range of 59.7% to 75.2%. Finally, this methodology was tested in the four agricultural raw soil samples (i. e. without any polymer enrichment). The values found in the soil samples were 2,517.5, 2,245.0, 3,867.5, and 1,725.0 pieces kg^{-1}, for the Ferralsols, Nitisols Gleysols, and Cambisols samples, respectively, with diverse shapes including fragments, granules, films, and fibers. This approach lays the groundwork for future studies on MP behavior in Brazilian tropical agricultural soils.

Keywords: Density separation, Extraction of microplastic, Spectroscopy, Tropical soils.

1 INTRODUCTION

Since the advent of synthetic plastics in the early twentieth century, their production and widespread utilization have experienced significant growth. Plastics play an integral role in nearly every facet of human activity, including agriculture, civil construction, medical equipment, industrial manufacturing, automotive, and electronics. This extensive application owes to their inherent plasticity, stable chemical properties, and remarkable impact resistance (1,2).

In agriculture, plastics find diverse uses, ranging from protective systems and coverings to irrigation, transportation, and storage of agricultural products. They serve in storing pesticides (herbicides and insecticides), and agricultural inputs (seeds and fertilizers), and contribute to irrigation systems and the controlled release of nitrogen, often in the form of nanocomposites (3–6). However, despite their manifold advantages, the environmental repercussions of plastic usage are undeniable. Although many thermoplastic polymers are theoretically recyclable, the current recovery rate remains dismally low, hovering below 6% (7,8).

Over time, improperly disposed plastics undergo weathering and degradation, transforming into fragile and brittle fragments, thus forming microplastics (MP) or nanoplastics (NPs). MP constitute solid plastic particles ranging in size from 1 μm to 5 mm, while NPs are particles smaller than 100 nm (8–10). Due to their diminutive size, these particles can be easily dispersed by wind and water currents over extensive distances, thereby infiltrating marine (11) and terrestrial ecosystems (4). This wide dissemination poses a significant threat to ecosystems, as these particles can be ingested by marine organisms, potentially entering the food chain and impacting human health (12,13).

In recent decades, numerous studies have focused on identifying and quantifying MP across various ecosystems (14,15). Research indicates that the majority of plastic waste originates from terrestrial sources (16–19). Studies conducted in Brazil have shown that microplastic pollution is widespread across different ecosystems, including beaches, rivers, and sediments (20,21). In agricultural soils, the primary sources of microplastics are polyethylene (PE), polypropylene (PP), polyvinyl Chloride (PVC), and polystyrene (PS) (22,23). Particularly, Low-Density polyethylene (LDPE) and PVC MP were found in large quantities in agricultural soils (24), which is not surprising as these plastics are widely used in modern agriculture.

For instance, LDPE mulch film, which is used as a covering material in agriculture (25), accounts for approximately 2% of global plastic production each year (26). PVC is also commonly used in irrigation devices (27). Therefore, it is crucial to assess and monitor the presence of MP in agricultural soils and their impact on the quality of the ecosystem, as well as the well-being of both biota and humans. Hence, identifying and quantifying plastic materials in agricultural soil may be of particular challenge, because it is a heterogeneous matrix of mineral solids, organic matter, and other constituents in a complex manner (28).

This study aims to develop and evaluate a method for extracting and analyzing LDPE and PVC microplastics in four agricultural tropical soil types that are representative of Southeastern Brazil: Gleissolo Melânico Tb Distrófico típico (GM), Latossolo Vermelho-Amarelo Distrófico típico (LVA), Nitossolo Háplico Distrófico típico (NX), and Cambissolo Háplico Tb distrófico típico (CX), according to the Brazilian System of Soil Classification Brazil (29). The MP extraction was done using the density separation method and their identification was done through optical microscopy and Fourier-transform infrared spectroscopy.

2 MATERIAL AND METHODS

2.1 Sample preparation

2.1.1 Microplastic samples

The microplastics used in the experimental procedures were specifically prepared for this study. Two types of polymers were selected due to their relevance as common sources of microplastics in agricultural environments (30,31). low-density polyethylene (LDPE) pellets and polyvinyl chloride (PVC) powder. Both materials were obtained from the Polymer Laboratory at the Federal University of Lavras. Additionally, fragments derived from a PVC irrigation pipe were included. The LDPE microplastics have densities ranging from 0.91 to 0.925 g cm^{-3}, while the PVC particles range between 1.25 and 1.60 g cm^{-3}.

To obtain plastic particles with micrometric dimensions, the plastics were grated using a metal file. Subsequently, the particles were sieved through meshes of 2000 µm, 1000 µm, 500 µm, 210 µm, and 105 µm to obtain microplastic particles with sizes ranging from 105 µm - 2000 µm. This size range was selected due to the significant prevalence of microplastics in soil within this range (12). The same mass proportion of the sieved microplastics was employed to produce the microplastic samples. Consequently, microplastic particles of varied sizes and shapes were generated through this process. Finally, the microplastic groups were prepared as follows: Group 1: LDPE microplastics, Group 2: PVC microplastics, and Group 3: samples with equal mass proportion of Groups 1 and 2.

2.1.2 Soil samples

Raw soil samples used comprised four tropical soil types: Gleissolo Melânico Tb Distrófico típico (GM), Latossolo Vermelho-Amarelo Distrófico típico (LVA), Nitossolo Háplico Distrófico típico (NX), and Cambissolo Háplico Tb distrófico típico (CX), according to the Brazilian System of Soil Classification (29). These correspond to Gleysols (GM), Ferralsols (LVA), Nitisols (NX), and Cambisols (CX), respectively, according to WRB (32). The samples were collected from the 0–20 cm soil layer at Muquem Farm and the Federal University of Lavras campus, in the municipality of Lavras, Minas Gerais state, Brazil, in an area destined for agricultural use, in August 2022. The soil samples were collected using a steel auger. Finally, samples were obtained with a mass of 500 g, which was stored in glass jars to prevent contamination. Chemical and physical analyses were performed according to Silva et al. (33). The landscape, location, land use, and physical and chemical characteristics of the studied soils are detailed in Table 1.

Table 1 Landscape, location, land use, physical and chemical properties of the studied soils.

Characteristics	**Soil Class**			
	LVA	NX	GM	CX
Location	21°12'16.62"S 44°58'55.14"O	21°11'56.09"S 44°58'51.02"O	21°12'4.23"S 44°58'44.48"O	21°13'49.59"S 44°59'0.44"O
Altitude (m)	996	978	960	918
Slope (%)	8 - 20	3 - 8	3 - 8	20 - 45
Current crop	Soybean	Soybean	Rice-Beans	Olive trees
Clay ($g\ kg^{-1}$)	490	530	310	550
Silt ($g\ kg^{-1}$)	100	60	220	170
Sand ($g\ kg^{-1}$)	410	410	470	280
Bulk density ($g\ cm^{-3}$)	1.36	1.29	0.75	0.92
Macroporosity ($cm^3 cm^{-3}$)	0.13	0.15	0.27	0.13
Microporosity ($cm^3\ cm^{-3}$)	0.39	0.38	0.46	0.27

Total Porosity (cm^3 cm^{-3})	0.52	0.52	0.73	0.40
pH (H_2O)	5.6	6.9	5.0	5.0
Al^{3+} ($cmol_c$ dm^{-3})	0.10	0.10	0.20	0.00
H+Al ($cmol_c$ dm^{-3})	2.70	1.20	4.00	1.70
SB ($cmol_c$ dm^{-3})	5.68	8.69	9.15	1.86
eCEC ($cmol_c$ dm^{-3})	5.78	8.79	9.35	1.86
tCEC ($cmol_c$ dm^{-3})	8.38	9.89	13.15	3.56
BS (%)	67.78	87.90	69.55	52.28
m (%)	1.73	1.14	2.14	0.00
SOM (g kg^{-1})	30.8	26.3	172.9	4.70

Note: LVA: Ferralsols; NX: Nitisols; GM: Gleysols; CX: Cambisols; Al^{3+}: Exchangable aluminum; SB: Sum of Bases; eCEC: effective cation exchange capacity; tCEC: Cation exchange capacity at pH 7; BS: Base saturation; m: Aluminum saturation; SOM: soil organic matter.

The samples were air-dried, sieved through a 2 mm mesh, and subjected to a 200 °C heat treatment for 24 hours. This process aimed to degrade the target microplastic particles in the soil while minimally affecting the soil organic matter (SOM) (34,35). By avoiding the combustion of SOM, we prevented any interference in the subsequent stages of the study.

Furthermore, researches indicate that the presence of organic matter in soil can affect the extraction of microplastics, leading to inaccurate estimations of their concentration in the soil (6,36,37). Therefore, before preparing the MP/soil samples, organic matter was removed using alkaline digestion, following the method described by Enders et al. (38). Briefly, ten grams of each soil sample were measured and transferred into a 200 mL beaker. Subsequently, 20 mL of a 30% KOH: NaClO solution was added to the soil and manually mixed for 2 minutes to ensure even distribution. The mixture underwent ultrasonic treatment in a water bath for 5 minutes to facilitate further dispersion and breakdown of soil aggregates. Following this, the mixture was transferred to an oven set at 50°C with forced air circulation to facilitate the evaporation of the alkaline solution. To ensure uniform digestion, the sample was manually shaken for 30 seconds every 4 hours during its incubation in the oven.

This digestion procedure was performed in triplicate to ensure consistency and reliability of results. Moreover, control soil samples were also prepared using the same protocol without adding the 30% KOH: NaClO solution. This control protocol was repeated in triplicate to serve as a baseline for comparison. The reagents were purchased from Neon and Alphatec Co. Ltda., Brazil.

2.1.3 Microplastic/soil samples

After the soil digestion procedure, the mixtures of microplastic and soil samples were prepared using 1 mg of microplastic per gram of soil (1 g kg^{-1} dry weight). Each soil sample was mixed with the respective groups of MP (Groups 1, 2, or 3) in triplicate. These samples were named as SOIL/LDPE, SOIL/PVA, and SOIL/LDPE: PVA (where SOIL is ferralsols, gleysols, cambisols, and Nitisols).

The chemicals were purchased from different Brazilian suppliers: sodium hypochlorite (NaClO) from Neon Co. Ltda., potassium hydroxide (KOH) from Alphatec, sodium chloride from Vetec, and zinc chloride ($ZnCl_2$) from Dinâmica Co., Ltda. All chemicals were of analytical grade, and purified distilled water was used throughout the experiments.

2.2 Extraction of microplastics: Density separation, centrifugation, and filtration

The method of density separation is widely employed to isolate microplastic particles from soil samples (8,16,22,24,25,39–41). In our study, the extraction of MP in soil samples followed the methodology outlined by (4,42), incorporating modifications. We applied the technique using sequentially three different liquids to isolate MP from soil: purified distilled water (DW) (ρ= 1.00 g cm^{-3}), a saturated solution of sodium chloride (NaCl) (S1) (ρ= 1.19 g cm^{-3}), and zinc chloride ($ZnCl_2$) (S2) (ρ= 1.5 g cm^{-3}). The chemicals were of analytical grade, purchased from different Brazilian suppliers: NaCl from Vetec, and $ZnCl_2$ from Dinâmica Co., Ltda.

Initially, we mixed 20 mL of distilled water with soil/MP sample (at a soil-to-MP ratio of 1g:1mg.). The mixture was manually stirred for 20 minutes and allowed to rest for 48 hours. Afterward, the mixture was sonicated for 5 minutes and centrifuged for 5 minutes. The supernatant was carefully removed and passed through a 2 µm nylon filter. To the solid mixture remaining in the beaker, we added 20 mL of S1. Again, this mixture was manually stirred for 20 minutes, sonicated for 5 minutes, and then centrifuged to remove the supernatant. The supernatant underwent two rounds of filtration using both DW and Solution S1.

Finally, 20 mL of S2 was added to the solid mixture in the beaker, and the previous procedure was repeated. In this instance, the supernatant was filtered through a nylon filter. All the nylon filters containing the MP were placed into Petri dishes, dried at room temperature, and then subjected to further analyses. The method of extracting MP from the soil samples is illustrated in Figure 1. Lastly, the potential contamination during the process was evaluated by conducting each extraction step on a soil-free solution.

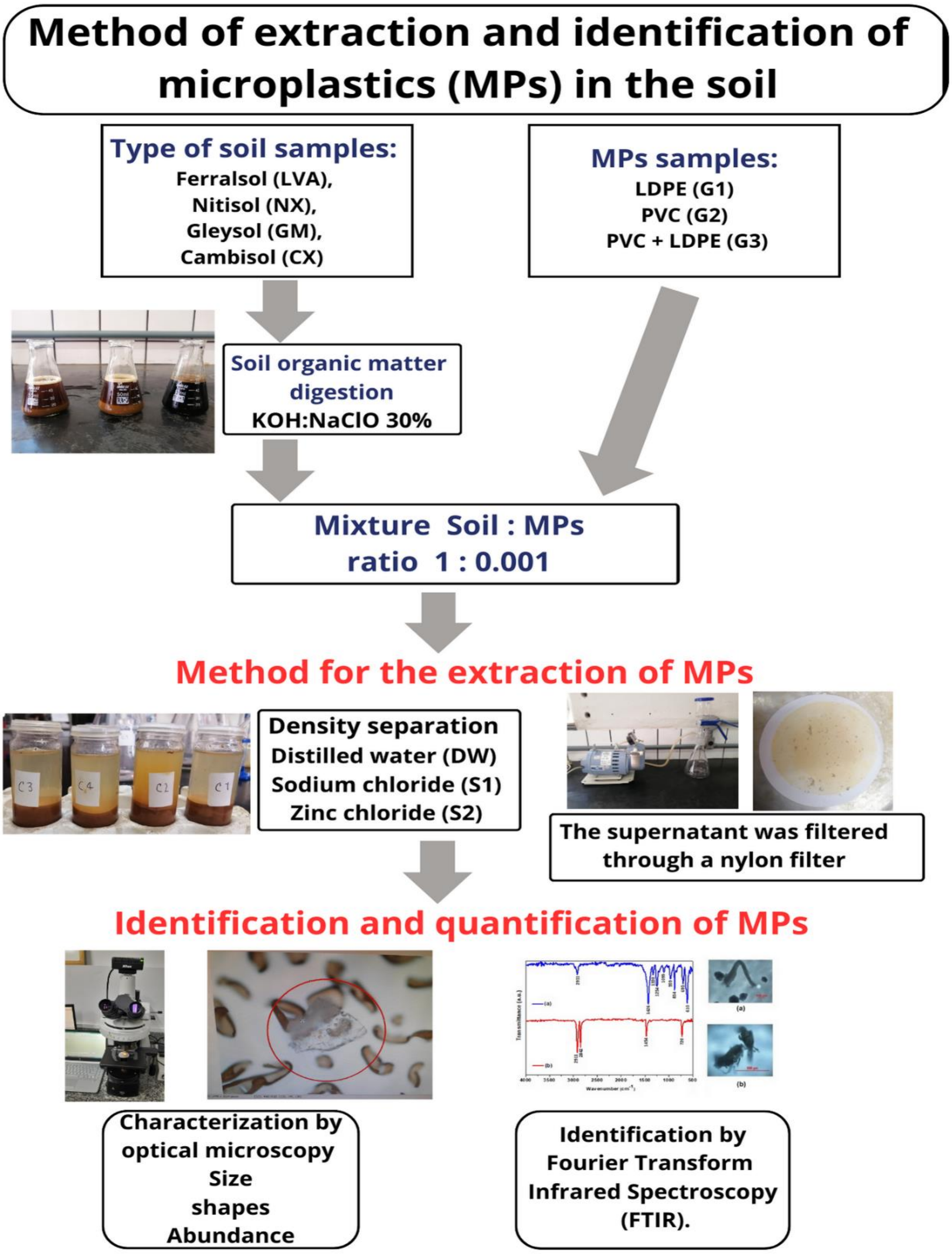

Figure. 1. Schematic diagram of test procedure used for MP extraction and identification of agricultural soils.

2.3 Evaluation of organic matter removal from the soil samples

The efficiency of removing organic matter using the KOH: NaClO solution was determined by comparing the organic matter content in soil samples with and without digestion. For this proposal, initially, we determined the organic matter content in the soil samples, using the loss-on-ignition method (LOI) (43). In brief, 10g of each soil sample was dried in an oven at 105 °C for 2 hours, until a constant dry weight was achieved. Then, it was combusted at 550 °C for 2 hours and it was cooled to room temperature. Then, the organic matter content in the soil samples was calculated through the following equation:

$$\mathrm{LOI} = \frac{\mathrm{W(105°C)} - \mathrm{W(550°C)}}{\mathrm{W(105°C)}} \mathrm{x}100\% \qquad (1)$$

Where W(105 ºC) represents the dry weight of the sample before combustion and W(550 ºC) is the dry weight of the sample after heating to 550 °C (both in g).

The efficiency of removing organic matter from the soil samples was done using the following equation:

$$Removedorganicmatter(\%) = \frac{SOM_a}{SOM_i} x100 \qquad (2)$$

where SOM_i represents the mass percent of organic matter in the soil samples that did not undergo the digestion step and SOM_a represents the mass percent of organic matter of soil samples after digestion.

2.4 Microplastic recovery rate

As mentioned before, the nylon filters containing the MP were placed onto a Petri dish. This filter was used to calculate the recovery rate of MP as follows:

$$recoveryrate[\%] = \frac{W_2 - W_1}{W_3} \times 100 \qquad (3)$$

Where W_1 is the weight (g) of the dry filters before extraction of MP, W_2 is the weight (g) of the dry filters with microplastics, and W_3 is the weight of MP mixed with soil samples. Using equation (3), the microplastic recovery rate was evaluated in two steps: i) after the density separation with distilled water and a sodium chloride solution (DW + S1), and ii) after the density separation with a zinc chloride solution (S2).

2.5 Identification and quantification of microplastics

The microplastics were characterized and identified using optical microscopy and Fourier transform infrared spectroscopy (FTIR) in two stages: i) before mixing with the soil samples, and ii) after the extraction method. The morphological characteristics of the particle surface and the size distribution of the MP were assessed using a Nikon Eclipse Ni 10X optical microscope and Imagin software version 4.6.0. Particles identified as potential plastics were identified using a Shimadzu IRAffinity 1S spectrometer. Measurements were made using the Attenuated Total Reflectance (ATR) method and spectra were recorded in the spectral range 400-4000 cm^{-1} with a scan rate of 16 and a spectral resolution of 4 cm^{-1}. The spectra were processed using OriginPro 2023b software (OriginLab Corporation, Northampton, Massachusetts, EUA), which allowed the spectra obtained to be compared with a polymer reference database. The identification was considered valid if the spectral match was at least 70%.

2.6 Application of microplastics extraction method in raw agricultural soils

The extraction method was evaluated on raw samples of the soils collected previously, by performing the same procedure outlined earlier, without the pre-treatment heat step pre-treatment in the soil and the addition of MP. For each sample tested, the quantification of the number of particles of MP was performed, accompanied by characterizing and quantifying the extracted polymers. The abundance of MP was recorded as pieces kg^{-1} of dry soil by counting the pieces of MP in the total area of the filter. The shape was classified as fragments (hard angular pieces), granules (circular or semicircular particles), fibers (elongated filaments), and films (soft, transparent flakes). In addition, the longest part of the particle length was measured and recorded in microns (µm) (52,53).

2.7 Statistical analyses

To assess potential disparities in the soil digestion process with the alkaline solution in the SOM content measured by the loss-on-ignition method in the soils, the differences between the studied polymers in the recovery rate of MP, and the differences in the quantity of MP particles.

The normality of the variables under study was verified using the Shapiro-Wilk test, the analysis of variance (ANOVA) was performed between treatments, and the Tukey test assessed the differences of means at a significance level of 5%. The data were transformed using the Box-Cox transformation. Statistical analyses and models were conducted using R Software (R Core Team, 2022) version 4.2.2 (44), using the Tidyverse and ggplot2 libraries.

3 Results and Discussion

3.1 Efficiency of Digestion Method for Organic Matter Removal in Soil Samples

The formation of aggregates in soil occurs when soil particles combine with different compounds and soil organic matter (SOM) (45,46). Recent studies have shown that microplastics combine with soil aggregates, including SOM (47), interfering with the extraction and identification of MP. Therefore, it is necessary to remove organic matter from soil samples without damaging the MP (48,49). The SOM content of samples without undergoing the digestion process, using the Loss on Ignition (LOI) method, was 17.9% for ferralsols, 22.5% for nitisols, 45.0% for gleysol, and 9.2% for cambisol. Similarly, the SOM content was determined in soil samples subjected to digestion. Consequently, on average, the SOM removal, expressed as percentages, were as follows: 70.9 ± 2.9% for ferralsol soil, 82.7 ± 17.9% for nitisols soil, 89.6 ± 1.3% for gleysol soil, and 46.7 ± 2.8% for cambisol (Figure 2). Statistical analysis shows a significant difference between the rate of organic matter removal in the four types of soil ($p < 0.05$). All estimates show a coefficient of variation of less than 23%.

According to these results, it is observed that the cambisol sample had the lowest SOM value, while the gleysol soil had the highest. This last result was expected, since, due to its redoximorphic characteristics (50), the gleysol soil type accumulates a large amount of SOM, thus confirming the higher removal content found. When comparing the rate at which SOM was removed from the gleysol, ferralsol, and nitisols samples, it is observed that the removal rate was lower in the latter two. This can be explained by the higher abundance of micro-aggregates in the ferralsol and nitisols soil types compared to the gleysol soil (50). These microaggregates in soil could hinder the SOM from the samples. On the other hand, the efficiency of SOM removal is also influenced by the organic matter content present in the soil samples. The soil samples with the lower SOM content (*e.g.,* cambisol) exhibit a correspondingly diminished rate of SOM removal. Radford et al. (40) observed that samples with low organic content displayed variations in the quantity of SOM removed depending on the employed digestion methods. In contrast, samples characterized by high SOM content did not exhibit notable differences in the amount of SOM removed under various treatments, including alkaline digestion. The alkaline digestion preserves the integrity of MP analysis in soil, unlike acid digestion (51) as will be elucidated later.

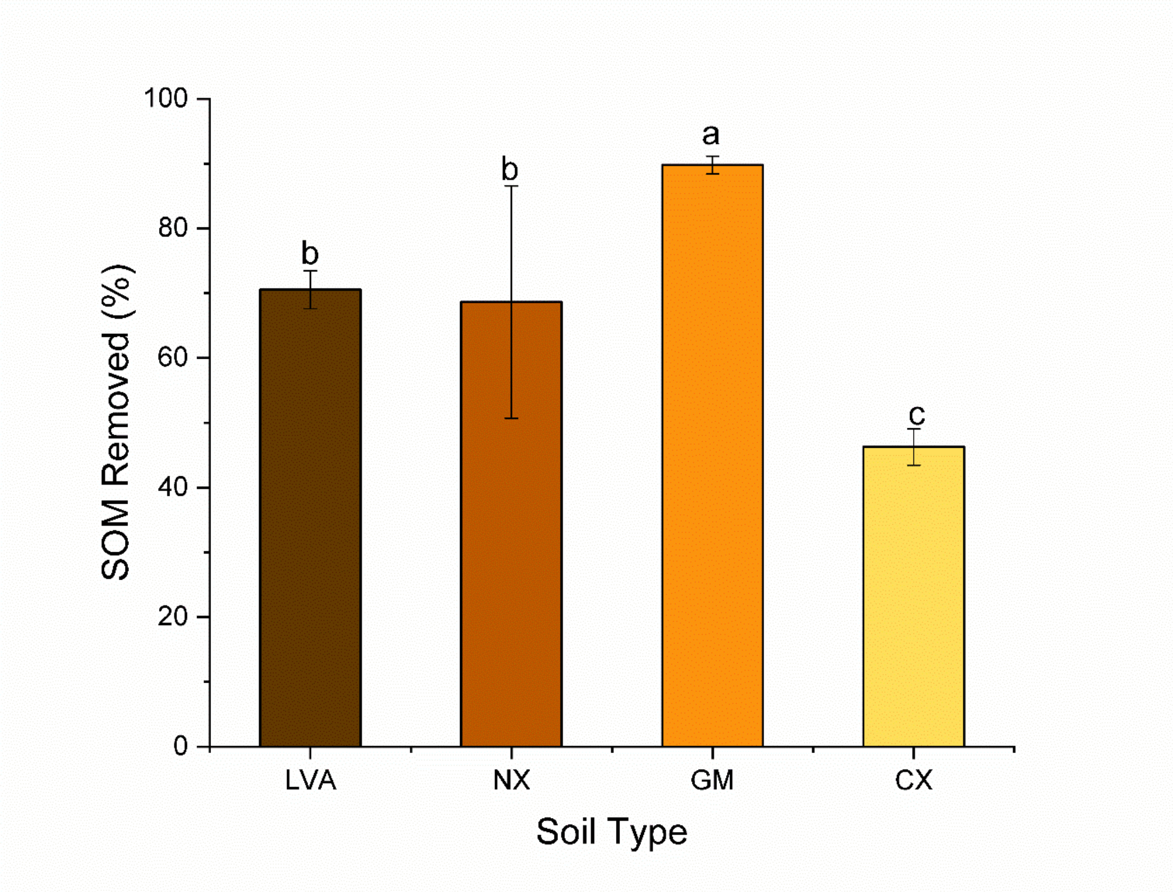

Figure 2. The recovery rate of organic matter from the soil samples after the digestion process, LVA: Ferralsols; NX: Nitisols; GM: Gleysols; CX: Cambisols.

3.2 Characterization of the microplastics before and after the extraction method

As previously mentioned, microplastics were created in the laboratory and sorted by size before being grouped for soil incorporation. Optical microscopy was employed to assess the size distribution of microplastics within each group (52,53), while FTIR spectroscopy was utilized for their characterization before soil insertion (54). The findings revealed that microplastics ranging from 105 to 1000 µm constituted 91.9% of Group 1, 81.5% of Group 2, and 89.4% of Group 3. Microplastics sized between 1000 and 2000 µm accounted for 6.8% in Group 1, 9.6% in Group 2, and 2.9% in Group 3. Samples from Groups 2 and 3 contained particles that were smaller than 105 µm. This was expected because PVC powder typically includes particles below 100 μm (8), which can pass through the sieve used in this study. Figure 3 illustrates the optical microscopic image of two samples of MP in different shapes and sizes, and the spectra recorded using FTIR.

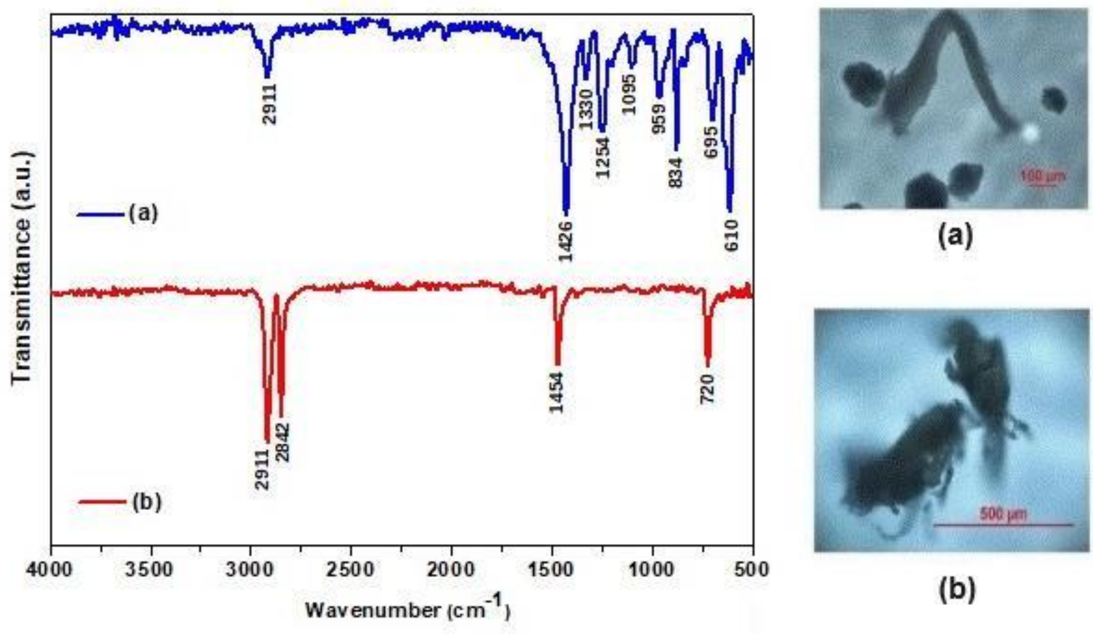

Figure 3. FTIR spectra and images of optical microscopy of PVC (a) and LDPE (b) microplastics created for experimental procedures.

In Figure 3(a), the characteristic FTIR bands of PVC are presented. The bands between 2958 and 2890 cm^{-1} correspond to different stretching vibration modes of the CH and CH_2 bonds. At 1426 cm^{-1}, it is observed the –CH_2–deformation vibrations (wagging of the methylene groups) (55). The 1254 and 1330 cm^{-1} bands correspond to C–H rocking deformation and C–H deformation of CHCl, respectively. The 1095 cm^{-1} band relates to C–C stretching vibrations, while the 959 cm^{-1} band is assigned to trans-CH wagging vibrations. The stretching vibration of the –C–Cl bond is associated with the 834 cm^{-1} band. Finally, the 610 and 695 cm^{-1} bands are attributed to the stretching of the C–Cl bond. FTIR spectrum for LDPE microplastics is presented in Figure 3(b), where the characteristic LDPE bands can be readily identified. Specifically, the spectrum reveals the 2915 and 2848 cm^{-1} bands corresponding to the asymmetric and symmetric C–H stretch of the methylene groups (CH_2), respectively. Additionally, the 1454 and 720 cm^{-1} bands can be attributed to the scissoring and rocking vibrations of the methylene groups (54,56).

After the extraction, a total of 191 microplastic particles were analyzed using optical microscopy, and their sizes were determined by calculating the maximum Feret diameter. Figure

4 shows the frequency distribution graph of microplastics recovered by size in the different soils studied.

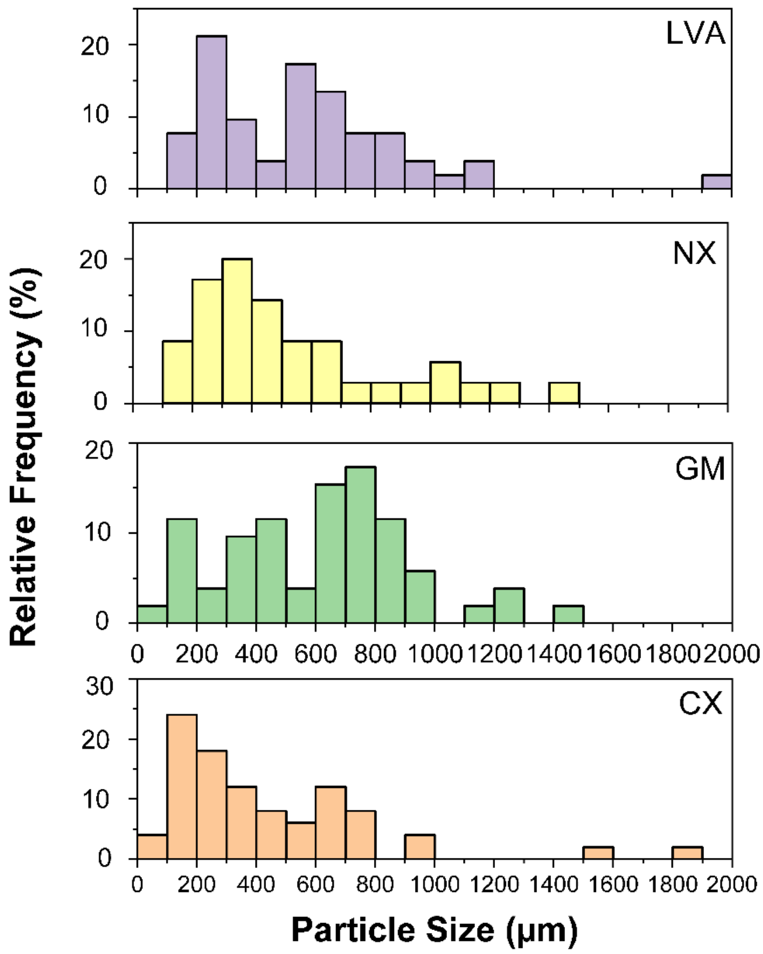

Figure 4 Frequency of recovered MP in the soil types as a function of their size distribution. LVA: Ferralsols; NX: Nitisols; GM: Gleysols; CX: Cambisols.

These results show that the microplastic particles recovered from all soil types ranged mostly from 105 to 1000 µm, with a small number detected between 1000 and 2000 µm (Figure. 4), similar to the sizes of microplastics observed before extraction. However, the proportion of MP removed by size distribution changes depending on soil type. The method utilized in this study demonstrates limited efficiency in extracting microplastics larger than 800 µm across all soil types, particularly in cambisols soils. These results suggest that MP of this size range were easily trapped in the soil, probably due to various factors involved in the separation process, including centrifugation time and speed. Similar results were observed by authors (4), which reported that the recovery of certain plastic particles may be hindered during centrifugation. During soil decantation, some plastic particles would be prevented from floating, thus reducing their recovery. Another hypothesis is related to the granular form of the PVC powder particles, which could not be completely separated from the fine soil particles during the isolation process, especially in clayey soils such as those studied in cambisols, nitisols, and ferralsols (Table 1). A similar situation was reported by author (57).

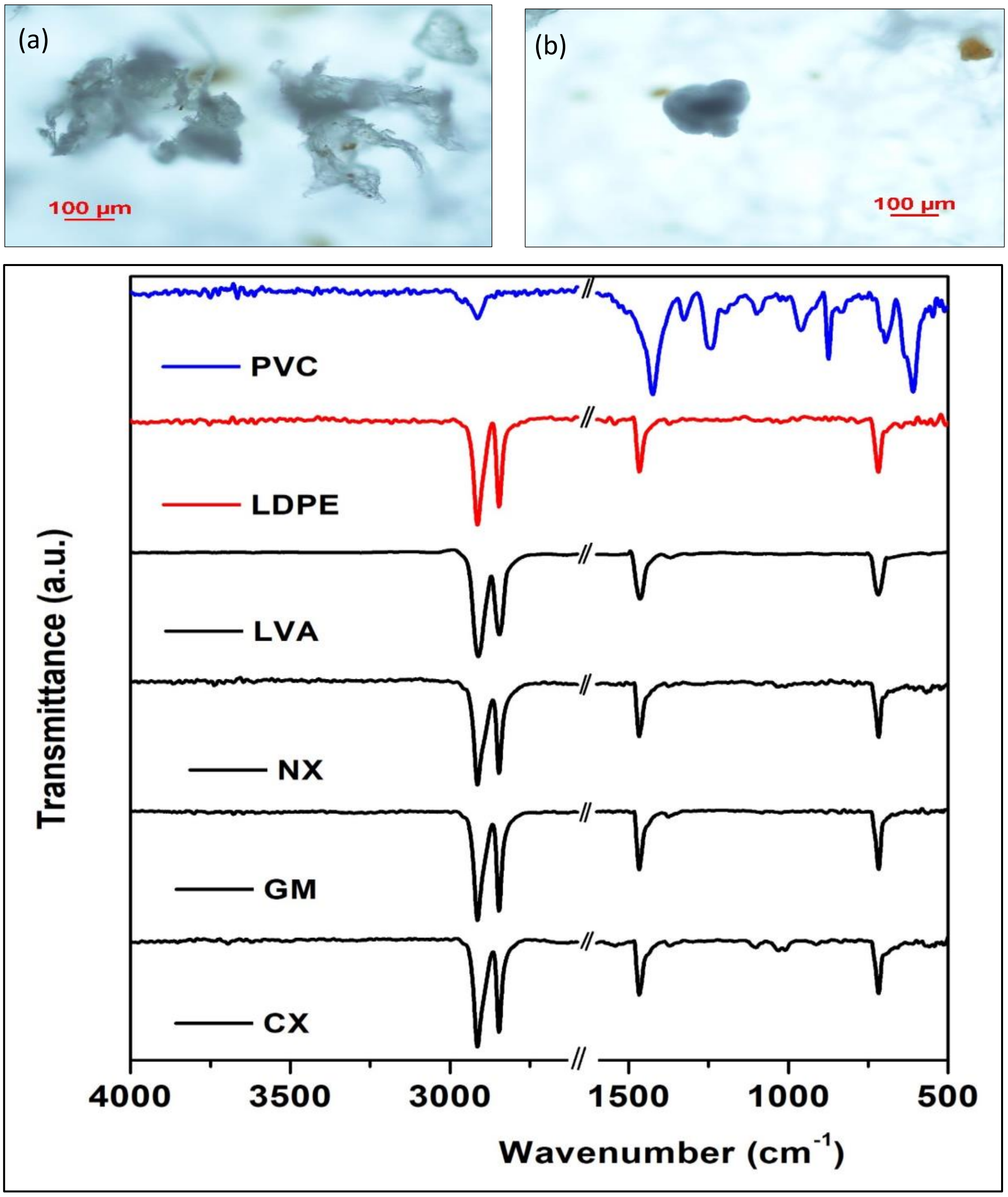

Figure 5. Images of the microplastics observed by optical microscopy: LDPE fragment shapes (a), PVC granule shapes (b), the spectrum of MP of LDPE: PVC mixture of Fourier Transform Infrared Spectroscopy (FTIR) (c) in different agricultural soil samples Ferralsols (LVA), Nitisols (NX), Gleysols (GM), and Cambisols (CX).

According to the FTIR results (Figure 5), after the separation density, the FTIR spectra did not show significant deviations from the initial spectra, making the identification of the polymer possible. This means that the characteristic band polymers kept their intensity allowing their identification after their extraction step.

3.3 Recovery efficiency of microplastics through extraction method

Figure 6 shows the recovery rates for microplastics extracted in two steps with distilled water and sodium chloride and with the zinc chloride solution. It also shows the total microplastic recovery rates for all soil samples. The results show a significant difference in the recovery rates of LDPE compared to PVC MP (Figure 6) when using the density separation method with DW and S1 solution across all soil types.

Specifically, the DW+S1 solution recovered over 50% of the mass of LDPE microplastics, whereas only about 25% of PVC was recovered. The average recovery rates of MP in LDPE: PVC/soil samples using DW and S1 solutions varied between different soil types. Specifically, the rates were 28.2% for ferralsols soil, 55.0% for NX soil, 43.9% for gleysols soil, and 47.9% for cambisols soil. In all cases, the recovery rates of MP were lower than those obtained from LDPE/soil and PVC/soil samples. Therefore, the separation method using a saturated NaCl solution did not result in high recovery rates of MP.

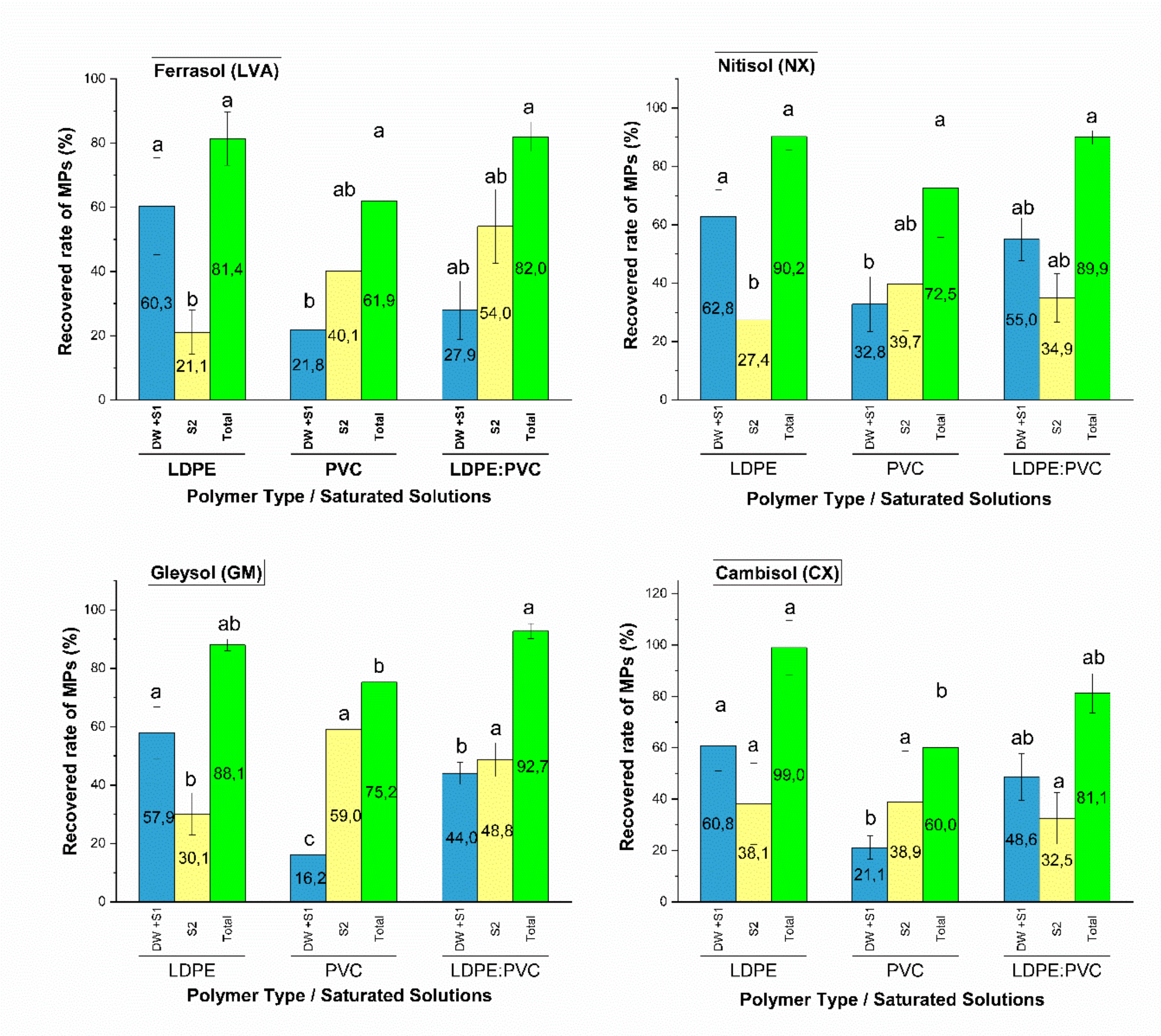

Figure 6. The recovery rate of microplastics was investigated using saturated solutions of distilled water and sodium chloride (DW + S1), as well as zinc chloride (S2), in four distinct soil types (Ferralsols, Nitisols, Gleysols, and Cambisols) and two different polymer types: low-density polyethylene (LDPE) and polyvinyl chloride (PVC). Different lowercase letters indicate significant differences between the type of saturated and total solutions at a significance level of $P < 0.05$ using Tukey's test.

The NaCl-saturated solution is commonly used to extract low-density MP, such as LDPE, from different environments because of its low cost and environmental benefits (25). However, our findings indicate that it is not effective when used in soils with high clay content, which is the case with our samples (Table 1). Quinn et al. (58) reported a similar situation in which they tested water and NaCl for extracting microplastics from PVC and PET polymers in sediment-type soil samples, obtaining a recovery rate of less than 60% particularly for sizes between 800 and 1000 µm. Andrei Kononov et al. (23), obtained low recovery rates of LDPE, reporting a rate of around 66% for particles smaller than 1 mm in agricultural soil, especially clay loam soil while using a saturated NaCl solution (59). According to the literature (40), the extraction of microplastics with sizes ranging from 0.25 to 1 mm from clayey soils depends mainly on the time process of density separation. This is because the clay content makes it difficult to separate the microplastics that adhere to it. In the case of our samples, the time used to mix the microplastics in the soil was probably not enough to separate the microplastics, allowing their flotation.

The results indicated that after using the S2 solution for extraction, the recovery rate of microplastics (MP) in the soil and low-density polyethylene (LDPE) samples ranged from 81.0% to 99.0%. In contrast, the recovery rate in the soil and polyvinyl chloride (PVC) samples ranged from 59.7% to 75.2%. Notably, a high recovery rate was achieved for low-density microplastics, while the extraction of PVC from all soil types yielded lower recovery rates.

The substantial challenge encountered in extracting PVC microplastics from the soil, particularly those smaller than 300μm, is worth noting, as emphasized in previous studies (58). Our observations underscored this difficulty, particularly evident in PVC/cambisols soil. This soil type's propensity for compaction increases soil density, posing hurdles in extracting smaller and denser microplastics, which tend to adhere to soil particles.

Finally, the study findings reveal that the average recovery rates of MP in soil/LDPE and Soil/PVC: LDPE samples were 89.6% ± 11.9% and 86.4% ± 8.4%, respectively. However, the average recovery rate for PVC polymers was 66.0% ± 22.9%.

3.4 Testing the recovery of microplastics from raw agricultural soils

The method of digestion of organic matter and density separation described above was used to analyze MP in raw agricultural soil samples ferralsols, NX, gleysols, and cambisols. This procedure enabled the determination of MP abundance per unit mass of soil. The values found in the soil samples were 2,517.5 ± 481 pieces kg^{-1}, 2,245 ± 501 pieces kg^{-1}, 3,867.5 ± 1120 pieces kg^{-1}, and 1,725 ± 95 pieces kg^{-1}, for the ferralsols, nitisols, gleysols, and cambisols samples, respectively (Figure 7c). The ferralsols, nitisols, and gleysols samples exhibit a higher abundance of microplastics in the soil. These soils stem from an area characterized by intensive agricultural practices, including semi-annual crops such as rice, soybeans, and beans. In contrast, the cambisols samples, which demonstrate a lower presence of MP in the soil, pertain to an area predominantly occupied by perennial olive trees, thus experiencing minimal agricultural activity. Consequently, the reduced occurrence of microplastics in the cambisols samples can be attributed to their land use, as this soil remains unaffected by major sources of soil microplastics, such as biosolids, organic fertilizers, mulch, and atmospheric deposition

(31,60). For instance, Leitão et al. (61) conducted a study on soil microplastics in Coimbra, Portugal, comparing sites with and without agricultural use. They reported an average of 104 x 10^3 pieces kg^{-1} microplastics in agricultural soils, while forested sites exhibited a lower average of 55 x 10^3 pieces kg^{-1}, higher than those reported in this study. In contrast, Bhavsar et al. (13) reported that the abundance of MP ranged from 21 to 210 particles per 100 g of dry soil sample, collected from critical MP pollution areas in Surat in Gujarat, India; these MP concentrations are close to those found in this study.

Moreover, agricultural soils are susceptible to erosion, facilitating the transport of microplastics through surface runoff (62). Consequently, soils at lower elevations tend to accumulate a higher abundance of microplastics. In the case of our samples, the gleysols, nitisols, and ferralsols soils are regions with slopes ranging from 3 to 8%, whereas the cambisols soil features a steeper slope, ranging from 20 to 45%. This difference in topography suggests that the lower-altitude location of gleysols soils enables them to receive microplastics through surface runoff, leading to a greater accumulation of microplastics in these areas (63)

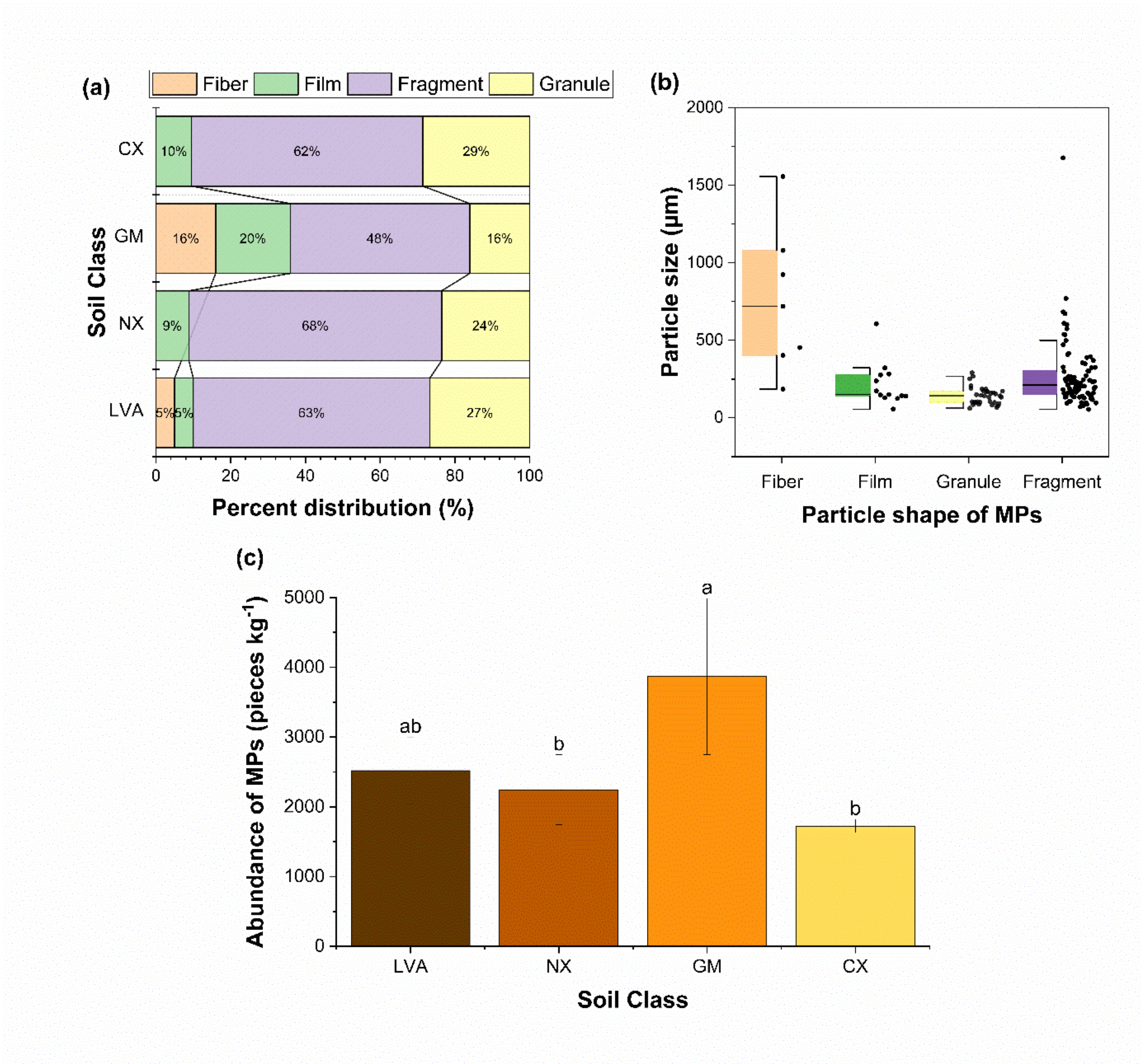

Figure 7. Microplastics distribution in samples collected: shape distribution (a); size distribution (b); and mean abundance of microplastics and standard deviation bar (item kg soil dry) (c), in different agricultural soil samples Ferralsols (LVA), Nitisols (NX), Gleysols (GM), and Cambisols (CX). Different letters indicate significant differences at P < 0.05).

The abundance of microplastics found in soil samples differs from those reported in other surveys carried out on agricultural soils. For instance, on Hainan Island in China, the concentration of MP in the study area ranged from 2.8 x10^3 to 82.5x10^3 particles kg^{-1}, with an average concentration of 15.461x10^3 particles kg^{-1}, and sizes between 20 and 200 µm (64). Thirty-two soil samples were collected from four agricultural farms in Bangladesh, and their mean microplastic concentration was found to be 21.3 x 103 particles kg^{-1}, the size range of microplastics was between 1.0 and 1.5 mm. (65) In a typical agricultural township near the southeast coast of China, the concentration of MP ranged from 70.2 to 851.3 particles kg^{-1}, with an average of 314 particles kg^{-1} in coastal plain soils (66).

Although the abundance of microplastics in Brazilian agricultural soils hasn't been reported yet, it has already been reported the abundance of MP in mangroves (67). According to a study by da Silva et al. (68) there was a remarkable presence of microplastics in six Brazilian mangrove soils, registering a value of 10.782 x10^3 particles kg^{-1} (max. = 31.087x10^3 particles kg^{-1}), the main microplastics being fibers with a dominant size between 150 and 200 µm. These results, which are higher than those of the present study, highlight the need for further research into the identification of microplastics and their distribution in different environments.

The average size of MP particles found in agricultural soils exhibits variability based on their shape (Figure 7). The majority of particles have a size of less than 300 µm, while only fibers have an average size of 750 µm. Wang et al. (70) reported that the highest proportion of MP, around 54.29% of the total pieces in all soils, had a size of less than 200 µm. A similar situation was reported by Yu et al. (71) where MP with a size less than 500 µm in agricultural soils, specifically in a layer between 10 to 25 cm depth, indicates that smaller MP tend to migrate to deeper layers of the soil. Yu et al. (71) noted that the predominant forms of MP were fragments (46.3%) and films (25.4%), similar proportions to those identified in this research.

These MP characterized here were clearly influenced by soil class and landscape position, rising opportunities for investigating diffuse pollution, and the development of environmental tracer studies (42,72–75)

The MP was further characterized under the microscope by measuring the size and shape of the particles. Figure 7(a) shows the percentage distribution of the different forms (fragment, film, fiber, and granule) in the four soil samples collected (ferralsols, nitisols, gleysols, and cambisols). Fragments were the form with the highest percentage of occurrence in all the soils, followed by granules > films > fibers. In general, the predominant form was a fragment, and, in particular, in the cambisols and nitisols soil samples there were no particles in the form of fibers. According to Figure 7(b), the MP in the shape of granules have an average size of 167.8 ± 55.7 µm, in the shape of fibers, 759.4 ± 469 µm, in the shape of films, 214.2 ± 140 µm, and in the shape of fragments, 268.8 ± 215.8 µm. The fiber-shaped particles showed the greatest variation in size compared to the other shapes.

4 Conclusions

In this study, it was proposed a methodology for the extraction, characterization, and identification of two microplastics (PVC and LDPE), and their testing in four Brazilian tropical agricultural soils. The procedure encompassed four key steps: (i) removal of organic matter; (ii) density-based separation; (iii) identification; and (iv) characterization of microplastics. The recovery efficiency exceeded 88% for LDPE and 66% for PVC. Remarkably, the $ZnCl_2$ extraction solution proved to be highly effective in recovering denser microplastics.

This methodology ensured an optimal extraction and characterization of MP in the four types of soils studied, the method used to extract MP from agricultural soils allowed finding significant differences between soil samples, highlighting the GM sample with a notably higher abundance of MP compared to nitisols and cambisols. The findings mentioned above emphasize the significance of comprehending the distribution and features of microplastics in agricultural areas. These tiny plastic particles can have a significant impact on soil health and the environment as a whole. The results further suggest the requirement for additional research and the creation of effective strategies to alleviate this environmental pollution problem.

Acknowledgments

This work was supported by the Federal University of Lavras (UFLA), the SurColombiana University (USCO), the National Council for Scientific and Technological Development (CNPq) (processes: 307950/2021-2 and 307059/2022-7), the Foundation for Research Support of the State of Minas Gerais (FAPEMIG) (processes: APQ 00802-18), and the Coordination for the Improvement of Personnel (CAPES) (code 001) for supplying the equipment and technical support for experiments involving infrared analyses and the Optical Laboratory of DFI-UFLA for obtaining images.

ABBREVIATIONS

MP: microplastics

LDPE: low-density polyethylene

PVC; poly(vinyl chloride)

GM: Gleysols

LVA: Ferralsols

NX: Nitisols

CX: Cambisols

NaClO: sodium hypochlorite

KOH: potassium hydroxide

NaCl: sodium chloride

$ZnCl_2$: zinc chloride

FTIR: fourier transform infrared spectroscopy

LOI: *loss-on-ignition method*

SOM : soil organic matter

REFERENCES

1. Ju, T.; Yang, K.; Chang, L.; Zhang, K.; Wang, X.; Zhang, J.; Xu, B.; Li, Y. Microplastics Sequestered in the Soil Affect the Turnover and Stability of Soil Aggregates: A Review. *Sci. Total Environ.* **2023**, *904*, 166776, doi:10.1016/j.scitotenv.2023.166776.

2. O'Kelly, B.C.; El-Zein, A.; Liu, X.; Patel, A.; Fei, X.; Sharma, S.; Mohammad, A.; Goli, V.S.N.S.; Wang, J.J.; Li, D.; et al. Microplastics in Soils: An Environmental Geotechnics Perspective. *Environ. Geotech.* **2021**, *8*, 586–618, doi:10.1680/jenge.20.00179.

3. He, D.; Luo, Y.; Lu, S.; Liu, M.; Song, Y.; Lei, L. Microplastics in Soils: Analytical Methods, Pollution Characteristics and Ecological Risks. *TrAC Trends Anal. Chem.* **2018**, *109*, 163–172, doi:10.1016/j.trac.2018.10.006.

4. Grause, G.; Kuniyasu, Y.; Chien, M.; Inoue, C. Separation of Microplastic from Soil by Centrifugation and Its Application to Agricultural Soil. *Chemosphere* **2022**, *288*, 132654, doi:10.1016/j.chemosphere.2021.132654.

5. Rychter, P.; Kot, M.; Bajer, K.; Rogacz, D.; Šišková, A.; Kapušniak, J. Utilization of Starch Films Plasticized with Urea as Fertilizer for Improvement of Plant Growth. *Carbohydr. Polym.* **2016**, *137*, 127–138, doi:10.1016/j.carbpol.2015.10.051.

6. Zhang, S.; Shen, T.; Yang, Y.; Li, Y.C.; Wan, Y.; Zhang, M.; Tang, Y.; Allen, S.C. Controlled-Release Urea Reduced Nitrogen Leaching and Improved Nitrogen Use Efficiency and Yield of Direct-Seeded Rice. *J. Environ. Manage.* **2018**, *220*, 191–197, doi:10.1016/j.jenvman.2018.05.010.

7. Sutherland, W.J.; Dias, M.P.; Lynn, V.D.; Helen, D.; Abigail, C.E.; Fleishman, E.; Gibbons, D.W.; Clout, M.; Côte, I.M.; Daszak, P.; et al. A Horizon Scan of Emerging Global Biological Conservation Issues for 2020. *Trends Ecol. Evol.* **2020**, *35*, 1–7, doi:https://doi.org/10.1016/j.tree.2009.10.003.

8. Junhao, C.; Xining, Z.; Xiaodong, G.; Li, Z.; Qi, H.; Siddique, K.H.M. Extraction and Identification Methods of Microplastics and Nanoplastics in Agricultural Soil: A Review. *J. Environ. Manage.* **2021**, *294*, doi:10.1016/j.jenvman.2021.112997.

9. Möller, J.N.; Löder, M.G.J.; Laforsch, C. Finding Microplastics in Soils: A Review of Analytical Methods. *Environ. Sci. Technol.* **2020**, *54*, 2078–2090, doi:10.1021/acs.est.9b04618.

10. Kumar, P.; Lee, J.; Brown, R.J.C.; Kim, K. Micro- and Nano-Plastic Pollution : Behavior, Microbial Ecology, and Remediation Technologies. *J. Clean. Prod.* **2021**, *291*, 1–22, doi:https://doi.org/10.1016/j.jclepro.2020.125240.

11. Crichton, E.M.; Noël, M.; Gies, E.A.; Ross, P.S. A Novel, Density-Independent and FTIR-Compatible Approach for the Rapid Extraction of Microplastics from Aquatic Sediments. *Anal. Methods* **2017**, *9*, 1419–1428, doi:10.1039/C6AY02733D.

12. Yang, X.; Bon, Y.; Hung, M.; Bernhart, R.; Lai, K. Environmental Health Impacts of Microplastics Exposure on Structural Organization Levels in the Human Body. *Sci. Total Environ.* **2022**, *825*, 154025, doi:10.1016/j.scitotenv.2022.154025.

13. Bhavsar, P.S.; Chovatiya, B. V; Kamble, S.B.; Gore, A.H. Extraction and Analysis of

Microplastics in the Soil of Diamond City, Surat (Gujarat, India): Ecological Risk, Pollution Indices, and Greenness Evaluation. *ACS Agric. Sci. Technol.* **2024**, *4*, 614–525, doi:10.1021/acsagscitech.4c00140.

14. Mengjie, W.; Chunping, Y.; Cheng, D.; Hongyu, L. Microplastics in Waters and Soils: Occurrence, Analytical Methods and Ecotoxicological Effects. *Ecotoxicol. Environ. Saf.* **2020**, *202*, doi:https://doi.org/10.1016/j.ecoenv.2020.110910.

15. Abdolahpur Monikh, Fazel Doornhein, N.; Romeijn, S.; Vijver, Martina G. Peijnenburg, W.J.G.M. Method for Extraction of Nanoscale Plastic Debris from Soil. *Anal. Methods* **2021**, *13*, 1576–1583, doi:10.1039/D0AY02308F.

16. Liu, M.; Song, Y.; Lu, S.; Qiu, R.; Hu, J.; Li, X.; Bigalke, M.; Shi, H.; He, D. A Method for Extracting Soil Microplastics through Circulation of Sodium Bromide Solutions. *Sci. Total Environ.* **2019**, *691*, 341–347, doi:https://doi.org/10.1016/j.scitotenv.2019.07.144.

17. Surendran, U.; Jayakumar, M.; Raja, P.; Gopinath, G. Microplastics in Terrestrial Ecosystem : Sources and Migration in Soil Environment. *Chemosphere* **2023**, *318*, 137946, doi:10.1016/j.chemosphere.2023.137946.

18. Kitahara, K.; Nakata, H. Plastic Additives as Tracers of Microplastic Sources in Japanese Road Dusts. *Sci. Total Environ.* **2020**, *736*, 139694, doi:10.1016/j.scitotenv.2020.139694.

19. Perez, C.N.; Carr, F.; Hoarau, A.B.; Joris, A.; Leonards, G.P.E.; Lamoree, M.H. Innovations in Analytical Methods to Assess the Occurrence of Microplastics in Soil. *J. Environ. Chem. Eng.* **2022**, *10*, 107421, doi:10.1016/j.jece.2022.107421.

20. Fernandes, A.N.; Bertoldi, C.; Lara, L.Z.; Stival, J.; Alves, N.M.; Cabrera, P.M.; Grassi, M.T. Microplastics in Latin America Ecosystems: A Critical Review of the Current Stage and Research Needs. *J. Braz. Chem. Soc.* **2022**, *33*, 303–326, doi:10.21577/0103-5053.20220018.

21. Rani-Borges, B.; Martins, T.F.G.; Pompêo, M. Status of Brazilian Research on Microplastics Present in Aquatic Ecosystems: Freshwater. *Panam. J. Aquat. Sci.* **2021**, *16*, 106–117.

22. Fan, W.; Qiu, C.; Qu, Q.; Hu, X.; Mu, L.; Gao, Z.; Tang, X. Sources and Identification of Microplastics in Soils. *Soil Environ. Heal.* **2023**, *1*, 100019, doi:https://doi.org/10.1016/j.seh.2023.100019.

23. Kononov, A.; Hishida, M.; Suzuki, K.; Harada, N. Microplastic Extraction from Agricultural Soils Using Canola Oil and Unsaturated Sodium Chloride Solution and Evaluation by Incineration Method. *Soil Syst.* **2022**, *6*, 1–11, doi:10.3390/soilsystems6020054.

24. Thomas, D.; Schutze, B.; Heinze, W.M.; Steinmetz, Z. Sample Preparation Techniques for the Analysis of Microplastics in Soil- A Review. *Sustainability* **2020**, *12*, 9074, doi:10.3390/su12219074.

25. Zhang, S.; Yang, X.; Gertsen, H.; Peters, P.; Salánki, T.; Geissen, V. A Simple Method for the Extraction and Identification of Light Density Microplastics from Soil. *Sci. Total Environ.* **2018**, *616–617*, 1056–1065, doi:10.1016/j.scitotenv.2017.10.213.

26. Quilez, M.A.I.; Uttam, C.P.; Merino, D.; Athanassiou, A. Composites of Thermoplastic Starch and Lignin-Rich Agricultural Waste for the Packaging of Fatty Foods. *ACS Sustain. Chem. Eng.* **2022**, *10*, 15402–15413, doi:10.1021/acssuschemeng.2c04326.

27. Yan, P.; Zhang, S.; Wang, J.; Xiao, Z.; Yan, S.; Wang, W.; Aurangzeib, M. Heterogeneity of Plastic Residue Was Determined by Both Mulch Film and External Plastic Pollutants in the Farmland of Northeast China. *Sci. Total Environ.* **2022**, *853*, doi:http://dx.doi.org/10.1016/j.scitotenv.2022.158681.

28. Bläsing, M.; Amelung, W. Plastics in Soil : Analytical Methods and Possible Sources. *Sci. Total*

Environ. **2018**, *612*, 422–435, doi:10.1016/j.scitotenv.2017.08.086.

29. Silva, B.M.; Santos, W.J.R.; Marques, J.J. *Detailed Soil Survey of Muquém Farm / UFLA, Lavras- MG*; Boletim Té.; Lavras MG, Brazil, 2014;

30. Wang, J.; Huang, M.; Wang, Q.; Sun, Y.; Zhao, Y.; Huang, Y. LDPE Microplastics Significantly Alter the Temporal Turnover of Soil Microbial Communities. *Sci. Total Environ.* **2020**, *726*, 138682, doi:10.1016/j.scitotenv.2020.138682.

31. Weithmann, N.; Möller, J.N.; Löder, M.G.J.; Piehl, S.; Laforsch, C.; Freitag, R. Organic Fertilizer as a Vehicle for the Entry of Microplastic into the Environment. *Sci. Adv.* **2018**, 1–7, doi:https://doi.org/10.1126/sciadv.aap8060.

32. IUSS Working Group WRB *World Reference Base for Soil Resources. International Soil Classification System for Naming Soils and Creating Legends for Soil Maps.*; (IUSS), I.U. of S.S., Ed.; 4th ed.; International Union of Soil Sciences (IUSS),: Vienna, Austria, 2022; ISBN 9798986245119.

33. Silva, A.E. da; Fontana, A.; Melo, A. da S.; Martins, A.L. da S.; Inda, A.V.; Santi, A.; Madari, B.E.; Mattos, B.B.; Almeida, B.G. de; Alves, B.J.R.; et al. *Manual de Métodos de Análise de Solo*; Empresa Br.; Rio de Janeiro, 2017;

34. Oden, C.P.; Werth, C.J.; Kienzle, B.A.; Katz, L.E. Impact of Organic Matter on Transformation during Thermal Remediation of Pyrene-Contaminated Substrates. *Sci. Total Environ.* **2024**, *906*, 167569, doi:10.1016/j.scitotenv.2023.167569.

35. Jia-ping, W.; Xiu-jun, W.; Juan, Z. Evaluating Loss-on-Ignition Method for Determinations of Soil Organic and Inorganic Carbon in Arid Soils of Northwestern China ∗ 1. *Pedosph. An Int. J.* **2013**, *23*, 593–599, doi:10.1016/S1002-0160(13)60052-1.

36. Me, M.; Boontanon, N.; Fujii, S.; Kitpati, S. Rapid and Ef Fi Cient Removal of Organic Matter from Sewage Sludge for Extraction of Microplastics. *Sci. Total Environ.* **2022**, *853*, 158642, doi:10.1016/j.scitotenv.2022.158642.

37. Al-azzawi, M.S.M.; Kefer, S.; Weißer, J.; Reichel, J.; Schwaller, C.; Glas, K.; Knoop, O.; Drewes, J.E. Validation of Sample Preparation Methods for Microplastic Analysis in Wastewater. *Water Re* **2020**, *12*, doi:doi:10.3390/w12092445.

38. Enders, K.; Lenz, R.; Beer, S.; Stedmon, C.A. Extraction of Microplastic from Biota: Recommended Acidic Digestion Destroys Common Plastic Polymers. *ICES J. Mar. Sci.* **2017**, *74*, 326–331, doi:10.1093/icesjms/fsw173.

39. Vermeiren, P.; Muñoz, C.; Ikejima, K. Microplastic Identification and Quantification from Organic Rich Sediments: A Validated Laboratory Protocol. *Environ. Pollut.* **2020**, *262*, 114298, doi:10.1016/j.envpol.2020.114298.

40. Radford, F.; Zapata-Restrepo, L.M.; Horton, A.A.; Hudson, M.D.; Shaw, P.J.; Williams, I.D. Developing a Systematic Method for Extraction of Microplastics in Soils. *Anal. Methods* **2021**, *13*, 1695–1705, doi:10.1039/d0ay02086a.

41. Scopetani, C.; Chelazzi, D.; Mikola, J.; Leiniö, V.; Heikkinen, R.; Cincinelli, A.; Pellinen, J. Olive Oil-Based Method for the Extraction, Quantification and Identification of Microplastics in Soil and Compost Samples. *Sci. Total Environ.* **2020**, *733*, doi:10.1016/j.scitotenv.2020.139338.

42. Corradini, F.; Meza, P.; Eguiluz, R.; Casado, F.; Huerta-Lwanga, E.; Geissen, V. Evidence of Microplastic Accumulation in Agricultural Soils from Sewage Sludge Disposal. *Sci. Total Environ.* **2019**, *671*, 411–420, doi:10.1016/j.scitotenv.2019.03.368.

43. Izquierdo, B.J.; Arévalo, H.J.J. Determinación Del Carbono Orgánico Por El Método Químico

y Por Calcinación. *Ing. y Región* **2021**, *26*, 20–28, doi:10.25054/22161325.2527.

44. R Core Team R: A Language and Environment for Statistical Computing. R Foundation for Statistical Computing 2024.

45. Zhang, H.; Huang, Y.; An, S.; Zhao, J.; Xiao, L.; Li, H.; Huang, Q. Microplastics Trapped in Soil Aggregates of Different Land-Use Types: A Case Study of Loess Plateau Terraces, China. *Environ. Pollut.* **2022**, *310*, 119880, doi:10.1016/j.envpol.2022.119880.

46. Lehndorff, E.; Rodionov, A.; Amelung, L.P.; Rottmann, P.; Spiering, B.; Wulf, S.D. Spatial Organization of Soil Microaggregates. *Geoderma* **2021**, *386*, 114915, doi:https://doi.org/10.1016/j.geoderma.2020.11491.

47. Liu, Y.; Zhong, Y.; Hu, C.; Xiao, M.; Diag, F.; Yu, Y.; Zhu, Z.; Chen, J.; Ge, T.; Ding, J. Distribution of Microplastics in Soil Aggregates after Film Mulching. *Soil Ecol. Lett.* **2023**, *5*, 230171, doi:10.1007/s42832-023-0171-9.

48. Prata, J.C.; João, P.; Girão, A. V; Lopes, I.; Duarte, A.C.; Rocha-santos, T. Identifying a Quick and Ef Fi Cient Method of Removing Organic Matter without Damaging Microplastic Samples. *Sci. Total Environ.* **2019**, *686*, 131–139, doi:10.1016/j.scitotenv.2019.05.456.

49. Pfohl, P.; Roth, C.; Meyer, L.; Heinemeyer, U.; Gruendling, T.; Lang, C.; Nestle, N.; Hofmann, T.; Wohlleben, W.; Jessl, S. Microplastic Extraction Protocols Can Impact the Polymer Structure. *Microplastics and Nanoplastics* **2021**, *1*, 1–13, doi:https://doi.org/10.1186/s43591-021-00009-9 (2021).

50. Guimarães, D.V.; Silva, M.L.N.; Beniaich, A.; Pio, R.; Gonzaga, M.I.S.; Avanzi, J.C.; Bispo, D.F.A.; Curi, N. Dynamics and Losses of Soil Organic Matter and Nutrients by Water Erosion in Cover Crop Management Systems in Olive Groves, in Tropical Regions. *Soil Tillage Res.* **2021**, *209*, doi:10.1016/j.still.2020.104863.

51. Thiele, C.J.; Hudson, M.D.; Russell, A.E. Evaluation of Existing Methods to Extract Microplastics from Bivalve Tissue: Adapted KOH Digestion Protocol Improves Filtration at Single-Digit Pore Size. *Mar. Pollut. Bull.* **2019**, *142*, 384–393, doi:10.1016/j.marpolbul.2019.03.003.

52. Schneider, C.A.; Rasband, W.S.; Eliceiri, K.W. NIH Image to ImageJ: 25 Years of Image Analysis. *Nat. Methods* 2012, *9*, 671–675.

53. Sierra, I.; Chialanza, M.R.; Faccio, R.; Carrizo, D.; Fornaro, L.; Pérez-Parada, A. Identification of Microplastics in Wastewater Samples by Means of Polarized Light Optical Microscopy. *Environ. Sci. Pollut. Res.* **2020**, *27*, 7409–7419, doi:. https://doi.org/10.1007/s11356-019-07011-y.

54. Smith, B.C. The Infrared Spectra of Polymers II: Polyethylene. *Spectroscopy* **2021**, *36*, 24–29, doi:https://doi.org/10.56530/spectroscopy.xp7081p7.

55. Käppler, A.; Fischer, D.; Oberbeckmann, S.; Schernewski, G.; Labrenz, M.; Klaus, J.E.; Voit, B. Analysis of Environmental Microplastics by Vibrational Microspectroscopy: FTIR, Raman or Both? *Anal. Bioanal. Chem.* **2016**, *408*, pages8377–8391, doi:https://doi.org/10.1007/s00216-016-9956-3.

56. Chouchene, K.; Tommaso, N.; Modugno, F.; Castelvetro, V.; Mohamed, K. Soil Contamination by Microplastics in Relation to Local Agricultural Development as Revealed by FTIR, ICP-MS and Pyrolysis-GC/MS. *Environ. Pollut.* **2022**, *303*, 119016, doi:https://doi.org/10.1016/j.envpol.2022.119016.

57. Zhang, G.S.; Liu, Y.F. The Distribution of Microplastics in Soil Aggregate Fractions in Southwestern China. *Sci. Total Environ.* **2018**, *642*, 12–20, doi:10.1016/j.scitotenv.2018.06.004.

58. Quinn, B.; Murphy, F.; Ewins, C. Validation of Density Separation for the Rapid Recovery of Microplastics from Sediment. *Anal. Methods* **2016**, *9*, 1491–1498, doi:https://doi.org/10.1039/C6AY02542K.

59. Monteiro, S.S. Methods for the Extraction of Microplastics in Complex Solid , Water and Biota Samples. *Trends Environ. Anal. Chem.* **2022**, *33*, e00151, doi:https://doi.org/10.1016/j.teac.2021.e00151.

60. Büks, F.; Kaupenjohann, M. Global Concentrations of Microplastics in Soils - A Review. *Soil* **2020**, *6*, 649–662, doi:10.5194/soil-6-649-2020.

61. Leitão, I.A.; van Schaik, L.; Ferreira, A.J.D.; Alexandre, N.; Geissen, V. The Spatial Distribution of Microplastics in Topsoils of an Urban Environment - Coimbra City Case-Study. *Environ. Res.* **2023**, *218*, doi:10.1016/j.envres.2022.114961.

62. Rehm, R.; Zeyer, T.; Schmidt, A.; Fiener, P. Soil Erosion as Transport Pathway of Microplastic from Agriculture Soils to Aquatic Ecosystems. *Sci. Total Environ.* **2021**, *795*.

63. Han, N.; Zhao, Q.; Ao, H.; Hu, H.; Wu, C. Horizontal Transport of Macro- and Microplastics on Soil Surface by Rainfall Induced Surface Runoff as Affected by Vegetations. *Sci. Total Environ.* **2022**, *831*, 154989, doi:doi.org/10.1016/j.scitotenv.2022.154989.

64. Amjad, M.; Huang, Q.; Khan, S.; Wang, Q.; Huang, J.; Fahad, X.; Sajjad, M.; Liu, Y.; Mašek, O.; Li, X.; et al. Abundance, Spatial Distribution, and Characteristics of Microplastics in Agricultural Soils and Their Relationship with Contributing Factors. *Rev. Gestão Ambient.* **2023**, *328*, doi:https://doi.org/10.1016/j.jenvman.2022.117006.

65. Hossain, M.N.; Rahman, M.M.; Afrin, S.; Akbor, M.A.; Bakar, S.A.; Malafaia, G. Identification and Quantification of Microplastics in Agricultural Farmland Soil and Textile Sludge in Bangladesh. *Sci. Total Environ.* **2023**, *858*, doi:10.1016/j.scitotenv.2022.160118.

66. Zhou, Y.; Jia, Z.; Zheng, G.; Chen, L.; Zhang, Q.; Su, B.; Zhou, S. Microplastics in Agricultural Soils on the Coastal Plain : Spatial Characteristics, Influencing Factors and Sources. *Sci. Total Environ.* **2023**, *901*, 1–12, doi:https://doi.org/10.1016/j.scitotenv.2023.165948.

67. Zamprogno, G.C.; Caniçali, F.B.; Cozer, C. dos R.; Otegui, M.B.P.; Graceli, J.B.; Costa, M.B. da Spatial Distribution of Microplastics in the Superficial Sediment of a Mangrove in Southeast Brazil: A Comparison between Fringe and Basin. *Sci. Total Environ.* **2021**, *784*, doi:10.1016/j.scitotenv.2021.146963.

68. Silva, P.E.; Vincent, T.; da Conceição, H.; Santos, T.; de Almeida, M.; Vinhas Costa, O.; Rebouças, M.; Gonzaca, J. Widespread Microplastic Pollution in Mangrove Soils of Todos Os Santos. *Environ. Res.* **2022**, *210*, 112952.

69. Wang, L.; Yen, H.; Wang, X.; Huang, C. hua; Sun, J.; Hammac, A.; Wang, Y. Deposition- and Transport-Dominated Erosion Regime Effects on the Loss of Dissolved and Sediment-Bound Organic Carbon: Evaluation in a Cultivated Soil with Laboratory Rainfall Simulations. *Sci. Total Environ.* **2021**, *750*, doi:10.1016/j.scitotenv.2020.141717.

70. Wang, J.; Li, J.; Liu, S.; Li, H.; Chen, X.; Peng, C.; Zhang, P.; Liu, X. Distinct Microplastic Distributions in Soils of Different Land-Use Types : A Case Study of Chinese Farmlands *. *Environ. Pollut.* **2021**, *269*, 116199, doi:https://doi.org/10.1016/j.envpol.2020.116199.

71. Yu, L.; Zhang, J. Di; Liu, Y.; Chen, L.Y.; Tao, S.; Liu, W.X. Distribution Characteristics of Microplastics in Agricultural Soils from the Largest Vegetable Production Base in China. *Sci. Total Environ.* **2021**, *756*, 1–9, doi:10.1016/j.scitotenv.2020.143860.

72. Batista, P.V.G.; Laceby, J.P.; Davies, J.; Tassinari, D.; Silva, M.L.N.; Curi, N.; Quinton, J.N. A Framework for Testing Large-Scale Distributed Soil Erosion and Sediment Delivery Models : Dealing with Uncertainty in Models and the Observational Data. **2021**, *137*,

doi:10.1016/j.envsoft.2021.104961.

73. Chen, B. Current Status and Trends of Research on Microplastic Fugacity Characteristics and Pollution Levels in Mangrove Wetlands. *Front. Environ. Sci.* **2022**, *10*, 1–13, doi:10.3389/fenvs.2022.1021274.

74. Redondo-hasselerharm, P.E.; Rico, A.; Koelmans, A.A. Risk Assessment of Microplastics in Freshwater Sediments Guided by Strict Quality Criteria and Data Alignment Methods. *J. Hazard. Mater.* **2023**, *441*, 129814, doi:10.1016/j.jhazmat.2022.129814.

75. Guo, Z.; Li, P.; Yang, X.; Wang, Z.; Lu, B.; Chen, W. Soil Texture Is an Important Factor Determining How Microplastics Affect Soil Hydraulic Characteristics. *Environ. Int.* **2022**, *165*, 107293, doi:10.1016/j.envint.2022.107293.

This paper was submitted and is under review in the journal ACS OMEGA.

PAPER 2 – PLASTIC DEBRIS IN AGROECOSYSTEMS: DISTRIBUTION AND ABUNDANCE PATTERNS, AND RELATIONSHIP WITH TERRAIN CHARACTERISTICS IN SOUTHEASTERN BRAZIL

ABSTRACT

Plastic pollution in agricultural soil is a major concern, affecting soil biodiversity and functionality. In this context, studies on agricultural soil plastic pollution that consider its use across different regions are essential. This study aimed to identify, quantify, and characterize plastic debris in various agroecosystems within a Southeast Brazil sub-basin, considering land use. Additionally, the sampled plastic debris was georeferenced, allowing its characteristics to be correlated with terrain features such as the LS factor and vegetation cover. Based on size, the plastic debris was categorized into macroplastics, mesoplastics, and coarse microplastics. The results revealed that agricultural areas accounted for 91.2% of the total plastic waste collected. The most common polymer types identified were polypropylene, polyethylene, and polyvinyl chloride, comprising 82.6% of the total. The accumulation of plastic debris in this region was primarily linked to intensive human activity and agricultural practices. Moreover, its distribution strongly correlated with terrain characteristics, particularly the LS factor and vegetation cover, with higher concentrations observed in smooth and moderately undulating terrain. These findings highlight the importance of monitoring plastic debris in the basin's terrain and identifying pollution sources to provide valuable insights for mitigating its environmental impact.

KEYWORDS: Diffuse pollution, Land use, polymers, spatial distribution

1. INTRODUCTION

Plastic products are extensively used in the agricultural sector due to their advantageous properties, such as durability, versatility, mechanical resistance, and low cost (1–3). These materials serve multiple purposes, including use as cover films, fertilizer and seed bags, irrigation pipes, pesticide containers, and protective netting, among others (4–6). While the utility of plastics in agriculture is undeniable, the increasing improper disposal of plastic products has led to significant socio-environmental impacts, including contamination that affects the food chain (7,8) and degrades soil quality (9).

Plastic pollution, resulting from waste of various sizes, has been extensively studied due to its significant impact on ecosystems (8–10). Once released into the environment, plastic debris is subjected to multiple degradation processes driven by factors such as moisture, oxygen, heat, radiation, light, and mechanical stress, leading to its progressive fragmentation into smaller particles (11,12). Research confirms the presence of plastic particles in various ecosystems (13,14). It has also been shown that the contaminating potential of these particles in biotic and abiotic environments is directly related to their size (15,16). For example, studies have shown that macroplastics in agricultural soils can reduce their bulk density, reduce macropores, and alter the distribution of water in the soil. On the other hand, microplastics can affect the growth and survival rate of soil organisms, thus altering soil functionality (17).

Plastic debris is classified by size into macroplastics (MaP, >25 mm), mesoplastics (MeP, 5–25 mm), microplastics (MP, 1 μm–5 mm), nanoplastics (NPs, <1 μm, typically 1–1000 nm) (17,18), and coarse microplastics (CMP, 2–5 mm), a subclass of MP (19–21). Plastic waste in agricultural soils comes from plastic mulch, input packaging, pesticides, organic fertilizers, rural household waste, sludge landfill, composting, wastewater irrigation, road runoff, and atmospheric deposition (11,22,23). The accumulation of such debris poses a growing threat to agroecosystems, with the degradation of macroplastics being a primary source of microplastics (6–8,24,25).

The fragmentation and degradation of plastics are influenced by factors including polymer type, debris thickness, and soil organisms (17,26). Common agricultural polymers include polyethylene (PE), low-density polyethylene (LDPE), high-density polyethylene (HDPE), polypropylene (PP), polystyrene (PS) and polyvinyl chloride (PVC). These polymers, composed of carbon-carbon chains, degrade through chain cleavage processes, with degradation times varying by polymer type (14,27).

Studies conducted worldwide have explored the abundance, distribution, polymer composition, shape, size, and migration of plastic debris in agricultural soils (26,28–31). On the other hand, the accumulation of plastic particles in agricultural soils depends on several factors, including soil type and use, vegetation cover (32), and climatic factors associated with its geographical location. Considering the geographical location, plastic debris could easily migrate to surrounding ecosystems, reaching seas and oceans or traveling along large river basins, causing far-reaching impacts. According to Cai et al. (33) humid tropical agricultural soils in China exhibited higher plastic debris accumulation due to the influence of regional climate (9,11,33). Climatic factors such as temperature and altitude also affect plastic debris accumulation in agricultural soils (33).

Despite existing studies, several factors linking agricultural soils to plastic debris remain unexplored, including the role of vegetation as a plastic sink, the influence of soil preparation and management, and the dynamics of particle size in agricultural soils.

This study aims to quantify and characterize the abundance, mass, and polymer composition of plastic debris in tropical agricultural soils, particularly in identifying the types and sources of contamination. Additionally, the study aims to analyze the spatial distribution of plastic debris and relate its characteristics (quantity, mass, area, diameter, and perimeter) to the topographic features of the terrain, such as slope, LS factor, and vegetation cover, to identify patterns and potential critical accumulation points. It is important to emphasize that the study area exhibits similar characteristics to those of other regions of Brazil and can serve as a reference for designing effective strategies for plastic pollution prevention and control, promoting sustainable agricultural development.

It is also important to emphasize that this is the first study to investigate characteristics, abundance, types, and spatial distribution of plastic debris (MaP, MeP, and CMP) in agricultural soils within a reference river basin in southeastern Minas Gerais. The study area encompasses forests, grasslands, and agricultural lands where activities such as soil preparation, fertilization, irrigation, and harvesting take place. These activities serve as a basis for understanding plastic waste pollution in tropical soils.

2. MATERIALS AND METHODS

2.1. Site description

The study area was the Muquém Experimental Farm of the Federal University of Lavras (UFLA), located in a sub-basin of the Rio Grande in southeastern Brazil. The farm covers an area of approximately 165 hectares of diversified land including forest, grassland, and agriculture (Figure. 1). The sub-basin is part of the Atlantic Plateau geomorphological unit, specifically on the surface of the Upper Rio Grande, a tributary of the Paraná River, located in the municipality of Lavras, Minas Gerais. It is between latitude -21°12'037"S and longitude -44°59'3.77"W, WGS 84 UTM 23S.

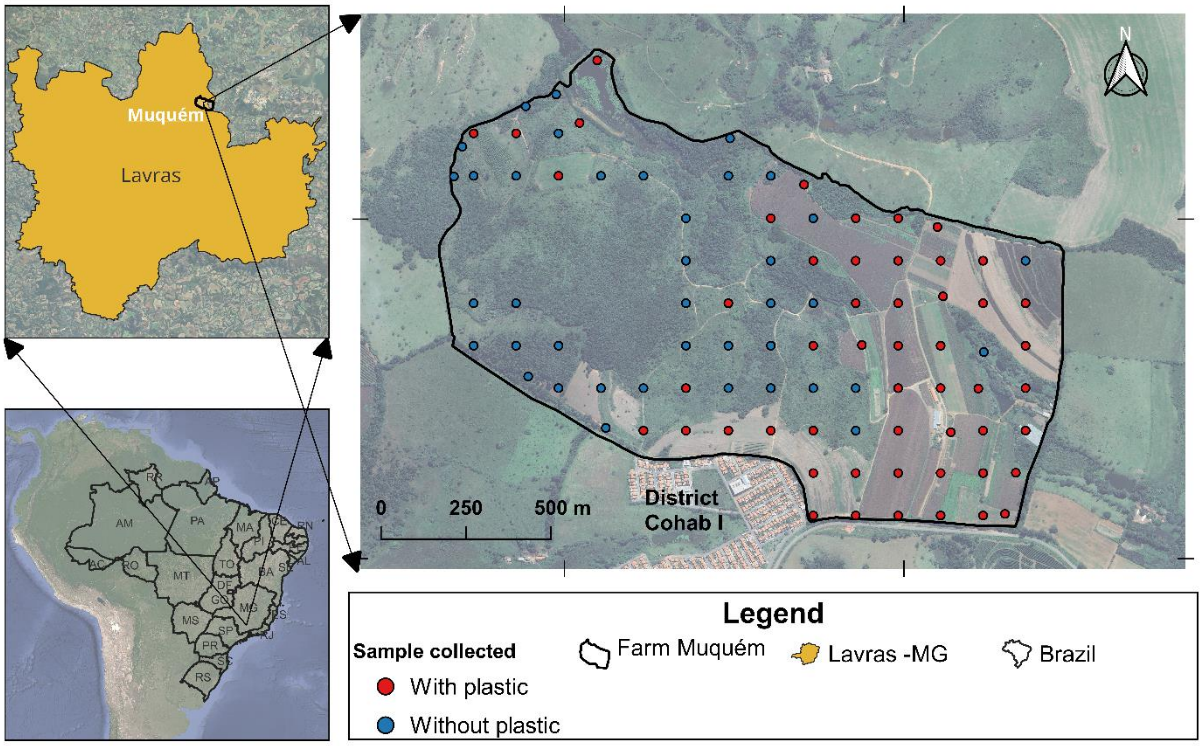

Figure 1. Map of the study area and geographic location of sampled points with and without plastic debris at sub-basin *from* Muquém farm, municipality of Lavras, Brazil.

The climate of the region is classified as Cwa, temperate rainy (mesothermal) according to the Köppen climate system, with a dry winter and subtropical rainy summer, with an average annual rainfall of 1,383.4 mm, concentrated in the summer, from October to February (34,35). According to the Meteorological Service in Brazil (INMET) database, the prevailing winds are easterly from March to September and northeasterly from November to February, with average wind speeds of 2.16 m s^{-1} and 1.64 m s^{-1}, respectively (36).

According to the international classification (37), the soil orders present in the study area correspond to Inceptisols (CX), which occupy 18.84 ha (11,41% of the area), Entisols Aquepts

(GM), which occupy 1.92 ha (1.16% of the area), Oxisols (LVA) occupy 63.60 ha (38.50%), Alfisols (NX) 8.30 ha (5.02%), Ultisols (PVA) 58.07 ha (35.15% of the area) and Lithic Orthents (RL) 14.48 ha, representing 8.76% of the total area of the farm.

The sub-basin has a minimum elevation of 877 m and a maximum of 1040 m, with varying landforms and slopes. Its landforms was classified according to Silva et al. (38) as: flat (< 3%), gently undulating (3 - 8%), undulating (8 - 20%), strongly (20 - 45%), mountainous (45 - 75%), corresponding to 2.7%, 17.8%, 58.8%, 20.1% and 0.6% of the total area of the farm, respectively (Figure 2b).

Land use on the farm was classified into three types (38). The first was agricultural use, with annual crops representing 29.15% of the agricultural land, with maize (*Zea mays*), soybean (*Glycine max* (L.) *Merrill*), wheat (*Triticum aestivum* L.), beans (*Phaseolus vulgaris*), sorghum (*Sorghum bicolor* L.), and rice (Oriza sativa L.), as well as perennial crops (0.91% of the area), coffee (*Coffea arabica*), eucalyptus (*Eucalyptus* sp.) and, to a lesser extent, other forest species. This is followed by grassland (mainly Poaceae species), with 39.33% cultivated grassland and 4.69% native grassland, and then forest, with 24.39% of the farm area.

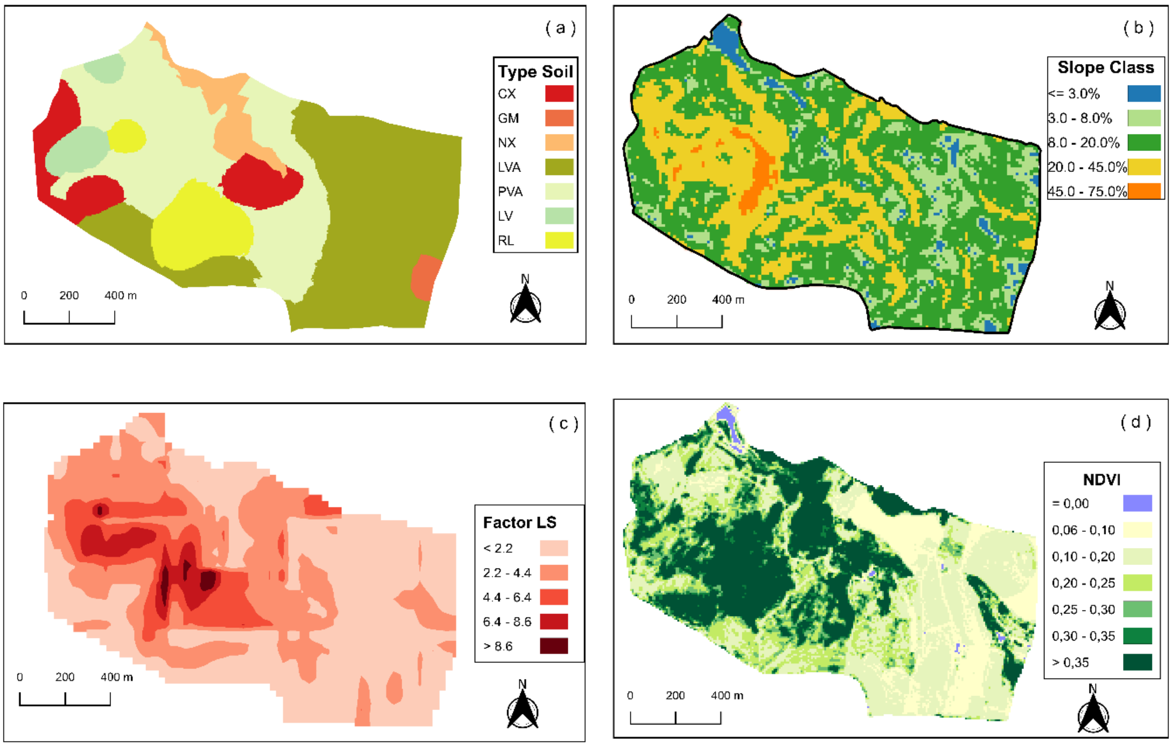

Figure 2. Map showing soil types (a), slope classes (b), LS factor map (c), and NDVI map (d) of the Muquém farm. Note: reliefs associated with their respective slopes, namely: flat (< 3%), slightly undulating (3 - 8%), undulating (8 - 20%), strongly (20 - 45%), and mountainus (45 -

75%). To Oxisols (LVA), Cambisols (CX), Ultisols (PVA), Alfisols (NX), Lithic Orthents (RL), and Entisols (GM).

2.2 Sampling of study materials

Plastic debris was collected between August 2022 and April 2023. First, the study area was surveyed, and sampling points were georeferenced. The surrounding vegetation, land use, and altitude were determined. Georeferencing was carried out using a Garmin Oregon 750 Global Positioning System (GPS) with an accuracy of 3 m, using a regular grid of 125 m × 125 m resolution. A total of 91 points were georeferenced, corresponding to a sampling density of 1.77 samples per hectare.

At each sampling point, the soil surface was visually inspected for plastic debris, which was collected within an area of approximately 19.63 m² per point. The samples were collected, stored and identified by mesh point, and transported to the laboratory for further analysis.

To determine the topographic characteristics of the study area, such as the topographic length and slope factor (LS factor) and the normalized difference vegetation index (NDVI), secondary geomorphometric information from the TOPODATA database of the National Space Research Institute (INPE) and maps from the CBERS 4 satellite in October 2022 were used.

The LS factor was determined using the tool SAGA-GIS, "LS-Factor, Field-Based". The NDVI and LS factor values were extracted using the Point Sampling Tool plugin available in the QGis software (39). Figures 2c and 2d show the map of the LS factor and vegetation index (NDVI).

2.3 Classification, characterization, and identification of plastic debris

The plastic debris collected at each sampling point was classified according to its mass, dimensions (length, perimeter, and area), and polymer type. The classification of plastic debris was also carried out considering land use. To follow, the collected plastic particles were first physically shaken and washed with distilled water to remove the remnants of soil and non-plastic materials adhering to their surface. They were then air-dried and stored in steel containers.

Each piece of plastic debris was then photographed using a high-resolution digital camera (Cannon EOS 60D). The digital images obtained were analyzed using ImageJ software, (40). The photographs of the debris, together with the scale of a caliper (± 0.5 mm), helped to determine the pixel of the digital image and hence the dimensions of the debris. Based on these measurements, plastic debris was classified as macroplastics (MaP) for particles > 25,000 µm, mesoplastics (MeP) for particles between 5,000 and 25,000 µm, and coarse microplastics (CMP) for particles between 2,000 and 5,000 µm.

To calculate the mass and abundance of plastic debris per sampling point, equations 1 and 2 were used, respectively. These values were then extrapolated to hectares using a conversion factor (f1).

$$Mass \left[\frac{kg}{ha}\right] = \frac{W_i}{S} \times f_1 \qquad (1)$$

$$Abundance \left[\frac{pieces}{ha}\right] = \frac{N_i}{S} \times f_1 \qquad (2)$$

Where Wi (g) is the total mass of plastic debris, S (m^2) is the surface area of the sampling point (approximately 19.63 m^2), Ni is the number of plastic particles per sampling point and f1 is the conversion factor to hectare. The data from equations (1) and (2) were recorded in a georeferenced database using QGIS software.

Raman spectroscopy was used to identify the type of polymer present in the plastic debris, collected at each point. Raman spectra were obtained at room temperature using a confocal Raman microscope (Alpha300 from Witec, Germany) with a 785 nm excitation laser and a 50x magnification objective. Depending on the sample analyzed, the laser power varied from 2 to 15 watts, the integration time from 1.0 to 2.0 s, and the accumulations from 20 to 30 cycles. All measurements were performed in the spectral range 300 - 3500 cm^{-1}. The Raman spectra were plotted using OriginPro 2024b software (41). Raman spectroscopy analysis was conducted by comparing the samples' Raman spectra with the Raman spectra of polymers of reference obtained from the literature. Thus, the march in the positions and intensities of the bands between the sample spectra and the reference spectra enabled the identification of the polymer type with high confidence. From this analysis, the identified Raman spectra corresponded to polypropylene (PP), polyethylene (PE), polyvinyl chloride (PVC), polyethylene terephthalate (PET), polystyrene (PS), polyamide (PA), rubber, and acrylic.

2.4 Statistical Data Analysis

The data analysis aimed to test whether there was a difference in the abundance, mass, and geometric dimensions of plastic debris depending on the land use in the study area. To achieve this, the distributions of the groups were compared using the Kruskal-Wallis test, which was suitable for data that did not follow a normal distribution. Dunn's test was then applied to perform multiple comparisons between group medians. Results were considered statistically significant if the P-value was less than 0.05. Point distribution maps of the abundance (pieces ha^{-1}) and mass (kg ha^{-1}) of plastic debris per sampling site were generated using QGIS software (39).

In addition, a multiple factor analysis (MFA) was performed (42,43), which explores the relationship between the topography variables (slope and LS factor) and the NDVI index with the abundance and size variables of plastic debris collected on the soil surface. Three databases corresponding to four slope bands, seven LS factor bands, and seven NDVI index bands were constructed to perform the MFA (Tables S1, S2, and S3).

In each table band, the average of two groups was recorded: the first called 'abundance', which includes the quantity and mass of plastic debris; and the second called 'dimensions', made up of the area, diameter, and perimeter of the plastic debris. Statistical analysis and MFA in software R (44) using the MVar.pt library (43).

3 RESULTS

3.1 Abundance and point distribution of plastic debris in the study area

The spatial distribution of plastic debris abundance (Figure 3a) and mass (Figure 3b) in the study area was analyzed based on land use. Out of 91 georeferenced sampling points on Muquém Farm, plastic debris was found at 56.52% of the points, with 44.56% in agricultural areas, 6.52% in forested areas, and 5.44% in grasslands. Conversely, no plastic debris was detected at 43.48% of the points, distributed as follows: 22.83% in forested areas, 15.22% in grasslands, and 5.43% in agricultural land. These results highlight the predominance of plastic debris in agricultural zones.

The abundance of plastic debris, estimated per soil area, ranged from 0.509 $x10^3$ pieces ha^{-1} to 104 $x10^3$ pieces ha^{-1}. In the distribution map (Figure 3a), the litter abundance was described according to the model proposed by Liu et al. (45) and Weber et al. (46). Very high represents abundance values greater than 80 $x10^3$ pieces ha^{-1}, high represents values between 25 $x10^3$ and 80 x103 pieces ha^{-1}, medium represents values between 15 $x10^3$ and 25 $x10^3$ pieces ha^{-1}, low represents values between 3 $x10^3$ and 15 $x10^3$ pieces ha^{-1} and very low represents values less than 3 $x10^3$ pieces ha^{-1}.

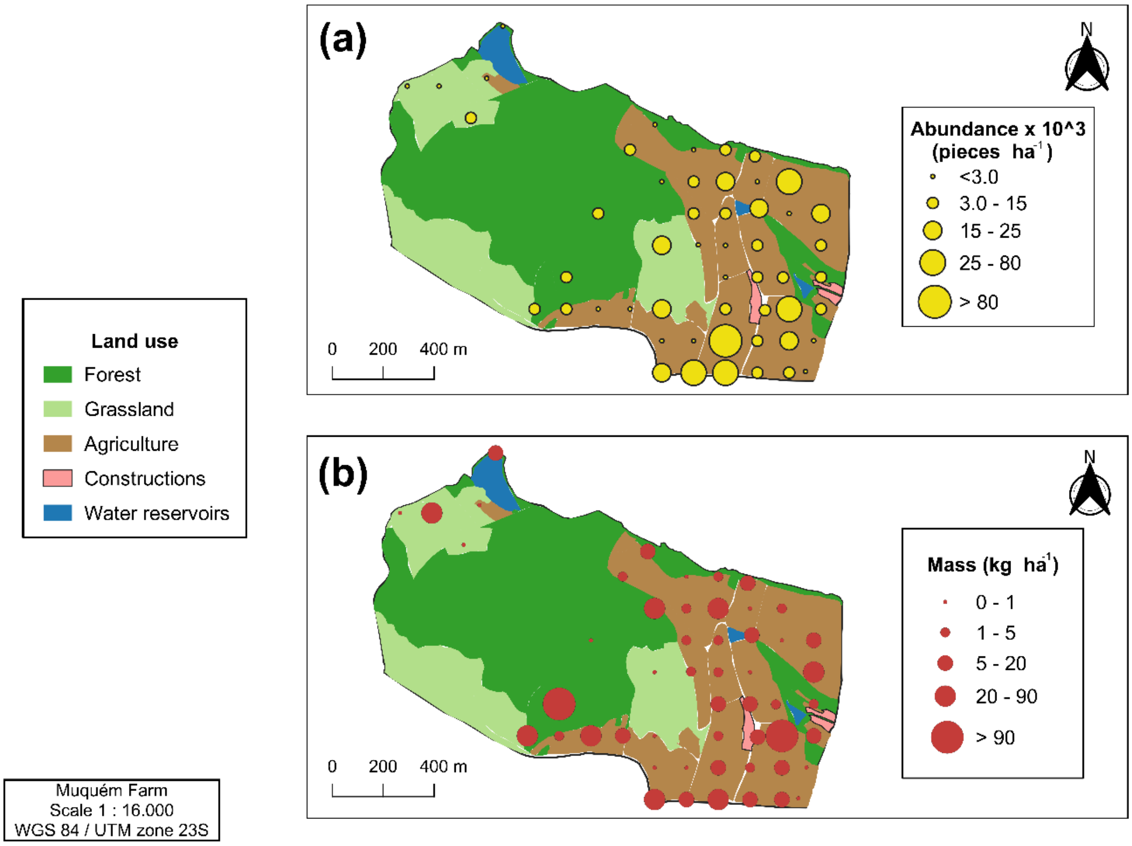

Figure 3. Map of the studio area showing the spatial distribution of the abundance (a) and mass (b) of plastic debris associated with land use.

The map of plastic debris mass distribution by soil area followed the same logic as above. Where the category very high represents mass values greater than 90 kg ha^{-1}, high represents values between 20 and 90 kg ha^{-1}, medium represents values between 5 and 20 kg ha^{-1}, low represents values between 1 and 5 kg ha^{-1} and very low represents values less than 1 kg ha^{-1}.

The cumulative abundance of plastic debris was dependent on the sites sampled (Figure 4a). The MaP and MeP plastic debris size classes were the most representative of the three land uses studied. When analyzing the total plastic debris by size, it was observed that the agricultural area had the highest average percentage of MaP, while the grassland and forest areas had the highest percentage of MeP. On the other hand, CMP was found in smaller quantities in all sampled areas compared to debris of other sizes (Figure 4a).

The mean abundance of plastic debris (Figure 4b) was 4.25 x 10^3 pieces ha^{-1}, 4.89 x 10^3 pieces ha^{-1}, and 12.80 x 10^3 pieces ha^{-1} as observed for the forest, grassland, and agriculture areas respectively.

The spatial distribution of the mass of plastic debris on the soil surface at each sampled site varied from 0.039 kg ha^{-1} to 405 kg ha^{-1} (Figure 3b). The total average as a function of land use was 83.60 kg ha^{-1} for forest, 10.18 kg ha^{-1} for grassland, and 12.05 kg ha^{-1} for agriculture (Figure 4c). There were no significant differences between the mean abundance and mass of plastic detritus for the three investigated land uses (forest, grassland, and agricultural land).

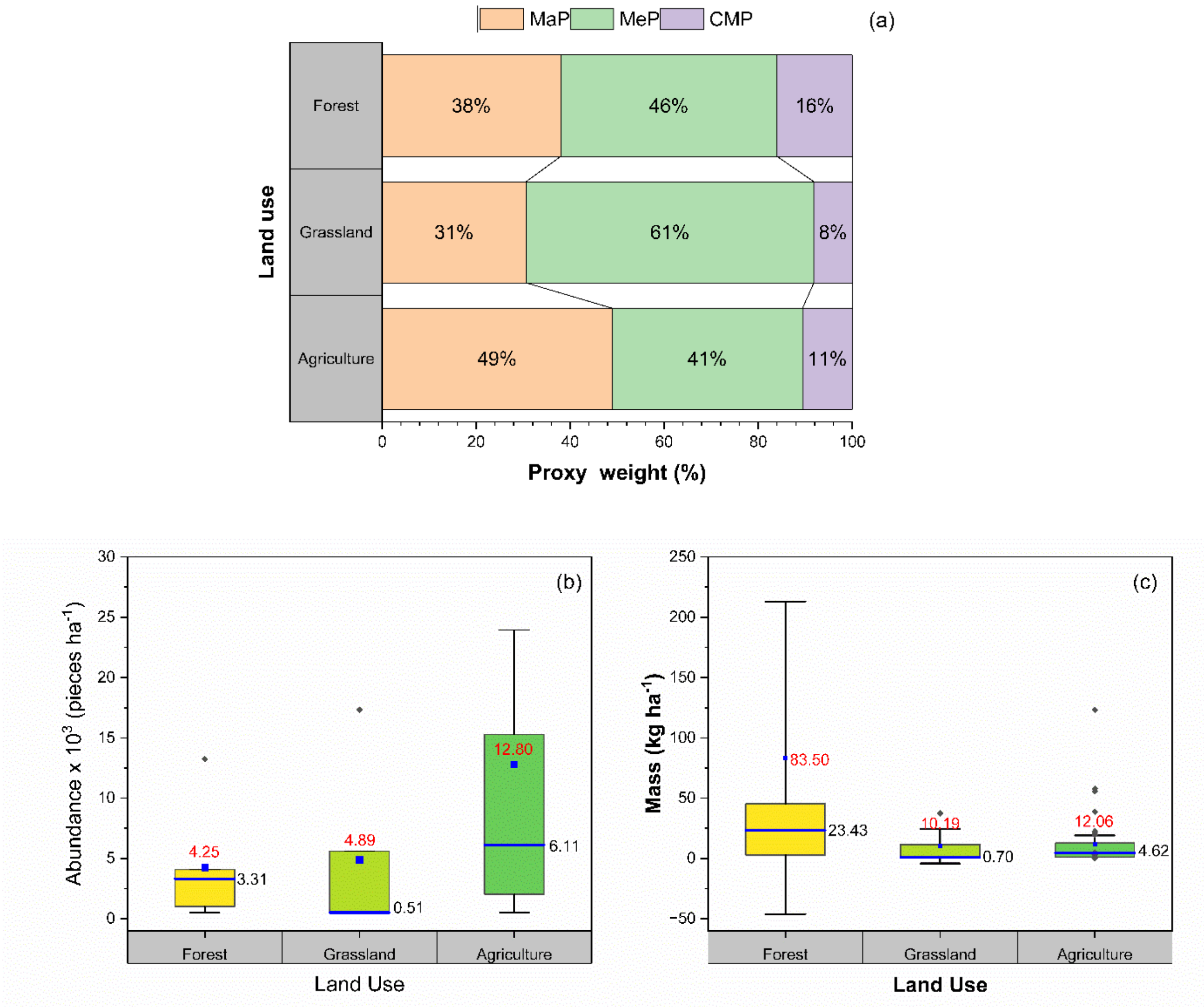

Figure 4. Cumulative percentage abundance of macroplastics (MaP), mesoplastics (MeP), and coarse microplastics (CMP) (a), Boxplot of abundance (b), and mass (c) of plastic debris collected about land use. The diagrams show extreme values (whiskers), the first and third quartiles (the bottom and top of the boxes, respectively), and the median value (the line inside the boxes with the black number next to the line). The average of the data is represented by the numbers in red.

3.2 Dimensions of plastic debris in the agricultural sub-basin

A total of 1123 pieces of plastic debris were collected from 52 points, representing a total abundance of 572.08 x10^3 pieces ha^{-1}. Table 1 shows the abundance of plastic debris classified by land use and debris size. The results show that 4.45% of the plastic debris was found in the forest area, 4.36% in the grassland area, and 91.2% in the agricultural area.

This indicates that the agricultural area has the highest concentration of debris on the soil surface. Specifically, in the agriculture area, MaP represented 44.6%, MeP 37.0%, and CMP 9.6% of the debris. In the grassland area MaP, MeP, and CMP made up 1.3%, 2.7%, and 0.4% of the debris, respectively. In the forest area, these values were 1.7% for MaP, 2.0% for MeP, and 0.7% for CMP (Table 1).

Table 1. Land use, size class of plastic debris (S), total abundance (n), and geometric dimensions of plastic debris. (Median and interquartile range (IQR)).

Land use	S	n x 10^3 (pieces ha^{-1})	FQR (%)	Area (cm^2)		Length (cm)		Perimeter (cm)	
				median	iqr	median	iqr	median	iqr
Forest	MaP	9.68	1,69	42.991	354.890	15.676	30.594	67.252	91.708
	MeP	11.72	2.05	0.251	0.531	0.778	0.557	2.215	2.191
	CMP	4.08	0.71	0.084	0.025	0.441	0.082	1.316	0.357
Grassland	MaP	7.64	1.34	15.570	42.286	7.360	5.916	28.580	26.095
	MeP	15.28	2.67	0.210	0.160	0.735*	0.528	2.520	1.178
	CMP	2,04	0.36	0.043	0.067	0.328	0.234	1.115	0.953
Agriculture	MaP	255.22	44.6	16.170	40.790	8.280	9.655	32.610	38.786
	MeP	211.41	36.5	0.210	0.325	1.090*	0.797	3.160	2.695
	CMP	55.02	9.62	0.030	0.030	0.340	0.150	0.865	0.392

Note: Macroplastic (MaP), mesoplastic (MeP), coarse microplastic (CMP). n: Total number of plastic debris by land use and size class (pieces ha-1). FRQ: fraction corresponding to the size of plastic debris in a given range out of the total number (1123 samples) * Significant differences by Dum test at significance level $P < 0.05$.

The Kruskal-Wallis test showed no significant differences between the area and perimeter of plastic litter in the three land uses. However, a significant difference was observed when comparing the litter length values according to the land use sampled (Table 1). The results showed that the plastic debris with the smallest area, length, and perimeter was found in the agricultural area, with the smallest values recorded being 0.01 cm^2, 0.20 cm, and 0.42 cm, respectively. On the other hand, the plastic debris with the largest area and length was found in the forest area, with maximum values of 5076 cm^2 and 94 cm, respectively.

Figure 5 presents the extrapolated dimensions of plastic debris (area, perimeter, and length) for each land use on Muquém farm, standardized to 1 hectare. Statistical analysis revealed no significant differences in the dimensions of plastic debris among the three land uses. Plastic debris collected from agricultural land exhibited the largest interquartile ranges for length (225.31 to 966.94 m ha⁻¹) and perimeter (734.38 to 4242.44 m ha⁻¹). In contrast, forest areas showed the widest interquartile range for the area of plastic debris, varying between 5.89 and 108.97 m² ha⁻¹. Agricultural land had the highest mean values for all dimensions, with an average area of 27.15 m² ha⁻¹, length of 739.92 m ha⁻¹, and perimeter of 2929.43 m ha⁻¹.

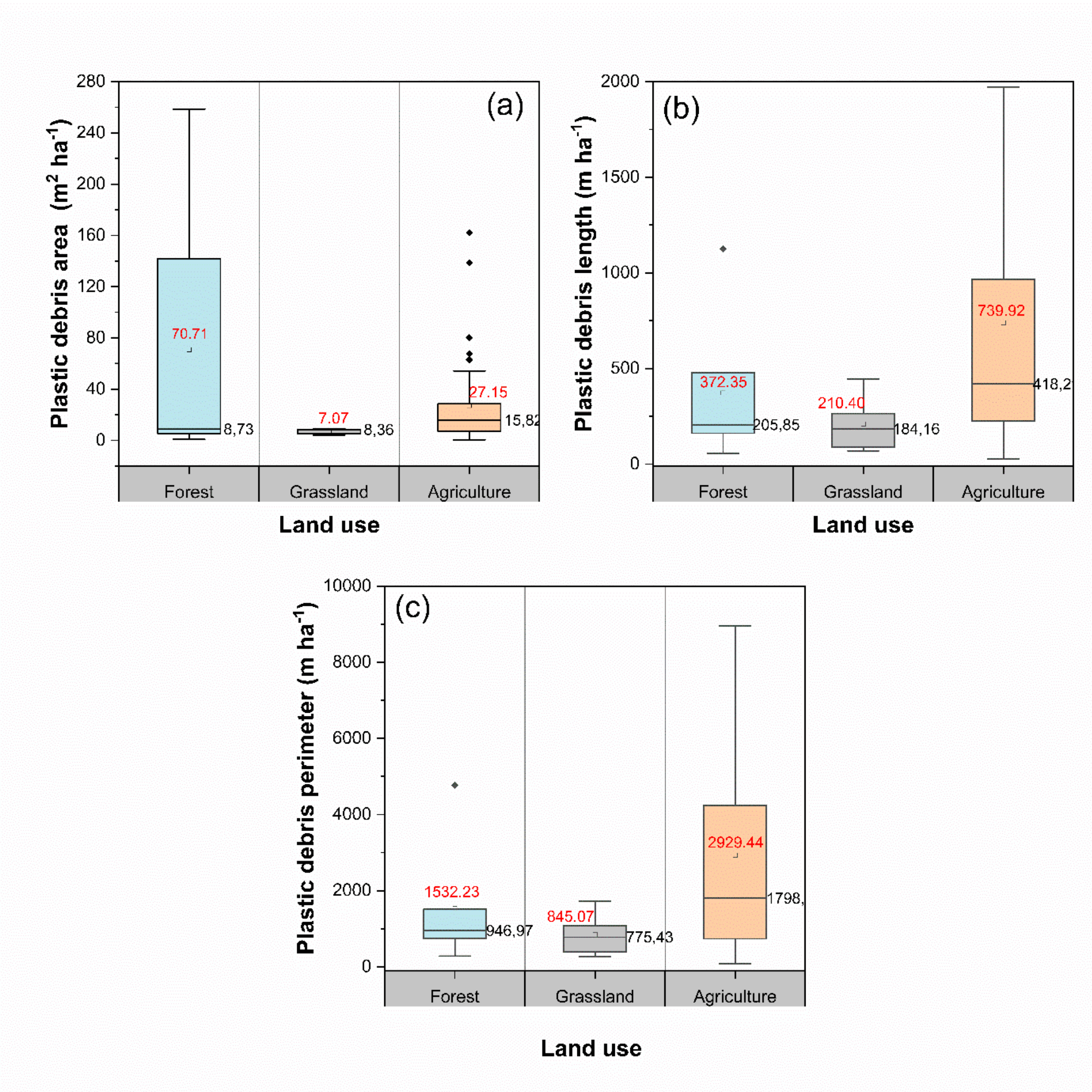

Figure 5. Box plots of the distribution of area (a), perimeter (b), and length (c) by land use on the Muquém farm. The plots show the extreme values (whiskers), the first and third quartiles (the bottom and top of the boxes, respectively), and the median (the line inside the boxes with the black number next to the line). The average of the data is represented by the numbers in red.

3.3 Relationship between the topographic conditions and the vegetation index (NDVI) of the study area and the abundance and size of the plastic debris.

The quantity, mass, area, diameter, and perimeter of plastic debris varied with land topography, specifically slope class, LS factor, and NDVI vegetation index. In forest areas, plastic debris was only found in undulating relief, despite covering all relief types. Grassland areas, dominated by undulating relief, showed the highest plastic debris accumulation. Agricultural areas contained plastic debris across all relief types except strongly and mountainous, which were scarce (Figure 2b).

Overall, 2% of debris was found in strongly terrain, 65% in undulating, 25% in gently undulating, and 8% in flat terrain. The LS factor ranged from 1.711–4.967 in forests, 2.123–3.160 in grasslands, and 0.126–2.748 in farmlands. Agricultural areas showed the highest debris presence and the lowest LS factor, particularly in the 0.126–2.201 range.

NDVI values ranged from 0.071–0.354 in forests, 0.119–0.229 in grasslands, and 0.060–0.380 in farmlands. Notably, 61% of agricultural sampling points fell within the NDVI range of 0.060–0.152 (Figure 2d).

The exploration analysis of these variables was performed using multiple factor analysis (MFA) (Figure 6), which includes three databases, with slope, LS factor, and NDVI index being the individuals for each database (Tables S1, S2, and S3, respectively). Five variables are grouped into two groups, the abundance group contains the variables quantity and mass, and the dimensions group contains the variables area, diameter, and perimeter of plastic debris.

For the MFA of the slope variable and groups (Figure 6a), two components were derived that are responsible for explaining 89.91% of the total variation. The first component shows a variability of 78.53%, with the variables in the dimension group consisting of area, diameter, and perimeter having a coefficient of 0.956, 0.921, and 0.930, respectively. The second component showed a variability of 11.38%. This variability was mainly explained by the plastic debris mass variable, with a coefficient of -0.509.

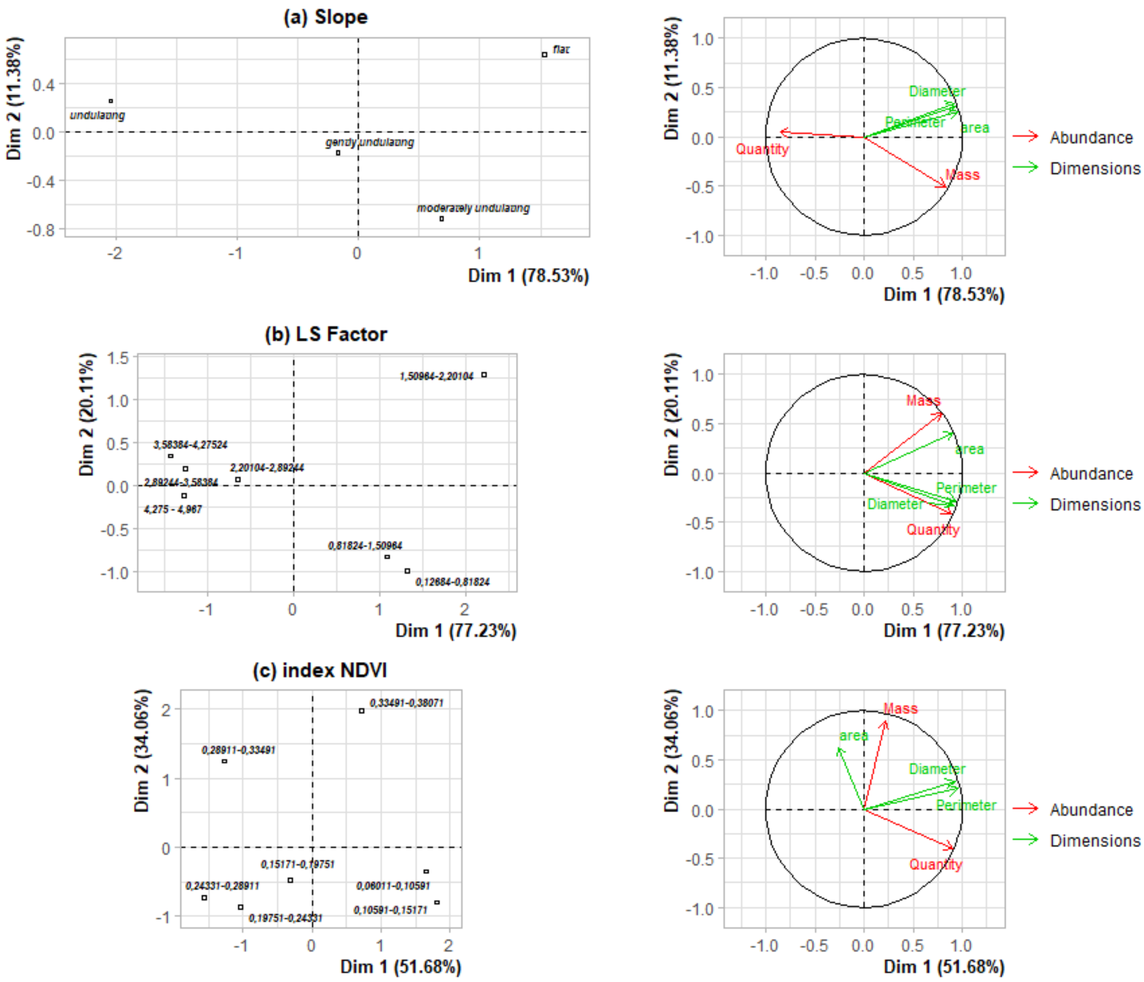

Figure 6. Multiple factor analysis (MFA) of the variables (a) slope, (b) LS factor, and (c) NDVI index as a function of plastic debris abundance and size groups.

For the MFA of the LS factor variable and the groups (Figure 6b), two components were derived that are responsible for explaining 97.34% of the total variation. The first component shows a variability of 77.23%, with the variables in the dimension group consisting of area, diameter, and perimeter having a coefficient of 0.907, 0.941, and 0.921, respectively. The second component showed a variability of 20.11% explained by the variables in the abundance group, made up of the quantity and mass of plastic debris, with a coefficient of -0.411 and 0.608, respectively.

For the MFA of the NDVI index variable and the groups (Figure 6c), two components were derived that are responsible for explaining 85.74% of the total variation. The first component shows a variability of 51.68%, where the variables perimeter, diameter, and quantity have a coefficient of 0.955, 0.923, and 0.907, respectively. The second component showed a variability of 34.06% explained by the variables mass and area of plastic debris, with a coefficient of 0.902 and 0.625, respectively.

3.4 Spectral composition of the polymers

Raman spectrometry was used to fingerprint each material and identify the type of polymer in the debris analyzed. From the total of 1,123 pieces of plastic debris collected at the 52 sampling points, 191 groups with very similar characteristics were formed. Representative samples were selected from each group based on the characteristics of the debris, such as size, shape, and color. In addition, the history of use in the sampled areas was taken into account, such as irrigation with water containing plastic, common litter such as plastic bags, debris from roads or nearby communities, and others.

Spectra were collected from different regions of the surface of each sample analyzed. The Raman spectra obtained showed baseline deviation and varying signal intensities, so corrections were made, including noise removal, baseline correction, and normalization.

The results indicated that the primary polymer types identified among the samples analyzed were PP, PE, PVC, PET, and PA. As shown in Figure 7a, PP and PE were the most prevalent, accounting for 40.94% and 30.2% of the total polymers, respectively. PVC, PET, and PA constituted 11.4%, 10.1%, and 4.7%, respectively, while other polymers, including rubber and acrylic, represented 2.68% of the total. The Raman spectra (Figure 7c) of the most representative polymers found in the samples analyzed were PP, PE, PVC, and PET. In all cases, the spectra showed characteristic peaks for each type of polymer.

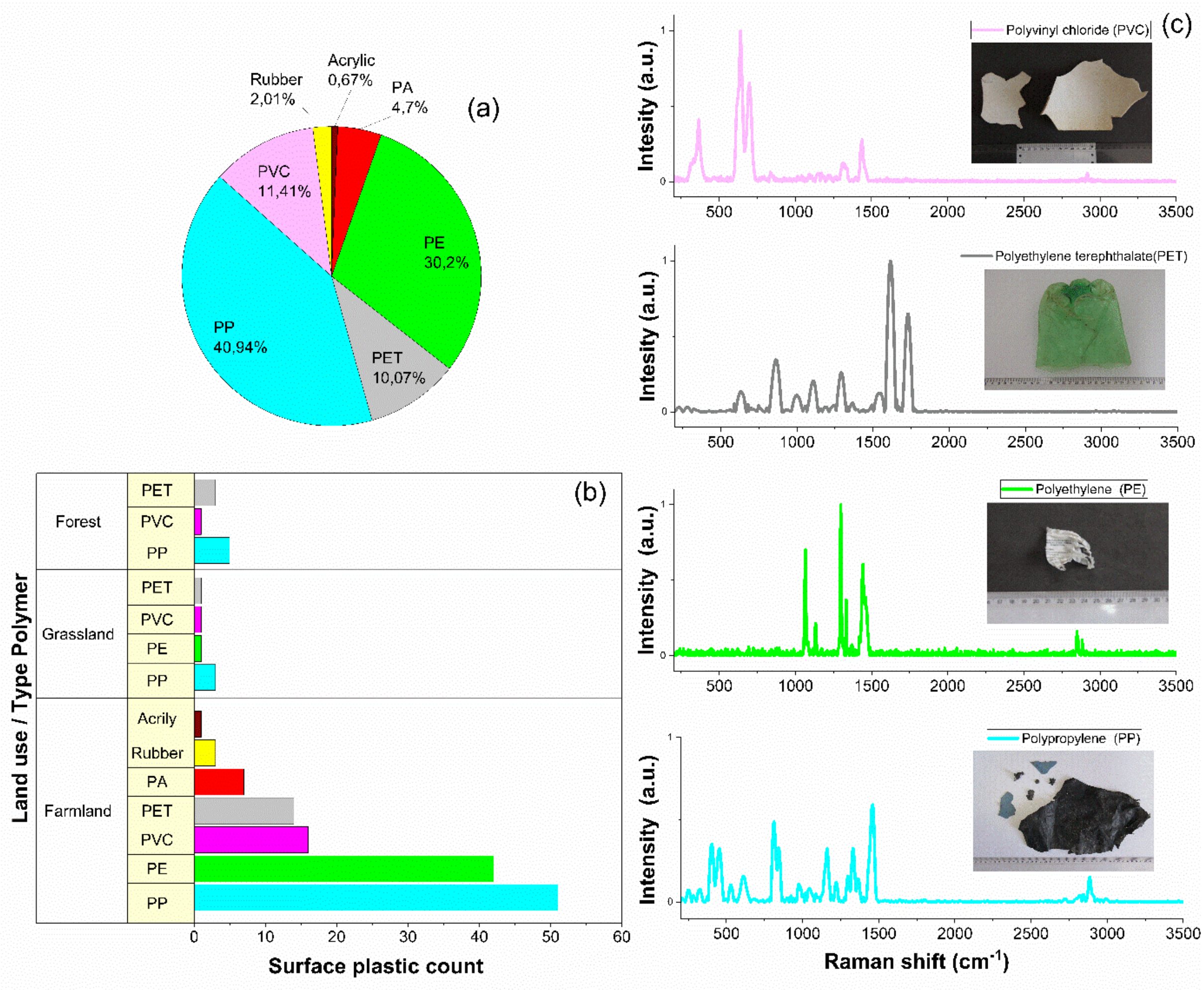

Figure 7. Polymer type and percentage distribution (a), number of plastic debris by polymer type and by land use (n=191) (b), spectrum of polymers by Raman spectroscopy (c), collected on the soil surface of the study area. PE, polyethylene; PP, polypropylene; PVC, polyvinyl chloride; PET, polyethylene terephthalate; PS, polystyrene; PA, polyamide.

The Raman spectra corresponding to PP showed a characteristic peak around 841 cm^{-1}, representing the vibrations of its helical molecules. The peak at 1330 cm^{-1} is associated with the vibration of PP macromolecules in the helical conformation, corresponding to a superposition of the deformation mode of the C-H bond and the torsion mode of the CH_2 groups. The peak at 1435 cm^{-1} can be attributed to the asymmetric bending mode of the -CH_3 group, while the peaks at 1252 and 1170 cm^{-1} are due to the stretching of the C-C structure.

In the Raman spectra of the samples identified as PE, characteristic peaks were observed in the 1000 - 1500 cm^{-1} and 2800 - 2900 cm^{-1} regions. The peaks with the highest intensity were located at 1066 cm^{-1}, 1298 cm^{-1}, and 1439 cm^{-1}. These peaks are attributed to C-C stretching, CH_2 torsion, and CH_2 symmetric deformation, respectively. In addition, a peak at 1132 cm^{-1} corresponding to C-C stretching was observed.

The PVC samples showed spectra with high-intensity Raman peaks at 640 and 698 cm^{-1} attributed to stretching vibrations of C-Cl bonds. The peak at 1435 cm^{-1} corresponds to the angular deformation of the CH_2 and CH_3 groups. Finally, the PET spectrum showed two dominant peaks located at 1615 cm^{-1} and 1729 cm^{-1}. These correspond to the C-C stretching vibrations of the aromatic ring and the stretching vibrations of the carbonyl groups.

The analysis of polymer identification by Raman spectroscopy revealed that polypropylene (PP) is the main source of plastic pollution in the sampled areas, regardless of the type of land use (Figure 7b). In addition, it was observed that agricultural soils accumulate a greater variety of polymer types compared to the other areas.

4 DISCUSSION

4.1 Land Use Related Plastic Debris

This study revealed the presence of plastic debris of varying sizes and chemical compositions on the soil surface of a sub-basin in southeastern Brazil. Most of the debris was concentrated in agricultural areas, while forest and grassland regions showed lower contamination levels. This pattern highlights the strong influence of anthropogenic activities on the accumulation of plastic waste, particularly agriculture activities. A similar situation was described by Parolini et al. (47). Furthermore, it has been reported that low-density polyethylene (LDPE) and polypropylene (PP) are commonly used in agricultural materials, such as greenhouse covers, nets, and films (24). Consistently, our study confirmed that PP and polyethylene (PE) prevailed at the study site, comprising 40.9% and 30.2% of the total debris analyzed, respectively (Figure 6a) as confirmed by Raman spectroscopy.

As previously mentioned, the Raman spectra of the analyzed plastic debris matched known polymer spectra in the reference library. These results are consistent with Raman analyses of plastic debris found in soils across different regions (48–50). However, the spectra of some samples exhibited bands that shifted toward lower wavenumbers compared to the reference spectra, as observed in the PP spectrum (Figure 7c). This result suggests that weathered plastics undergo structural changes related to variations in molecular bond lengths, as indicated by Phan et al. (48).

Wang et al. (16) reported an abundance of $266.2 \times 10^4 \pm 507.9$ pieces ha^{-1} of PE plastic waste used as mulch film in agricultural soils in northwest China. In southeastern Germany, 56% of the plastic debris found in agricultural soils was identified as PE polymers, with an average abundance of 206 pieces ha^{-1}. In agricultural soils in central Germany, the predominant polymers detected were PS, PP, and PE, with a total abundance of 637 pieces ha^{-1} (46). These findings align with Kawecki and Nowack's (7) study, which highlighted similar trends in macroplastic and microplastic emissions in agricultural regions of China.

At our experimental site, the average abundance of plastic debris was 12.79 $x10^3$ pieces ha^{-1} in the agricultural area, 4.89×10^3 pieces ha^{-1} in the grassland area, and 4.24×10^3 pieces ha^{-1} in the forest area (Figure 4b). These results show variations in the abundance of plastic debris compared to other studies. Such differences can be attributed to several factors, one of which is the management of plastic materials in soils under agricultural use (51).

The results showed that the highest mass concentration of plastic debris was recorded in the forest area, averaging 83.50 kg ha^{-1} (Figure 4). This result was expected since no anthropogenic activities in this region significantly affected the size of the debris. In contrast, agricultural land exhibited a higher abundance of MaP, MeP, and CMP particles (Table 1), consistent with Meng et al. (17), who reported that intensive tillage practices accelerate plastic fragmentation, increasing microplastic (MP) concentrations compared to other land uses (52).

The mass of plastic debris in agricultural soil (12.06 $kg \cdot ha^{-1}$) was lower than values reported in previous studies. For instance, Wang et al. (16) documented an average of 47.2 $kg \cdot ha^{-1}$ for MaP-sized debris, while Meng et al. (17) reported 53.7 $kg \cdot ha^{-1}$ in agricultural soils of Northwest China. Berenstein et al. (51) found a range of 25 to 31 $kg \cdot ha^{-1}$ in Argentinian horticultural soils, and Lero et al. (31) recorded an average of 60 $kg \cdot ha^{-1}$ of MaP in the topsoil of forest islands formed by the Dunajec River in southern Poland. Despite the lower plastic debris mass in agricultural areas, continuous monitoring and regulatory measures are essential to mitigate plastic pollution in these environments.

We observed that in forest areas, the type and density influence the accumulation of plastic debris. Specifically, the highest NDVI values correspond to points with the highest mass concentration of plastic debris (Figures 2d and 4b). The type and density of vegetation play a key role in retaining plastic debris within these agroecosystems, preventing its mechanical fragmentation and transport. Vegetation acts as a physical barrier, limiting the direct exposure of plastic debris to environmental degradation factors such as UV radiation, wind, water, and erosion (31,52).

In summary, it is well known that a significant part of the plastic debris in agricultural soils remains buried as mesoplastics for long periods, and another part will fragment into micro- and nanoplastics (9,47), further aggravating the contamination of the soil and terrestrial ecosystem. An interesting macroplastic fragmentation process is explained by Berenstein et al.

(51). These authors explain that the natural cycles of hydration and dehydration of agricultural soils play a critical role in the decomposition of macroplastics into mesoplastics, microplastics and even nanoplastics. These natural processes act as plastic shredders in the environment, contributing to the formation of particles smaller than 2 mm. (4,7). Therefore, detecting and identifying plastic debris in agricultural soils is essential to mitigate their growing presence and environmental impact.

4.2 The relationship of plastic debris to landforms and vegetation

Our findings revealed a correlation between the quantity and mass of plastic debris and the topography of the land, particularly in gently to moderately rolling terrains. These areas, which accounted for 76.6% of the total study site, are predominantly associated with agricultural activities (Figure 6a).

Several studies have explored the relationship between the migration of plastic debris, ground conditions, vegetation, and human activities. Cao et al. (51) highlight that most plastic debris tends to accumulate at depths of 0–10 cm, where agricultural activities and soil disturbance are more prevalent. In sloping terrains, plastic debris often concentrates in depressions or less steep areas. Similarly, Wang et al. (52) identify the application of organic fertilizers and sewage sludge on agricultural land as significant sources of plastic debris. Furthermore, areas with moderate slopes experience slower water runoff, facilitating the accumulation of plastic waste (53). High concentrations of plastic debris are also strongly linked to regions with intense anthropogenic activities, particularly agricultural zones (54).

The LS factor ranges between 0.126 - 0.818 and 0.818 - 1.509, located in agricultural areas, were found to be associated with a higher concentration of plastic debris (Figure 6b). On gentle slopes, plastic accumulation may be greater due to the reduction in water flow velocity, which facilitates plastic deposition on the bottom according to Cesarini and Scalici (30). These observations are consistent with the results of Wang et al. by (55), who indicated that the shorter length of slopes and the low gradient contribute to an increase in the abundance of plastic debris.

Concerning the NDVI index, the lowest bands, between 0.060-0.105 and 0.105-0.151, correspond to areas with low vegetation cover (agricultural use), where a greater amount of low-mass plastic debris was found (Figure 6c). However, Cesarini et al.(19) describe the opposite scenario on sloping land with greater vegetation cover, plastic debris retention may be more efficient, while areas without vegetation and with a slope favor the dispersal of this debris. However, Figure 6c shows that the mass of plastic debris was greater in the higher NDVI bands, between 0.335 and 0.381, which were associated with forest areas, albeit with less debris (Figures 3a and 3b). In these areas, plastic fragmentation and degradation were less intense due to less exposure to physical factors and less human disturbance, which explains the presence of debris with greater mass in regions with higher NDVI index (56).

As mentioned previously, vegetation cover can act as a natural barrier that traps plastic debris, limiting its migration by reducing surface runoff (9) and promoting localized accumulation. However, the effectiveness of this barrier depends on the density and type of vegetation present (51). For example, agricultural areas with homogeneous crops and vacant lots exhibited greater dispersion and abundance of plastics compared to grassland and forest areas, which are characterized by denser and more diverse vegetation, and consequently were found to have higher plastic concentrations, as observed in Figures 3b and 4c.

The size of the plastic debris is related to the flat terrain (Figure 6a), values lower than 2.201 for the LS factor (Figure 6b), and the higher percentage of CMP-type plastic debris is more related to forest areas, which can be explained by the influence of tree foliage, which can trap airborne microplastics, as reported by Huang et al. (57) and Falakdin et al. (60).

Under these premises, it is assumed that the abundance, size variation, accumulation, and directional redistribution of plastic debris in the soil has multiple possibilities of occurrence, such as the characteristics of the terrain, slope, land use, and variables such as wind, surface runoff, wind erosion [53,61], the density and type of vegetation (30), in addition to human activities in agriculture (60). Therefore, a deeper understanding of the mechanisms and processes involved in the distribution and accumulation of plastic debris in soils is essential for advancing knowledge in this field.

4.3 Limitations, future research, and recommendations

The spatial distribution map of plastic debris (Figure 3) identifies key accumulation zones, providing a valuable tool for guiding the placement of waste collection points. This is particularly relevant for agricultural areas with flat or gently undulating terrain and sparse vegetation, as highlighted by the multiple-factor analysis (Figure 6). Implementing targeted collection strategies in these high-concentration areas could significantly reduce plastic waste accumulation and reduce its environmental impact.

A limitation of this study was the smaller number of samples from forest areas and grassland compared to agricultural areas. Dense vegetation in forest areas hindered access, while several sampling points in grassland areas contained no plastic debris of the sizes analyzed. Thus, further research in these areas is necessary. Additionally, there is a lack of studies analyzing other factors influencing plastic accumulation, such as wind patterns, surface runoff dynamics, and temporal variations in plastic debris migration and degradation, as highlighted by Billings et al. (63).

5 CONCLUSIONS

We present the first study into the distribution of plastic debris on a medium-sized farm with different types of use, as commonly found in Brazil. The abundance and mass of plastic debris were spatially heterogeneous, ranging from 0.509 x103 pieces ha^{-1} to 104 $x10^3$ pieces ha^{-1} and from 0.039 kg ha^{-1} to 405 kg ha^{-1}, respectively.

In conclusion, these findings highlight the influence of land topography and vegetation density on the accumulation of plastic debris. Areas with gentle slopes and sparse vegetation facilitate plastic dispersion, while denser vegetation in forested areas acts as a natural barrier, retaining debris with a higher mass concentration. Our research has demonstrated that agricultural practices contribute to the fragmentation of macroplastics into smaller particles, such as mesoplastics and microplastics, which can worsen soil contamination.

The types of polymers identified in the study area were polypropylene (PP), polyethylene (PE), and polyvinyl chloride (PVC). However, our results indicate that contamination was largely attributed to the widespread use of PE and PP in agricultural operations. In general, this plastic debris primarily originates from materials used for plant labeling, agrochemical storage, irrigation systems, and various types of bags. Additionally, degraded plastic debris was found predominantly in agricultural areas, which exhibited the highest abundance and mass of plastic waste. In summary, our findings emphasize that agricultural practices are the main drivers of plastic debris accumulation. Therefore, effective management strategies to mitigate environmental impacts are essential.

ASSOCIATED CONTENT

Supporting Information.

Tables S1, S2, and S3 show the slope data, LS factor, NDVI index of the study site, and the quantity and size of plastic debris used for multiple factor analysis (MFA) (PDF).

ACKNOWLEDGMENT

This work was supported by the Federal University of Lavras (UFLA), the SurColombiana University (USCO), the National Council for Scientific and Technological Development (CNPq) (processes: 307950/2021-2 and 307059/2022-7), the Foundation for Research Support of the State of Minas Gerais (FAPEMIG) (processes: APQ 00802-18), and the Coordination for the Improvement of Personnel (CAPES) (code 001). The authors would to thank the Laboratory of Electron Microscopy and Analysis of the Ultrastructural Federal University of Lavras.

ABBREVIATIONS

MaP; Macroplastics, MeP; mesoplastics, CMP; coarse microplastics, MP; microplastics, PE; polyethylene, PP; polypropylene, PS; polystyrene, PVC; polyvinyl chloride, GM; Gleysols, LVA; Oxisols, NX; Nitisols, CX; Cambisols, SOM; soil organic matter.

REFERENCES

1. Vox, G.; Loisi, R.V.; Blanco, I.; Mugnozza, G.S.; Schettini, E. Mapping of Agriculture Plastic Waste. *Agric. Agric. Sci. Procedia* **2016**, *8*, 583–591, doi:10.1016/j.aaspro.2016.02.080.

2. Ng, L.E.; Yu, S.; Dungan, A.M.; Colwell, J.M.; Ede, S.; Huerta, E.; Meng, K.; Geissen, V.; Louise, L.; Chen, D. Microplastic Pollution Alters Forest Soil Microbiome. *J. Hazard. Mater.* **2021**, *409*, 124606, doi:10.1016/j.jhazmat.2020.124606.

3. Borg, R.; Camilleri-Fenech, M. Investigating the Agricultural Use and Disposal of Plastics in Malta. *Sustainability* **2024**, *16*, 954, doi:10.3390/su16030954.

4. Piehl, S.; Leibner, A.; Löder, M.G.J.; Dris, R.; Bogner, C.; Laforsch, C. Identification and Quantification of Macro- and Microplastics on an Agricultural Farmland. *Sci. Rep.* **2018**, *8*, 1–9, doi:10.1038/s41598-018-36172-y.

5. Roy, P.; Mohanty, A.K.; Misra, M. Microplastics in Ecosystems: Their Implications and Mitigation Pathways. *Environ. Sci. Adv.* **2022**, *1*, 9–29, doi:10.1039/d1va00012h.

6. Amjad, M.; Huang, Q.; Khan, S.; Wang, Q.; Huang, J.; Fahad, X.; Sajjad, M.; Liu, Y.; Mašek, O.; Li, X.; et al. Abundance, Spatial Distribution, and Characteristics of Microplastics in Agricultural Soils and Their Relationship with Contributing Factors. *Rev. Gestão Ambient.* **2023**, *328*, doi:https://doi.org/10.1016/j.jenvman.2022.117006.

7. Kawecki, D.; Nowack, B. A Proxy-Based Approach to Predict Spatially Resolved Emissions of Macro- and Microplastic to the Environment. *Sci. Total Environ.* **2020**, *748*, 141137, doi:10.1016/j.scitotenv.2020.141137.

8. Gao, H.; Liu, Q.; Yan, C.; Mancl, K.; Gong, D.; He, J.; Mei, X. Macro-and/or Microplastics as an Emerging Threat Effect Crop Growth and Soil Health. *Resour. Conserv. Recycl.* **2022**, *186*, 106549, doi:10.1016/j.resconrec.2022.106549.

9. Yan, P.; Zhang, S.; Wang, J.; Wang, W.; Xu, B.; Hao, X.; Aurangzeib, M. Field Management Changes the Distribution of Mesoplastic and Macroplastic in Mollisols of Northeast China.

Chemosphere **2022**, *308*, doi:10.1016/j.chemosphere.2022.136282.

10. Li, S.; Ding, F.; Flury, M.; Wang, Z.; Xu, L.; Li, S.; Jones, D.L.; Wang, J. Macro- and Microplastic Accumulation in Soil after 32 Years of Plastic Film Mulching. *Environ. Pollut.* **2022**, *300*, doi:10.1016/j.envpol.2022.118945.

11. Gui, J.; Sun, Y.; Wang, J.; Chen, X.; Zhang, S.; Wu, D. Microplastics in Composting of Rural Domestic Waste : Abundance, Characteristics, and Release from the Surface of Macroplastics *. *Environ. Pollut.* **2021**, *274*, 116553, doi:https://doi.org/10.1016/j.envpol.2021.116553.

12. Yan, P.; Zhang, S.; Wang, J.; Xiao, Z.; Yan, S.; Wang, W.; Aurangzeib, M. Heterogeneity of Plastic Residue Was Determined by Both Mulch Film and External Plastic Pollutants in the Farmland of Northeast China. *Sci. Total Environ.* **2022**, *853*, doi:http://dx.doi.org/10.1016/j.scitotenv.2022.158681.

13. Cera, A.; Pierdomenico, M.; Sodo, A.; Scalici, M. Spatial Patterns of Mesoplastics and Coarse Microplastics in Fl Oodplain Soils as Resulting from Land Use and Fl Uvial Processes. *Environ. Pollut. J.* **2020**, *267*, 115390, doi:https://doi.org/10.1016/j.envpol.2020.115390.

14. Schwarz, A.E.; Lensen, S.M.C.; Langeveld, E.; Parker, L.A.; Urbanus, J.H. Plastics in the Global Environment Assessed through Material Fl Ow Analysis, Degradation and Environmental Transportation. *Sci. Total Environ.* **2023**, *875*, 162644, doi:10.1016/j.scitotenv.2023.162644.

15. Paes, E. da S.; Gloaguen, T.V.; Silva, H. dos A. da C.; Duarte, T.S.; de Almeida, M. da C.; Costa, O.D.A.V.; Bomfim, M.R.; Santos, J.A.G. Widespread Microplastic Pollution in Mangrove Soils of Todos Os Santos Bay, Northern Brazil. *Environ. Res.* **2022**, *210*, doi:10.1016/j.envres.2022.112952.

16. Wang, S.; Fan, T.; Cheng, W.; Wang, L.; Zhao, G.; Li, S.; Dang, Y.; Zhang, J. Occurrence of Macroplastic Debris in the Long-Term Plastic Fi Lm-Mulched Agricultural Soil : A Case Study of Northwest China. *Sci. Total Environ.* **2022**, *831*, 154881, doi:https://doi.org/10.1016/j.scitotenv.2022.154881.

17. Meng, F.; Fan, T.; Yang, X.; Riksen, M.; Xu, M.; Geissen, V. Effects of Plastic Mulching on the Accumulation and Distribution of Macro and Micro Plastics in Soils of Two Farming Systems in Northwest China. *PeerJ* **2020**, *8*, 1–20, doi:10.7717/peerj.10375.

18. Li, P.; Li, Q.; Hao, Z.; Yu, S.; Liu, J. Analytical Methods and Environmental Processes of Nanoplastics. *J. Environ. Sci. (China)* **2020**, *94*, 88–99, doi:10.1016/j.jes.2020.03.057.

19. Kumar, P.; Lee, J.; Brown, R.J.C.; Kim, K. Micro- and Nano-Plastic Pollution : Behavior, Microbial Ecology, and Remediation Technologies. *J. Clean. Prod.* **2021**, *291*, 1–22, doi:https://doi.org/10.1016/j.jclepro.2020.125240.

20. Cesarini, G.; Cera, A.; Battisti, C.; Taurozzi, D.; Scalici, M. Is the Weight of Plastic Litter Correlated with Vegetal Wrack ? A Case Study from a Central Italian Beach. *Mar. Pollut. Bull.* **2021**, *171*, 112794, doi:10.1016/j.marpolbul.2021.112794.

21. Weber, C.J.; Opp, C. Spatial Patterns of Mesoplastics and Coarse Microplastics in Floodplain Soils as Resulting from Land Use and Fluvial Processes. *Environ. Pollut.* **2020**, *267*, 115390, doi:10.1016/j.envpol.2020.115390.

22. Shi, X.; Chen, Z.; Wei, W.; Chen, J.; Ni, B.-J. Toxicity of Micro/Nanoplastics in the Environment: Roles of Plastisphere and Eco-Corona. *Soil Environ. Heal.* **2023**, *1*, 100002, doi:10.1016/j.seh.2023.100002.

23. Bonnevie, J.; Ervik, H.; Aasen, A.; Hellevik, C. Macroplastic in Soil and Peat. A Case Study from the Remote Islands of Mausund and Froan Landscape Conservation Area, Norway ; Implications for Coastal Cleanups and Biodiversity. *Sci. Total Environ.* **2021**, *787*, 0–8, doi:https://doi.org/10.1016/j.scitotenv.2021.147547.

24. Kawecki, D.; Nowack, B. Polymer-Specific Modeling of the Environmental Emissions of Seven Commodity Plastics As Macro- and Microplastics. *Environ. Sci. Technol.* **2019**, *53*, 9664–9676, doi:10.1021/acs.est.9b02900.

25. Guo, J.; Huang, X.; Xiang, L.; Wang, Y.; Li, Y.; Li, H.; Cai, Q. Source, Migration and Toxicology of Microplastics in Soil. *Environ. Int.* **2020**, *137*, 105263, doi:10.1016/j.envint.2019.105263.

26. Fan, W.; Qiu, C.; Qu, Q.; Hu, X.; Mu, L.; Gao, Z.; Tang, X. Sources and Identification of Microplastics in Soils. *Soil Environ. Heal.* **2023**, *1*, 100019, doi:https://doi.org/10.1016/j.seh.2023.100019.

27. He, D.; Luo, Y.; Lu, S.; Liu, M.; Song, Y.; Lei, L. Microplastics in Soils: Analytical Methods, Pollution Characteristics and Ecological Risks. *TrAC Trends Anal. Chem.* **2018**, *109*, 163–172, doi:10.1016/j.trac.2018.10.006.

28. Klaus, J.; Seeger, M.; Bigalke, M.; Weber, C.J. Microplastics in Vineyard Soils: First Insights from Plastic-Intensive Viticulture Systems. *Sci. Total Environ.* **2024**, *947*, 174699, doi:10.1016/j.scitotenv.2024.174699.

29. Cozzolino, L.; Nicastro, K.R.; Zardi, G.I.; Santos, C.B.D.L. Species-Specific Plastic Accumulation in the Sediment and Canopy of Coastal Vegetated Habitats. *Sci. Total Environ.* **2020**, *723*, 138018, doi:https://doi.org/10.1016/j.scitotenv.2020.138018.

30. Helcoski, R.; Yonkos, L.T.; Sanchez, A.; Baldwin, A.H. Wetland Soil Microplastics Are Negatively Related to Vegetation Cover and Stem Density. *Environ. Pollut.* **2020**, *256*, 113391, doi:10.1016/j.envpol.2019.113391.

31. Cesarini, G.; Scalici, M. Riparian Vegetation as a Trap for Plastic Litter. *Environ. Pollut.* **2022**, *292*, 118410, doi:https://doi.org/10.1016/j.envpol.2021.118410.

32. Lero, M.; Mikus, P.; Wyzga, B. First Insight into the Macroplastic Storage in a Mountain River : The Role of in-River Vegetation Cover, Wood Jams and Channel Morphology. *Sci. Total Environ.* **2022**, *838*, 0–11, doi:https://doi.org/10.1016/j.scitotenv.2022.156354.

33. Cai, L.; Zhao, X.; Liu, Z.; Han, J. The Abundance, Characteristics and Distribution of Microplastics (**MPs**) in Farmland Soil — Based on Research in China. *Sci. Total Environ.* **2023**, *876*, 162782, doi:10.1016/j.scitotenv.2023.162782.

34. Rillig, M.C.; Kim, S.W.; Zhu, Y.G. The Soil Plastisphere. *Nat. Rev. Microbiol.* **2023**, 1–11, doi:10.1038/s41579-023-00967-2.

35. Alvares, C.A.; Stape, J.L.; Sentelhas, P.C.; De Moraes Gonçalves, J.L.; Sparovek, G. Köppen's Climate Classification Map for Brazil. *Meteorol. Zeitschrift* **2013**, *22*, 711–728, doi:10.1127/0941-2948/2013/0507.

36. Dantas, A.A.A.; Carvalho, L.G. de; Ferreira, E. Classificação e Tendências Climáticas Em Lavras, MG. *Ciência e Agrotecnologia* **2007**, *31*, 1862–1866, doi:10.1590/s1413-70542007000600039.

37. Soil Survey Staff *Keys to Soil Taxonomy*; USDA, U.S.D. of A., Ed.; 13. ed.,.; USDA- Natural

Resources Conservation Service: United States Department of Agriculture, 2022;

38. Silva, B.M.; Santos, W.J.R.; Marques, J.J. *Levantamento detalhado do solo da Fazenda Muquém / UFLA, Lavras- MG*; Boletim Té.; Lavras MG, Brazil, 2014;

39. QGIS Development Team QGIS Geographic Information System Versão 3.28.2 Firenze 2024.

40. Schneider, C.A.; Rasband, W.S.; Eliceiri, K.W. NIH Image to ImageJ: 25 Years of Image Analysis. *Nat. Methods* 2012, *9*, 671–675.

41. OriginPro Lab Corporation OriginPro 2024, Version 2024b.

42. Greenacre, M.; Blasius, J. *Multiple Correspondence Analysis and Related Methods.*; Taylor and.; 1th. ed.: New York, 2006;

43. Ossani, P.C.; Cirillo, M.A. MVar.Pt: Analise Multivariada (Brazilian Portuguese). 2024, 1–60.

44. R Core Team R: A Language and Environment for Statistical Computing. R Foundation for Statistical Computing 2024.

45. Liu, H.; Sun, K.; Liu, X.; Yao, R.; Cao, W.; Zhang, L.; Wang, X. Spatial and Temporal Distributions of Microplastics and Their Macroscopic Relationship with Algal Blooms in Chaohu Lake, China. *J. Contam. Hydrol.* **2022**, *248*, doi:10.1016/j.jconhyd.2022.104028.

46. Weber, C.J.; Santowski, A.; Chifflard, P. Investigating the Dispersal of Macro- and Microplastics on Agricultural Fields 30 Years after Sewage Sludge Application. *Sci. Rep.* **2022**, *12*, 1–13, doi:10.1038/s41598-022-10294-w.

47. Parolini, M.; De Felice, B.; Lamonica, C.; Cioccarelli, S.; Crosta, A.; Diolaiuti, G.; Ortenzi, M.A.; Ambrosini, R. Macroplastics Contamination on Glaciers from Italian Central-Western Alps. *Environ. Adv.* **2021**, *5*, 100084, doi:10.1016/j.envadv.2021.100084.

48. Sobhani, Z.; Amin, A.; Naidu, R.; Megharaj, M.; Fang, C. Identification and Visualisation of Microplastics by Raman Mapping. *Anal. Chim. Acta* **2019**, *1077*, 191–199, doi:10.1016/j.aca.2019.05.021.

49. Phan, S.; Padilla-Gamiño, J.L.; Luscombe, C.K. The Effect of Weathering Environments on Microplastic Chemical Identification with Raman and IR Spectroscopy: Part I. Polyethylene and Polypropylene. *Polym. Test.* **2022**, *116*, doi:10.1016/j.polymertesting.2022.107752.

50. González-córdova, J.A.; Ariza-flores, D.; Pérez-huerta, J.S.; Madrigal-melchor, J. Optical Anisotropy Raman Response of Polyethylene Terephthalate Strained Thin Films. *Phys. B Condens. Matter* **2023**, *654*, 414693, doi:10.1016/j.physb.2023.414693.

51. Berenstein, G.; Córdoba, P.; Díaz, Y.B.; González, N.; Ponce, M.B.; Montserrat, J.M. Macro, Meso, Micro and Nanoplastics in Horticultural Soils in Argentina: Abundance, Size Distribution and Fragmentation Mechanism. *Sci. Total Environ.* **2024**, *906*, doi:10.1016/j.scitotenv.2023.167672.

52. Steinmetz, Z.; Schröder, H. Plastic Debris in Plastic-Mulched Soil — a Screening Study from Western Germany. *PeerJ* **2022**, 1–14, doi:10.7717/peerj.13781.

53. Cyvin, B.J.; Ervik, H.; Kveberg, A.A.; Hellevik, C. Macroplastic in Soil and Peat. A Case Study from the Remote Islands of Mausund and Froan Landscape Conservation Area, Norway ; Implications for Coastal Cleanups and Biodiversity. *Sci. Total Environ.* **2021**, *787*, 147547, doi:10.1016/j.scitotenv.2021.147547.

54. Cao, J.; Gao, X.; Hu, Q.; Li, C.; Song, X.; Cai, Y.; Siddique, K.H.M.; Zhao, X. Distribution Characteristics and Correlation of Macro- and Microplastics under Long-Term Plastic Mulching in Northwest China. *Soil Tillage Res.* **2023**, *231*, doi:10.1016/j.still.2023.105738.

55. Wang, W.; Ge, J.; Yu, X.; Li, H. Environmental Fate and Impacts of Microplastics in Soil Ecosystems : Progress and Perspective. *Sci. Total Environ.* **2020**, *708*, 134841, doi:10.1016/j.scitotenv.2019.134841.

56. Chai, L.; Zhou, Y.; Dong, H.; Gong, P.; Wang, X. Soil Contamination and Carrying Capacity across the Tibetan Plateau Using Structural Equation Models. *Environ. Pollut.* **2023**, *337*, 122640, doi:10.1016/j.envpol.2023.122640.

57. Yang, Z.; Lü, F.; Zhang, H.; Wang, W.; Xu, X.; Shao, L.; Che, Z.; Lu, B.; Ye, J.; He, P. A Neglected Transport of Plastic Debris to Cities from Farmland in Remote Arid Regions. *Sci. Total Environ.* **2022**, *807*, 150982, doi:https://doi.org/10.1016/j.scitotenv.2021.150982.

58. Guo, S.; Zhang, J.; Liu, J.; Guo, N.; Zhang, L.; Wang, S.; Wang, X.; Zhao, M. Organic Fertilizer and Irrigation Water Are the Primary Sources of Microplastics in the Facility Soil, Beijing. *Sci. Total Environ.* **2023**, *895*, 165005, doi:10.1016/j.scitotenv.2023.165005.

59. Huang, X.; Chen, Y.; Meng, Y.; Liu, G.; Yang, M. Are We Ignoring the Role of Urban Forests in Intercepting Atmospheric Microplastics? *J. Hazard. Mater.* **2022**, *436*, 129096, doi:10.1016/j.jhazmat.2022.129096.

60. Falakdin, P.; Lopez-Rosales, A.; Andrade, J.; Terzaghi, E.; Di Guardo, A.; Muniategui-Lorenzo, S. Comparison of Microplastic Type, Size, and Composition in Atmospheric and Foliage Samples in an Urban Scenario. *Environ. Pollut.* **2024**, *349*, 123911, doi:10.1016/j.envpol.2024.123911.

61. Cai, L.; Zhang, L.; Liu, Z.; Zhao, X.; Han, J. The Factors Affecting Microplastic Pollution in Farmland Soil for Different Agricultural Uses : A Case Study of China. *Catena* **2024**, *239*, 107972, doi:10.1016/j.catena.2024.107972.

62. Nohara, L.M.N.; Ariza-tarazona, M.C.; Triboni, R.E.; Nohara, L.E.; Villarreal-chiu, J.F.; Cedillo-gonz, E.I. Are You Drowned in Microplastic Pollution ? A Brief Insight on the Current Knowledge for Early Career Researchers Developing Novel Remediation Strategies. *Sci. Total Environ.* **2024**, *918*, 170382, doi:10.1016/j.scitotenv.2024.170382.

63. Billings, A.; Carter, H.; Cross, R.K.; Jones, K.C.; Pereira, M.G.; Spurgeon, D.J. Co-Occurrence of Macroplastics, Microplastics, and Legacy and Emerging Plasticisers in UK Soils. *Sci. Total Environ.* **2023**, *880*, doi:10.1016/j.scitotenv.2023.163258.

SUPPORTING INFORMATION FOR

Plastic debris in agroecosystems: Distribution and abundance patterns, and relationship with terrain characteristics in Southeastern Brazil

Table S1: Average values of the abundance group (number and mass) and the dimension group (area, perimeter, and diameter) of plastic debris collected on the soil surface as a function of four slope classes.

Class_slope	Abundance Group		Dimension Group		
	Quantity (pieces x10^3 ha^{-1})	Mass (kg ha^{-1})	Area (m^2 ha^{-1})	Perimeter (m ha^{-1})	Diameter (m ha^{-1})
Flat	9.297	16.343	54.021	3543.976	898.599
Gently undulating	9.366	10.513	19.934	2128.444	542.859
Undulating	11.717	24.809	32.126	2645.922	662.571
Strongly	17.320	0.695	5.292	1718.594	443.709

Table S2: Average values of the abundance group (quantity and mass) and the dimension group (area, perimeter, and diameter) of plastic debris collected on the soil surface as a function of seven LS factor intervals.

Class_slope	Abundance Group		Dimension Group		
	Quantity (pieces x10^3 ha^{-1})	Mass (kg ha^{-1})	Area (m^2 ha^{-1})	Perimeter (m ha^{-1})	Diameter (m ha^{-1})
[0.12684-0.81824]	15.419	15.750	26.560	2947.622	724.660
[0.81824-1.50964]	11.292	12.720	29.794	3183.372	841.919
[1.50964-2.20104]	10.507	58.594	67.789	2797.517	666.544
[2.20104-2.89244]	6.477	13.306	9.349	932.711	233.874
[2.89244-3.58384]	3.057	6.076	8.730	732.606	136.900
[3.58384-4.27524]	1.019	6.299	7.522	738.808	161.330

Table S3: Average values of the abundance group (quantity and mass) and the dimension group (area, perimeter, and diameter) of plastic debris collected on the soil surface as a function of seven NDVI index intervals.

Class_slope	Abundance Group		Dimension Group		
	Quantity (pieces x10^3 ha^{-1})	Mass (kg ha^{-1})	Area (m^2 ha^{-1})	Perimeter (m ha^{-1})	Diameter (m ha^{-1})
[0.06011-0.10591]	12.335	18.583	33.728	3514.991	830.615
[0.10591-0.15171]	15.390	9.603	26.490	3031.534	802.155
[0.15171-0.19751]	6.914	16.876	18.407	1618.361	392.364
[0.19751-0.24331]	6.028	2.735	5.392	762.798	199.266
[0.24331-0.28911]	2.802	0.419	3.336	658.591	147.972
[0.28911-0.35491]	0.509	40.560	258.584	1507.896	478.859

This paper was submitted in the Journal Agriculture, Ecosystems & Environment

PAPER 3 – ASSESSMENT OF SOIL MICROPLASTICS AND THEIR RELATION TO SOIL AND TERRAIN ATTRIBUTES UNDER DIFFERENT LAND USES IN SOUTHEASTERN BRAZIL

ABSTRACT

The assessment of microplastics (MP) in terrestrial ecosystems has gained increasing global attention, due to their potential impact on soil health, biodiversity, and agricultural production. While numerous studies have explored MP contamination in aquatic environments, research on their distribution and interactions in soil remains limited, particularly in tropical regions. This study aimed to characterize MP extracted from tropical soil samples and relate their abundance to soil and terrain attributes under different land uses (forest, grassland, and agriculture). Soil samples were collected from an experimental farm in Lavras, Minas Gerais, Southeastern Brazil, to determine soil physical and chemical attributes and MP abundance in a micro-basin. These locations were also used to obtain terrain attributes from a digital elevation model and the normalized difference vegetation index (NDVI). The majority of microplastics found in all samples were identified as polypropylene (PP), polyethylene (PE), polyethylene terephthalate (PET), and vinyl polychloride (PVC). The spatial distribution of MP was rather heterogeneous, with average abundances of 3,826, 2,553, and 3,406 pieces kg^{-1} under forest, grassland, and agriculture, respectively. MP abundance was positively related to macroporosity and sand content and negatively related to clay content and most chemical attributes. Regarding terrain attributes, MP abundance was negatively correlated with plan curvature, convergence index, and vertical distance to channel network and positively related to topographic wetness index. These findings indicate that continuous water fluxes at both the landscape and soil surface scales play a key role, suggesting a tendency for higher MP accumulation in lower-lying areas and soils with greater porosity. These conditions promote MP transport and accumulation through surface runoff and facilitate their entry into the soil.

Keywords: Distribution, Plastic polymer, Raman spectroscopy, Soil structure, Tropical Soils

1. INTRODUCTION

Microplastics (MP) are plastic particles formed either directly during manufacturing or by the fragmentation of larger plastic products (Li et al., 2020) due to exposure to ultraviolet radiation, weathering, hydrolysis, mechanical abrasion, physicochemical processes, and microbial action in the environment (Castelvetro et al., 2021; Orona et al., 2022; Zhou et al., 2023). MP can persist in soils for hundreds of years due to their chemical stability and physical resistance (Li et al., 2021), raising growing concerns about their potential impacts on the environment and human health (Li et al., 2020), and on soil biological health (Sarkar et al., 2022). The slow degradation of MP facilitates their dissemination across terrestrial and aquatic ecosystems (Lwanga et al., 2022), leading to their recognition as a globally persistent pollutant (Munno et al., 2020).

The scientific community and policymakers are increasingly concerned about the global contamination of soil by microplastics (MP), recognizing them as a marker of the Anthropocene. Over the past eight years, research has focused on understanding the magnitude and consequences of MP contamination (He et al., 2018), both in ecosystems and in human health (Hu et al., 2022).

Early studies primarily quantified and characterized MP in soils. Since the 2020s, however, more systematic investigations have emerged that address the effects of land use and environmental factors on the spatial and temporal distribution of MP (Feng et al., 2023), the influence of soil properties (Zhang et al., 2024), vertical migration (Li et al., 2021), terrain effects (Padha et al., 2022), and interactions with soil flora and fauna (Dogra et al., 2024).

Agricultural soils have been identified as one of the ecosystems most susceptible to MP pollution (Akca et al., 2024), originating from sources such as microfibers released from clothing, primary MP discarded in their original forms, manufacturing of cosmetics and cleaning products (Souza Machado et al., 2017), and the degradation of plastic debris already present in the environment (Amjad et al., 2023; Piehl et al., 2018). These particles can be easily transported by air and rain to the soil (Corradini et al., 2019; Guo et al., 2020; Nizzetto, Lu et al., 2016; Rillig et al., 2023), or by runoff into aquatic environments (Campanale et al., 2022). Such sources significantly contribute to MP accumulation in agricultural soils, leading to their long-term buildup in soil profiles (Büks and Kaupenjohann, 2020; Lwanga et al., 2022).

Microplastics particles can act as carriers for other pollutants, such as heavy metals and persistent organic pollutants, posing substantial risks to organisms (Amjad et al., 2023) and increasing their environmental impacts (Li et al., 2020). Additionally, MP may alter soil properties (Xiang et al., 2022), affecting soil structure and water dynamics (Souza Machado et al., 2019). These changes can have significant and lasting effects on soil carbon dynamics (Li et al., 2022), with yet unknown consequences for sustainability and food security (Nizzetto et al., 2016). The ubiquity of MP in the environment has led some authors to propose their use as a potential marker of the Anthropocene (Weber et al., (2021).

The amount of MP in soil at a given location is influenced by various factors, including polymer type, land use, soil attributes (Li et al., 2020), the heterogeneity of soil mineral and organic components (Piehl et al., 2018), etc. Additionally, the extraction and removal of microplastics from soil remain challenging, requiring particular approaches for each type of soil analyzed (Samanta et al., 2022). Among the methods for extracting MP from soils, the density separation method is the most used. This method involves the removal of organic matter, followed by the use of solutions with varying densities to the separation MP (Grause et al., 2022; Liu et al., 2019; Quinn et al., 2016; Radford et al., 2021), resulting in high recovery rates for MP ranging in size from 40 µm to 5000 µm (Samanta et al., 2022), finishing with filtration and isolation of MP (Li et al., 2020; Thomas et al., 2020).

Studies requiring the quantification and characterization of MP are conducted using stereoscopic microscopy, where particles are counted and classified by color, size, and shape, assisted by image acquisition and processing software (Samanta et al., 2022; Zhang and Liu, 2018). Additionally, polymer spectra identification is performed using non-destructive techniques such as Fourier-transform infrared spectroscopy (FTIR) and Raman spectroscopy (Munno et al., 2020; Souza Machado et al., 2019; Thomas et al., 2020).

Recent studies highlight the urgent need to prioritize research on MP in agroecosystems (Guimarães et al., 2024; Yang Zhou et al., 2023). While previous studies have documented the distribution and characterization of MP in river sediments, lakes, and Brazilian mangrove soils (Gerolin et al., 2020; Paes et al., 2022; Sarti et al., 2022), research on relationship between MP and soil attributes in tropical regions remains scarce. Therefore, investigating their distribution, characterization, and interactions with land use and terrain features in tropical soils is essential.

This study was based on the hypothesis that land use, soil attributes, and topography influence MP abundance in the topsoil. Therefore, the study aimed to quantify and characterize MP extracted from the 0–20 cm soil layer under different land uses on an micro-watershed in Southeastern Brazil and to relate MP abundance to soil physical and chemical properties, terrain attributes, and the normalized difference vegetation index (NDVI).

2. MATERIAL AND METHODS

2.1. Study area

The study was conducted in a watershed from the Muquém Experimental Farm of the Federal University of Lavras (UFLA), in the municipality of Lavras, Minas Gerais state, Brazil, It is between latitude -21°12'037"S and longitude -44°59'3.77"W, WGS 84 UTM 23S. It covers an area of approximately 165 hectares and features a diversified land use system comprising forest, grassland, and agriculture (Figure 1). The farm is located within the geomorphological unit of the Atlantic Plateau, specifically in the Upper Rio Grande surface, a tributary of the Paraná River (Silva et al., 2014).

The regional climate is classified as Cwb (subtropical highland) according to the Köppen climate classification system, mesothermic with dry mild winters and rainy warm summers (Alvares et al., 2013; Dantas et al., 2007). The area receives an average annual rainfall of 1,383.4 mm, concentrated during the rainy season from October to February. Predominant winds are easterly from March to September and northeasterly from November to February, with average wind speeds of 2.16 m s^{-1} and 1.64 m s^{-1} respectively, and a mean annual temperature of 20.6°C (INMET, 2022).

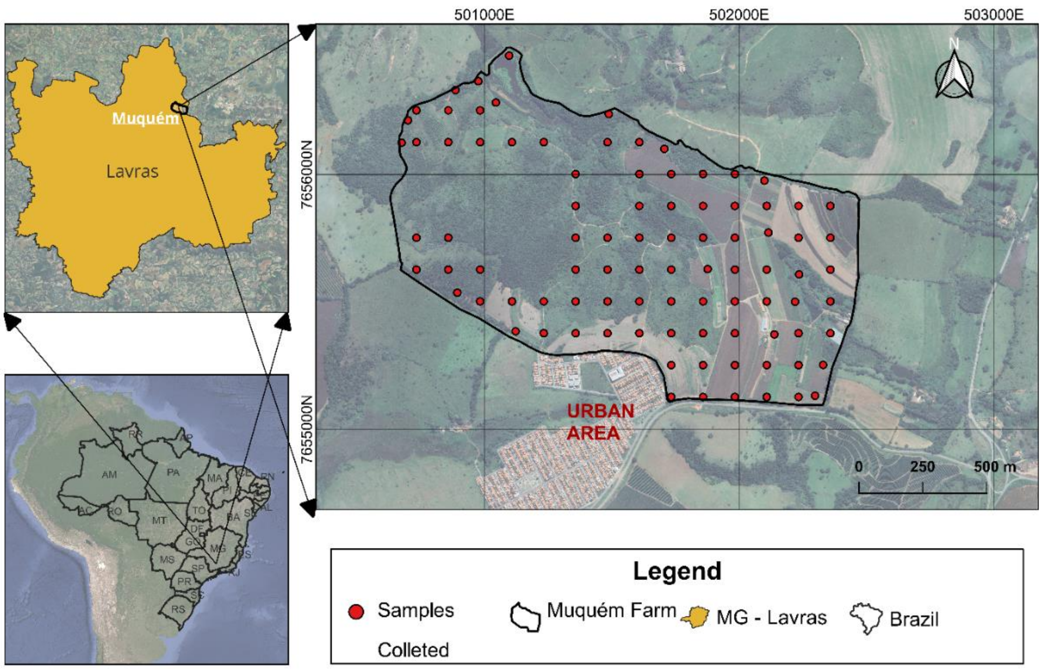

Figure 8. Map of the study area and geographic position of the sampled points at the watershed *from* Muquém farm, municipality of Lavras, Brazil.

The characteristics of the study site have already been detailed in Arevalo-Hernandez et al. (2025). Beginning with soil classification in the study area, the major soil orders in the micro-basin (Figure 2a) according to WRB-FAO (IUSS Working Group WRB, 2022) correspond to Cambisols (CX), which occupy 18.84 ha (11,41% of the area), Gleysols (GM), covering 1.92 ha (1.16% of the area), Ferrasols (LVA), occupying 63.60 ha (38.50%), Nitisols (NX) at 8.30 ha (5.02%), Acrisols (PVA) covering 58.07 ha (35.15% of the area), and Leptosols (RL) at 14.48 ha, representing 8.76% of the total area (Silva et al 2014).

The altitude in the study area ranges from 877 to 1,010 meters (Figure 2c), encompassing a topographic gradient from flat to mountainous terrains. Flat areas (slope < 3%) represent approximately 2.7% of the total area, while gently undulating areas (3–8% slope) account for 17.8%. The majority of the landscape (58.8%) is classified as undulating, with slopes between 8% and 20%. Strongly undulating areas (20–45% slope) cover 20.1% of the area, and mountainous regions (slope > 45%) represent the remaining 0.6% (Figure 2b).

Land uses in the study area were classified as agriculture, grassland, and forest. Agricultural use is composed of annual crops that occupy 29.2% of the area, including corn (*Zea mays*), soybean (*Glycine max* (L.) Merrill), wheat (*Triticum aestivum* L.), common bean (*Phaseolus vulgaris*), sorghum (*Sorghum bicolor* L.), and rice (*Oriza sativa* L.), while perennial crops occupy 0.9% of the farm, mainly coffee (*Coffea arabica*). Grasslands are the most common land use, with 39.3% of the area corresponding planted pastures (*Brachiaria* sp.) and 4.7% to native grassland. Forests occupy 24.4% of the area and the remaining 1.5% corresponds to water reservoirs and buildings. The forests are dominated by planted eucalyptus forests (*Eucalyptus* esp.) and native forest.

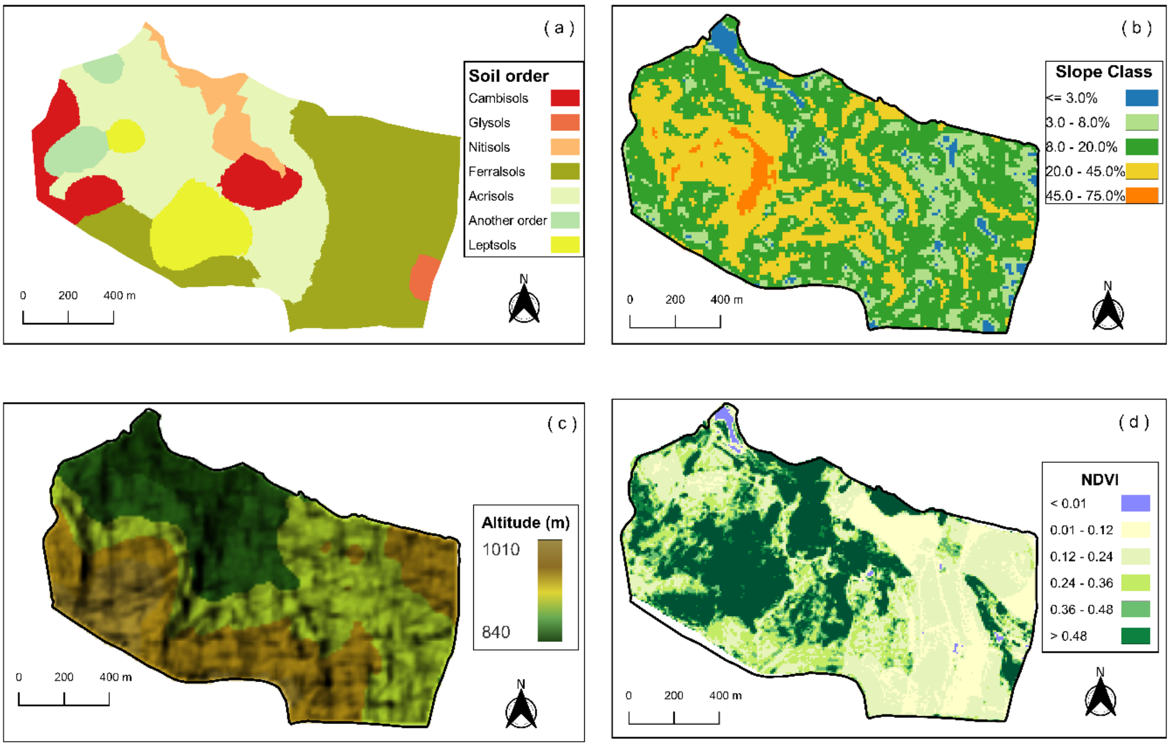

Figure 2. Maps representing soil order (a), slope classes (b), Altitude (c), and NDVI (d) of the watershed from Muquém Farm in Lavras, Southeastern Brazil. Note: reliefs associated with their respective slopes, namely: flat (< 3%), gently sloping (3 – 8%), strongly sloping to moderately steep (8 – 20%), steep to very steep (20 – 45%), and extremely steep (45 – 75%).

2.2. Soil sampling

Soil sampling was conducted from August 2022 to April 2023 using a predefined regular grid of 91 georeferenced points covering 165 ha, resulting in a sampling density of 1.77 ha per sample, with a resolution of 125 m × 125 m (Figure 1). Samples were collected from a 0–20 cm depth, with 100 g of soil stored in glass jars for microplastic analysis. Additionally, both disturbed and undisturbed samples were collected to assess soil physical and chemical properties.

The analyzed physical properties included soil texture (clay, sand, and silt), determined by the pipette method (Dane and Topp, 2002); aggregate stability (GMD), assessed using the wet sieving method, with mean weight diameter as the stability index (Kemper and Rosenau, 1986; Silva et al., 2017). Soil bulk density (Bd), total porosity (PT), macroporosity (pores > 0.05 mm diameter, Macro), and microporosity (Micro) were measured using the volumetric cylinder method, with microporosity determined under a suction of 6 kPa (Dane and Topp, 2002).

Chemical propeerties of the fine earth fraction (< 2 mm) included pH (determined at a 1:2.5 soil: water ratio); organic carbon content (determined via wet oxidation with 0.0667 mol L^{-1} potassium dichromate and concentrated sulfuric acid); exchangeable divalent cations (Ca^{2+} and Mg^{2+}) and exchangeable acidity (Al^{3+}), extracted using 1 mol L^{-1} KCl and quantified via inductively coupled plasma optical emission spectrometry (ICP-OES). Exchangeable potassium (K^{+}), available phosphorus (P), and sodium (Na) were extracted using Mehlich-1 solution and quantified by ICP-OES. Potential acidity (H + Al) was determined volumetrically using 0.5 mol L^{-1} calcium acetate at pH 7.0. Based on these results, sum of exchangeable cation (SB), effective cation exchange capacity (eCEC), aluminum saturation (m), cation saturation (V), and total cation exchange capacity (tCEC) were calculated. Methods followed Brazilian standards (Teixeira et al., 2017).

Sampling points were located using a Garmin Oregon 750 GPS with 3 m accuracy. Auxiliary data such as altitude, surrounding vegetation type, and current land use were also recorded. Terrain attributes were derived from a digital elevation model with spatial resolution of 12.5 m (high-resolution terrain corrected ALOS PALSAR scene ALPSRP243456750 from August 2010), data courtesy of JAXA/METI (2010). Terrain attributes were obtained from the basic terrain analysis in SAGA-GIS (Conrad et al., 2015) implemented into QGIS software version 3.36.3 (QGIS Development Team, 2024) and included slope, valley depth, distance to channel network, channel network base level, flat curvature, profile curvature, convergence index, topographic wetness index, relative slope position, and LS-factor. These values were extracted to the sampling grid by the Point Sampling Tool plugin using bilinear interpolation.

2.3. Extraction, Identification, and Quantification of Soil Microplastics

Soil MP extraction and assessment followed a three-phase procedure: 1) pre-processing, 2) MP separation, and 3) MP identification and quantification (Zhou et al., 2019).

The first stage, pre-processing, involved digesting the organic matter present in the soil samples using 10 g of soil and 20 mL of an alkaline solution of KOH: NaClO 30%. This mixture was dispersed in an ultrasonic bath at 35 W and 40 kHz for 5 minutes. After dispersion, the samples were placed in an oven at 50–60 °C and manually stirred for 30 seconds every 4 hours until reaching a constant mass.

During the second stage, MP separation, the samples were centrifuged in solutions of sequentially increasing density (ρ): distilled water (ρ = 1.00 g cm^{-3}), saturated NaCl solution (5.33 mol L^{-1}, ρ = 1.19 g cm^{-3}), and $ZnCl_2$ solution (5.06 mol L^{-1}, ρ = 1.5 g cm^{-3}). Soil samples treated with distilled water underwent ultrasound dispersion for 5 minutes to separate MP from soil aggregates. Subsequently, the solution was centrifuged at 2500 rpm for 5 minutes. The high speed allowed MP to float in the supernatant, which was then collected with a pipette and filtered using a vacuum pump and a 2 µm nylon membrane. Next, 20 mL of saturated NaCl solution was added to the precipitated soil in the tube. Again, the material was subjected to ultrasound dispersion and subsequently centrifuged at 2700 rpm for 5 minutes, repeating the supernatant collection and filtration processes. The final density separation was conducted with $ZnCl_2$ solution, where 20 mL was added to the tube with soil. The suspension underwent ultrasound dispersion followed by centrifugation and the supernatant was collected and filtered on a 2 µm nylon membrane. The process was repeated until no particles were observed in the supernatant. The particles retained on the filter were air-dried at room temperature (approximately 23°C) and stored in glass boxes.

In the third stage, MP identification and quantification, a Nikon Eclipse Ni microscope (10x magnification) was used. Images were recorded with a Nikon DS-Fi3 digital camera, supported by NIS Elements software version 4.6 for data processing. MP abundance was recorded in pieces kg^{-1} of dry soil by counting MP pieces in the total filter area. Regarding shape, MP were classified as fragments (angular hard pieces), granules (circular or semi-circular particles), fibers (elongated threads), and films (soft and transparent flakes). Additionally, MP were categorized by color, with the most relevant colors being white, black, blue, red, yellow, green, brown, and transparent (Yang et al., 2021b). MP size was categorized into the following groups: group 1 (20 to 200 µm), group 2 (200 to 500 µm), group 3 (500 to 1000 µm), and group 4 (1000 to 3000 µm) (Wang et al., 2021; Yang et al., 2021a).

Polymer identification was performed using spectral analysis with a Raman microscope model Alpha300 equipped with a 785 nm laser (Witec, 2022). Spectra were measured in the range of 300–3500 cm^{-1} with an acquisition time of 1 second, 20 accumulations, and a power filter of 2 to 15% to avoid sample burning. Raman spectroscopy analysis was conducted by comparing the samples' Raman spectra with the Raman spectra of polymers of reference obtained from the literature. Thus, the march in the positions and intensities of the bands between the sample spectra and the reference spectra enabled the identification of the polymer type with high confidence. From this analysis, the identified Raman spectra corresponded to polypropylene (PP), polyethylene (PE), polyvinyl chloride (PVC), polyethylene terephthalate

(PET), polystyrene (PS), polyamide (PA), rubber, and acrylic. Finally, this database was compared with the spectra of the MP isolated from the soil and processed using OriginPro Lab Corporation (2024).

2.4. Laboratory Contamination Prevention and Recovery Tests

Field samples were stored in glass jars. To avoid contamination, all materials used in sample analysis were made of glass and rinsed with a disinfectant solution (filtered distilled water and 30% ethanol) during all steps. Nitrile gloves and cotton clothing were also worn during the experiments, and access to the laboratory area was restricted to research personnel to prevent contamination from external sources. The same procedure for extracting MP from soil was conducted on five control samples, which did not any soil. Control samples were stored in petri dishes and inspected at the end of the analysis to verify potential contamination in the laboratory (Corradini et al., 2019; Weber et al., 2021).

Recovery tests were also conducted to ensure methodological precision. These were performed on four clean soil samples from the study area, along with low-density polyethylene (LDPE) and polyvinyl chloride (PVC). In this context, recovery rates for LDPE particles ranged from 81.0% to 98.8%, while PVC recovery rates ranged from 59.7% to 75.2% (Arevalo-Hernandez et al., 2025b).

2.5. Statistical Analysis

Statistical analysis was performed on the abundance of MP isolated from soil sampling locations (pieces kg^{-1}) in the 0–20 cm layer. After testing normality and heteroscedasticity, the data exhibited a non-normal distribution. Principal component analysis (PCA) and Spearman correlation were applied to examine relationships between land use (forest, grassland, and agricultural), soil physical and chemical properties, terrain attributes, and the normalized difference vegetation index (NDVI) for each sampling site. Multivariate analyses were conducted using R software (Core Team, 2024). Polymer graphs and spectra were generated using OriginLab Corporation software (2024).

3. RESULTS

3.1. Microplastic abundance

Microplastics (MP) were detected in all soil samples collected from the study area. These samples were distributed across land uses as follows: 19 from forest, 27 from grassland, and 45 from agricultural areas. The mean MP abundance ± standard deviation was 3,825.9 ± 338.5 pieces kg^{-1} for forest soils, 2,552.6 ± 230.9 pieces kg^{-1} for grassland, and 3,406.6 ± 231.2 pieces kg^{-1} for agricultural soils.

Microplastics abundance was categorized into five groups based on the classification (Liu et al., 2022; Rafique et al., 2020; Weber et al., 2022): very low (< 1500 pieces kg^{-1}); low (1500 - 3000 pieces kg^{-1}); medium (3000 - 4500 pieces kg^{-1}); high (4500 - 6000 pieces kg^{-1}); and very high (> 6000 pieces kg^{-1}). Seven values were classified as very high, corresponding to 8% of the total points, while 16% (n = 15) were categorized as high. Medium values were observed at 35% of the points (n = 32), low values for 30% (n = 27), and very low values for 11% (n = 10).

The point-based spatial distribution of MP abundance within the study area is shown in Figure 3. Overall, most points with high and very high MP abundance were located along the central strip and the eastern portion of the micro-watershed, particularly in the southern half, near an urban area and an inter-municipal road.

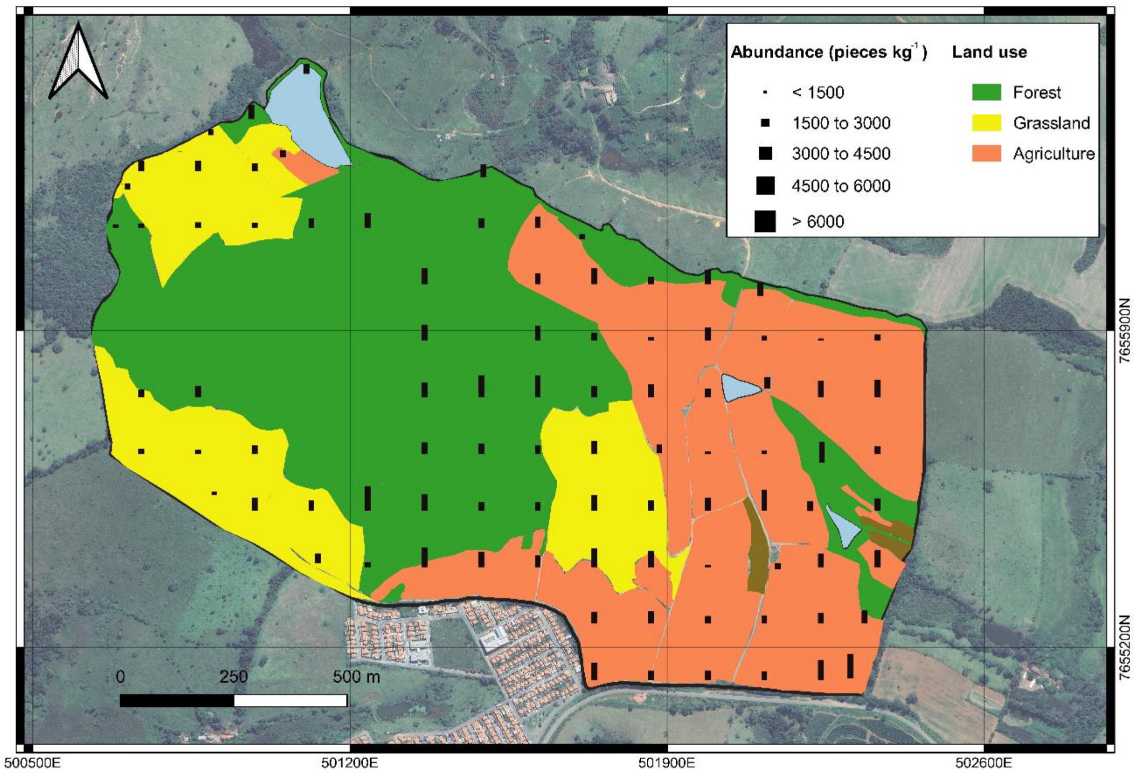

Figure 3. Distribution of sampling points at the watershed from Muquém Experimental Farm, Lavras, MG, Brazil, according to MP abundance and land use.

3.2. Microplastics composition

In this study, eight polymer types were identified using Raman spectroscopy. Their relative abundances in the 0–20 cm soil layer was: polypropylene (PP) 33.3%, polyethylene terephthalate (PET) 22.2%, polyethylene (PE) 14.8%, polyvinyl chloride (PVC) 8.6%, polyamide (PA) 8.6%, polycarbonate (PC) 6.2%, rubber 3.7%, and polystyrene (PS) 2.5% (Figure 4a). The prevalence of polymer types varied according to land use. In forest soils, the predominant polymers were PP (43.8%), PET (25%), PVC (12.5%), and PE (9.4%) (Figure 4b). In grassland soils, seven polymer types were identified, with PP, PET, PE, and PC being the most common, each representing 18.2% (Figure 4c). For agricultural soils, the most abundant polymers were PP (28.9%), PET (21.1%), and PE (18.4%) (Figure 4d).

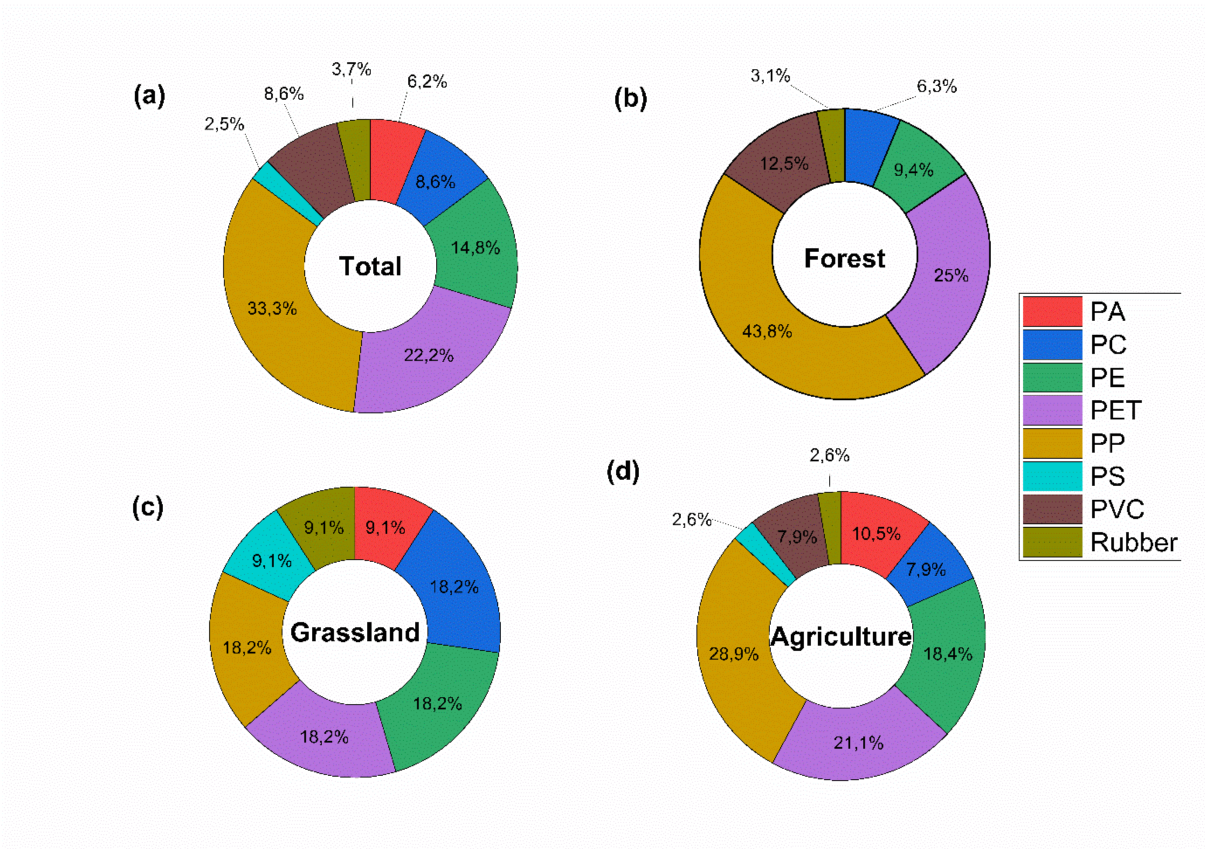

Figure 4. Polymer types identified in soil MP from the 0–20 cm soil layer under different land uses. (a) Total MP found (b) Forest, (c) Grassland, (d) Agriculture. PA: polyamide; PC: polycarbonate; PE: polyethylene; PET: polyethylene terephthalate; PP: polypropylene; PS: polystyrene; PVC: polyvinyl chloride.

Raman spectra of the most representative polymers found in soil samples from the study area were PP, PE, PET, and PVC (Figure 5). These spectra exhibited baseline shifts and variations in signal intensity, therefore different corrections were applied, including noise removal, baseline adjustment, and normalization. In all cases, the spectra revealed characteristic peaks specific to each polymer type.

For PP (Figure 5a), the Raman spectrum showed a characteristic peak around 2964 cm^{-1}, attributed to asymmetric CH stretching vibration. The peak at approximately 1463 cm^{-1} corresponded to asymmetric bending vibrations of the $–CH_3$ group, while the peak near 1162 cm^{-1} was associated with C–C stretching. Another peak at 890 cm^{-1} represented vibrations of helicoidal molecular structures. For this polymer, slight shifts in peak positions and changes in intensity were observed. These phenomena indicated weathering-induced chemical modifications on the polymer structure (Phan et al., 2022), suggesting oxidation, degradation, or cross-linking processes within the polymer chains.

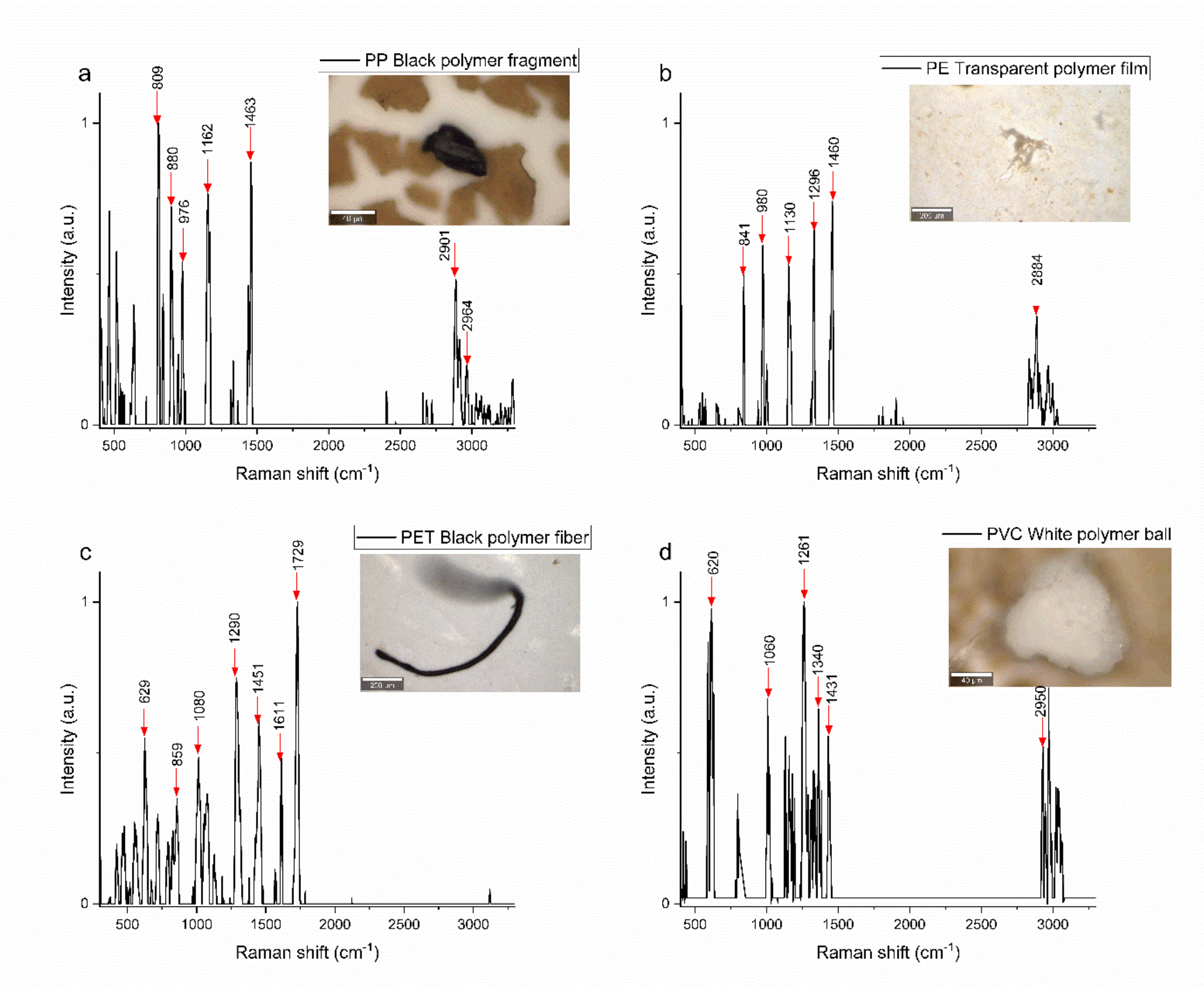

Figure 5. Raman spectra and photographs of the most abundant microplastics found in the 0–20 cm soil layer (PP, PE, PET, and PVC), observed using Raman spectroscopy.

In the PE spectrum (Figure 5b), characteristic peaks were observed in the regions 840–1450 cm^{-1} and 2884 cm^{-1}. The most intense peaks occurred at 980 cm^{-1}, 1130 cm^{-1}, and 1450 cm^{-1}, attributed to C-O stretching, symmetric C-C stretching, and symmetric CH_2 deformation, respectively. These findings align with previous studies on PE plastic debris in other regions (González-Córdova et al., 2023; Phan et al., 2022; Sobhani et al., 2019).

On the PET Raman spectra (Figure 5c), two dominant peaks were observed at 1611 cm^{-1} and 1729 cm^{-1}, corresponding to aromatic ring C-C stretching vibrations and carbonyl group stretching vibrations. Similar results were reported by González-Córdova et al., (2023). The PVC samples exhibited Raman spectra (Figure 5d) with high-intensity peaks at 620 cm^{-1}, associated with C-Cl bond stretching vibrations. Peaks at 1281 cm^{-1} and 1340 cm^{-1} corresponded to CH and CH-Cl bending vibrations, respectively, while the peak at 1431 cm^{-1} was related to angular deformation of the CH_2 group.

3.3. Color, Shape, and Size of Microplastics

A total of 3,118 MP particles were analyzed for color, shape, and size (Figure 6). Nine colors were identified (Figure 6a), with the respective percentages: black (34.9%), transparent (24.7%), brown (13.7%), white (12.6%), blue (8.1%), and yellow, red, green, and gray collectively accounting for 6.0%. Black and transparent were the predominant colors in all land uses, followed by brown or white depending on the land use.

Four MP shapes were recorded across all samples (Figure 6b): films (33%), fragments (28%), granules (25%) and fibers (14%). Generally, fibers were blue, films were transparent, and fragments and granules were black. Films were in the dominant shape, representing 31% in forest, 32% in grassland, and 34% in agricultural. Fragments and granules were found in similar proportions across all land uses, while fibers had the lowest occurrence, at 15% in forest and grassland and 13% in agricultural.

MP were categorized into four size groups: 20 – 200 μm, 200 – 500 μm, 500 – 1000 μm, and 1000 – 3000 μm. MP in the smallest size category (20 – 200 μm) were most abundant (Figure 6c), particularly for fragments and granules, accounting for 66%, 54%, and 63% of MP in the forest, grassland, and agricultural, respectively. MP larger than 1000 μm, mostly fibers, were the least abundant across all land uses.

In grassland, black granules and transparent films were the most common MP, with average sizes of 112.4 μm and 282.2 μm, respectively. In forest, transparent films, along with black fragments and granules, were the dominant forms, with average sizes of 207.6 µm, 151.1 µm, and 102.1 µm, respectively. For agricultural, transparent films and black fragments and granules were the most abundant, with average sizes of 220 µm, 143.3 µm, and 105.9 µm, respectively.

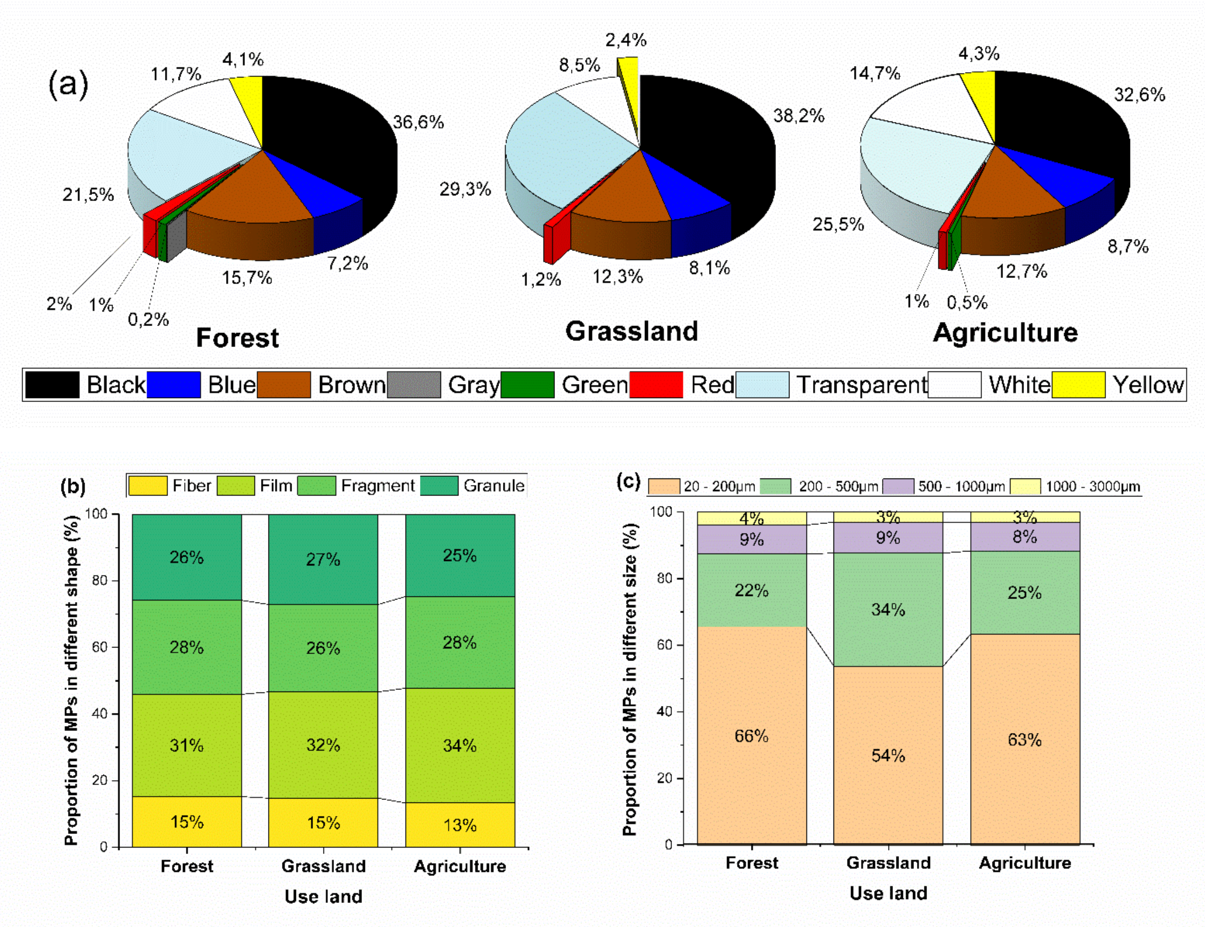

Figure 6. Percentage of microplastics sorted by (a) color, (b) shape, and (c) size for forest, grassland, and agricultural uses.

3.4. Relating microplastics to soil and terrain attributes

The first principal components (PC) accounted for 46.1% of the total variance in soil attributes (Figure 7a) and 62.5% of the total variance in terrain attributes (Figure 7b). For soil attributes, PC1 and PC2 seemed to represent soil chemical (SOM, tCEC, eCEC, SB, Ca, Mg, m) and physical attributes (PT, Bd, Clay, Sand, Micro), respectively. Although a clear trend regarding MP abundance was not clear, there was an evident trend according to land use, with agriculture observations scattering towards higher clay content and forest and grassland observations scattering towards higher sand content and bulk density.

This segregation between agriculture and other land uses was more evident in the PCA for the terrain attributes (Figure 7b). The first PC represented the vertical position of the sampled points, reflecting measures of curvature, distance to the channel network, and altitude, whereas the second PC was more strongly affected by slope and NDVI. In this case, the agriculture land use points were scattered towards higher altitudes and greater distances to the valley bottoms, whilst forest and grassland observations were related to higher Slopes.

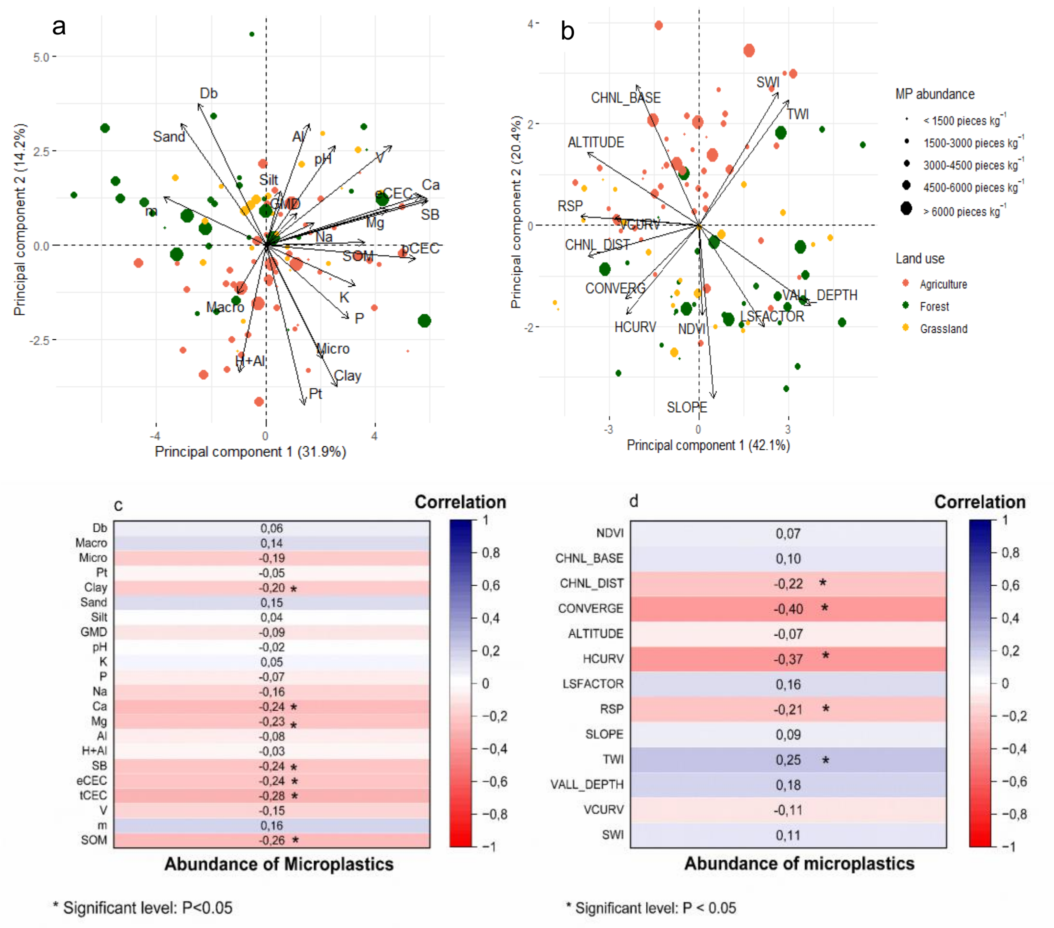

Figure 7. Principal component analysis of (a) soil physical and chemical properties and (b) terrain attributes and NDVI. Spearman's correlation between microplastic abundance and (c) soil physical and chemical properties and (d) terrain attributes and NDVI. Note: bulk density (Bd), macroporosity (Macro), microporosity (Micro), total soil porosity (PT), geometric mean diameter (GMD), exchangeable cations (SB), effective cation exchange capacity (eCEC), total cation exchange capacity (tCEC), total acidity (H+Al), cation saturation (V), aluminum saturation (m), soil organic matter (SOM), normalized difference vegetation index (NDVI), channel network base level (CHNL_BASE), channel network distance (CHNL_DIST), Convergence index (CONVERG), altitude, plan curvature (HCURV), LS-factor, relative slope position (RSP), slope, topographic wetness index (TWI), valley depth (VALL_ DEPTH), profile curvature (VCURV), SAGA wetness index (SWI).

4. DISCUSSION

4.1. Microplastic abundance

Numerous studies report the presence of microplastics (MP) in soils under different conditions, with their abundance and characteristics varying significantly depending on factors such as geographical location, land use, sampling depth, production systems employed, irrigation method, duration of plastic use, thickness, and type of plastic films used (Berenstein et al., 2024; Guo et al., 2023; Yoon et al., 2024). Additionally, atmospheric deposition, tire wear, and the use of sludge as an amendment are significant contributors (Corradini et al., 2019). The abundance of MP in soils reported by various authors is summarized in Table 1 according to location and land use to highlight their ubiquity and heterogeneity. Additionally, the lack of standardized methods for extracting MP from soils, along with variations in sampling methods, analysis techniques, and other natural or artificial factors, may influence MP abundance (Yang Zhou et al., 2023).

Table 1. Microplastic abundance (range, mean, and standard deviation) in soils according to location and land use as reported by various authors.

Location	Land use	Range	Average ± standard deviation.	Source
		pieces kg^{-1}		
Middle Franconia, southeast Germany	Agriculture	NA	0.34 ± 0.36	(Piehl et al., 2018)
Lahore, Pakistan	Agriculture Public Parks House lawns Industrial areas Drain, roadsides	1750 - 12200	4483 ± 2315	(Rafique et al., 2020)
Central Valley, Chile	Agriculture Grassland	NA	306 ± 360 184 ± 266	(Corradini et al., 2021)
Jiangxi Province, China	Agriculture	NA	43.8 ± 16.2	(Yang et al., 2021b)
Shandong Province, China	Agriculture	310 - 5698	1444 ± 986	(Yu et al., 2021)
Beijing, China	Greenhouse Agriculture	500 - 1240	891 ± 316	(Wang et al., 2022)
Yunnan, China	Agriculture Grassland Forest	50 - 3450	1236.36 ± 843.18 200 ± 228 85 ± 22.9	(Zhang et al., 2022)
Bangladesh	Agriculture	NA	$2.13 \times 10^4 \pm 0.13 \times 10^4$	(Hossain et al., 2023)

Buenos Aires, Argentina	Horticultural soil	27 - 69	43 ± 30	(Berenstein et al., 2024)
Rhineland-Palatinate, Germany	Viticulture farmland soil	400 - 13000	4200 ± 2800	(Klaus et al., 2024)
Northern, China	Legumes Farmland soil	1600 – 36200	11058	(La et al., 2024)
Lavras, Minas Gerais, Brazil	Forest	1000 - 7400	3826 ± 338	Present study
	Grassland	1000 - 4700	2553 ± 231	
	Agriculture	600 - 7300	3407 ± 231	

The MP abundance varied somewhat between land uses, with slight differences in size, color, shape, and polymer type across the three land uses studied. MP are ubiquitous, but their concentration depends on plastic usage in human activities (Rafique et al., 2020). For instance, our results for agricultural soils were higher than those researchers which found MP ranging from 6.0 to 444 pieces kg^{-1} with an average of 86 pieces kg^{-1} in surface agricultural soils in the Huangshui watershed, northeastern Qinghai-Tibet Plateau (Zhou et al. 2023). In contrast, other studies recorded MP abundances between 1,600 and 36,200 pieces kg^{-1}, averaging 11058 pieces kg^{-1} in agricultural land used under extensive plastic film and organic fertilizer application in northern China (La et al., 2024), with results markedly higher than our findings.

MP levels in agricultural soils similar to those in our study were founded ranging from 2,783 to 6,366 pieces kg^{-1} in Chinese agricultural soils (Wang et al., 2021). In the present study, MP concentrations ranged from 600 to 7,300 pieces kg^{-1}, with an average abundance of 3,407 ± 231 pieces kg^{-1} on agricultural use. Similar values were observed in Lahore, Pakistan, with MP concentrations ranging from 2200 to 6875 pieces kg^{-1}, averaging 3712 ± 2156 pieces kg^{-1} (Rafique et al., 2020). Variations in MP concentrations may be linked to differences in anthropogenic activity intensity, proximity to MP sources, vehicular traffic within the study area, and environmental conditions (La et al., 2024; Yoon et al., 2024; Zhang et al., 2022).

A similar scenario was observed for MP pollution in forest and grassland, with heterogeneity in results among the studies described (Table 1). In our data, MP concentrations in forest soils averaged 3,826 ± 338 pieces kg^{-1}, a much higher value than those reported in other studies, such as 85 ± 22.9 pieces kg^{-1} in Yunnan Province, China (Zhang et al., 2022), and 1097 pieces kg^{-1} in Gangdong, Seoul (Yoon et al., 2024). However, a study conducted in central China found a significantly higher MP abundance of 410,000 pieces kg^{-1} in forest soils. This was attributed to pollution sources such as wastewater from textile industries, sewage sludge, and exhaust emissions (Zhou et al., 2019).

In the present study, a similar MP abundance was found in the forest as in the agricultural (Figure 3). Although there is minimal human activity in the forest, it is believed that the detected MP may have been transported by atmospheric deposition (Padha et al., 2022).

Findings suggest that tree leaves can act as a long-term sink for airborne MP, which are typically smaller than 100 µm and shaped as fragments, granules, and fibers (Sunaga et al., 2024). Similarly, identified MP on tree leaves as fibers and fragments, ranging from 20 to 500 µm, in a semi-urban area near Coruña, Spain (Falakdin et al., 2024). In the present study, MP with similar shapes and sizes were identified in soils, as seen in Figures 6a and 6b, contributing to the explanation of high MP abundance in forests.

Another possible source is the degradation of plastic waste found on the surface along forest trails. The presence of plastic debris on the soil surface at the sampling sites may explain the higher MP abundance recorded in the forest. These findings suggest that the occurrence of MP may be influenced by human activities (Yoon et al., 2024; Zhang and Liu, 2018).

For grasslands, an average of 2,552.6 ± 230.9 pieces kg^{-1} was quantified, a much higher value than those reported in other studies, with recorded an average of 200 ± 228 pieces kg^{-1} (Table 1) (Corradini et al., 2021; Zhang et al., 2022). Compared to literature findings (Table 1), our MP abundances in grasslands were higher, likely due to sampling site selection with increased human activity levels and vehicle access within the study area, contributing to tire debris, plastic waste remnants, and road dust (Praveena et al., 2023; Yoon et al., 2024).

4.2. Distribution of microplastics in soil

The spatial distribution of MP was irregular and highly heterogeneous across the study region, being present in all soil samples regardless of land use. Causes for irregular MP abundance distribution include climatic factors, irrigation conditions, cultivation intensity, severe storms, and natural weathering (Feng et al., 2023; Ling et al., 2023; Liu et al., 2023). Figure 3 illustrates that the highest concentrations of MP were detected in the southern part of the study area, adjacent to a residential zone and municipal roads. This proximity appears to be closely linked to MP abundance, with MP concentrations tending to increase as the distance to these areas decreases (Wang et al., 2025).

Urbanization and anthropogenic activities contribute to soil contamination by MP (Amjad et al., 2023). Studies have concluded that MP abundance in soil is higher in residential areas compared to commercial and industrial areas, as population density influences MP contamination levels (Prajapati et al., 2023).

In this study, one of the areas with high MP abundance is located in the forest, where plastic debris deposited on the soil surface was displaced by runoff or wind from higher altitudes to lower areas, being intercepted by tree and shrub vegetation, leading to its deposition. These are probable causes of the high MP abundance (Falakdin et al., 2024; Sunaga et al., 2024). Similar results were reported with high MP abundance in northwestern Germany caused by high sludge production due to population density and intensive agricultural soil use (Brandes et al., 2021).

Studies suggest that MP pollution in agricultural soils is independent of fertilizer or compost applications and that nearby roads and urban areas do not significantly contribute to soil MP pollution (Corradini et al., 2021). Thus, it is necessary to investigate potential MP sources in the study area and compare findings with other research reports from similar locations with comparable sampling methods and procedures. This approach would facilitate the development of standardized and more universal analytical methods (Ling et al., 2023).

4.3. Visual characterization and composition of microplastics

The size, shape, color, and polymer type may help to understand their relationship to soil physicochemical attributes (Figures 4 and 6), such as pH, soil structure, hydrodynamics, and water-stable aggregates (Huang et al., 2022). These characteristics may also aid in tracking potential pollution sources of these plastic particles (La et al., 2024).

In this study, MP were categorized into four forms: fragments, films, fibers, and granules, and were found in varying proportions, regardless of land use (Figure 6). Similar forms were observed in other studies (La et al., 2024; Xiaoting et al., 2022). Films (32%) and fragments (28%) represented the highest proportions among soil samples, with equivalent results reported by Ling et al., (2023). Fibers and fragments have also been found as the most common, often originating from polyester and polyethylene debris (Yang et al., 2021b).

The shape of the MP particles can influence soil structure and integrate into the soil matrix in different ways. For instance, polyethylene fragments interact loosely with other soil particles, whereas polyester fibers form the framework for larger soil structures (Souza Machado et al., 2018). This behavior may impact aggregate stability and consequently soil susceptibility to erosion, a hypothesis requiring further investigation through studies comparing different soil textures and MP concentrations (Huang et al., 2022).

Results from this study revealed that MP varied in size according to shape: fragments ranged from 43.6 to 2,017 µm, films from 42.44 to 2,345 µm, fibers from 60.58 to 2,752 µm, and granules from 16.32 to 585 μm (Figure 6c). MP were classified into four size classes, with most particles falling between 20 and 200 μm (Figure 6c), similar to other research (La et al., 2024; Zhou et al., 2019). The analyzed MP covered a wide size range from 20 to 3,000 μm, which may explain the higher abundance values compared to studies that only characterized MP larger than 1 mm, (Piehl et al., 2018). Over 80% of the extracted MP from the three soil uses measured less than 500 μm, aligning with the other studies in Chinese agricultural uses (Ling et al., 2023; Wang et al., 2021). This degradation of plastic particles and debris into smaller pieces may be due to physical forces like compaction, friction, and soil tillage (Guo et al., 2023) or environmental influences such as weathering over a relatively brief time (Yoon et al., 2024).

In the present study, black, white, and transparent MP were the most common pieces across all three land uses (Figure 6a). Related results were reported by La et al. (2024). The color of MP particles may reveal their font (Akca et al., 2024). Black MP may originate from agricultural mulches and fertilizer bags, while white plastics are more common in greenhouses, including white plastic bags, transparent plastic films, and packaging materials (Guo et al., 2023; Wang et al., 2020). Meanwhile, colored MP often derives from fragments of bottles, clothing, and packaging found in everyday life and agricultural production (Ling et al., 2023).

The types of polymers identified using Raman spectroscopy in this study (Figure 4) were also observed in other studies analyzing MP in different land uses (Corradini et al., 2021; Praveena et al., 2023; Yoon et al., 2024). The most prevalent polymers, in order of their abundance, were PP, PET, PE, PVC, PA, PS, and rubber (Figure 4a), similar to findings in a review of 177 articles on MP in agricultural soils (Pérez et al., 2022). The spectra of the polymers found in the samples for each land use (Figure 5) contained the most representative functional groups of the polymers identified in numerous studies (Falakdin et al., 2024). Previous research has shown that agricultural soils mainly contain MP in the form of fibers and granules, with PS, PE, PP, and PET being the most common materials (Ding et al., 2022).

In our study, PP, PET, and PE components were the most abundant polymers identified, accounting for 73.3% of the particles identified (Figure 4). A similar proportion was reported using infrared spectroscopy (Ling et al., 2023). The PP can be attributed to the widespread use of woven sacks in agricultural production and plastic films for mulches (Guo et al., 2023). PET derives from discarded bottle fragments and packaging materials, while PE is commonly found in plastic bags, food packaging, and agricultural films (Ling et al., 2023). These MP types may result from the degradation of larger pieces of conventional plastics that contaminate the environment (Yang et al., 2021b).

The results highlighted a high variety of polymer types, colors, sizes, and shapes of MP found in the study area, with similar proportions across the three land uses studied (Figures 4 and 6). This indicated a somewhat homogeneous contamination process throughout the study area. A similar pattern was reported which found consistent MP characteristics across two metropolitan cities with similar plastic consumption patterns and human activities (Rafique et al., 2020).

4.4. Relating microplastic abundance to soil and terrain attributes and NDVI

In the present study, the correlation results in Figure 7c suggested a weak positive relationship between MP abundance and sand content and a significant negative correlation with clay content and SOM. Similar behavior was, which reported indicating that soils with higher sand content may facilitate MP accumulation, whereas clay-rich soils may retain less MP due to their structure and physical properties (Akca et al., 2024). This observation regarding soil structure was also noted in the PCA (Figure 7a), where the variables clay and microporosity were positively correlated, while sand content and bulk density (Bd) were inversely correlated with these attributes.

In this context, several studies have reported that MP can alter soil structure and microbial activity. The effects of MP on soil attributes were observed, with findings indicating that different concentrations and types of MP added to the soil could slightly increase Bd, although not significantly (Wen et al., 2022). Additionally, the MP affects soil Bd, but these changes depend on the shape, type, and concentration of MP (Souza Machado et al., 2018). These properties can influence water retention capacity and the adsorption of MP by colloidal solids and soluble matter, thereby affecting soil aggregate formation (Wen et al., 2022).

Our results indicated that the abundance of MP in agricultural exhibited a negative correlation with high Bd values and a positive correlation with high total porosity (PT) values (Figure 7a). This suggests that in compacted agricultural uses, MP abundance may be reduced, a trend also (Zhang et al., 2024).

A significant negative correlation was observed between MP abundance and soil chemical properties, such as Mg, Ca, tCEC, eCEC, SBT, and SOM (Figure 7a). The presence of MP may alter cation exchange in the soil due to their large specific surface area and adsorption capacity (He et al., 2018; La et al., 2024), potentially reducing long-term soil fertility and crop health (Souza Machado et al., 2019).

Although a negative correlation between MP abundance and SOM was observed (Figure 7a), the literature presents varying conclusions regarding this relationship. Study found that MP abundance in soil was negatively correlated with SOM stability (Akca et al., 2024). Other found that MP abundance was associated with a decrease in SOM quality, suggesting that MP may interfere with the relationship between organic matter and soil structure (Hu et al., 2022). The MP weathering has the potential to directly and indirectly alter the molecular properties of organic matter (Li et al., 2022; Wen et al., 2022). These changes in MP properties can transform the composition of soil organic matter from simple structures to more complex and aromatic organic compounds, impacting microbial community structure, abundance, biomass, and microbial activity (Liu et al., 2022; Souza Machado et al., 2019; Wang et al., 2019, 2020).

It is important to emphasize that MP effects on soil can vary depending on soil properties (texture, mineralogy, acidity, CEC, among others). These attributes influence soil response mechanisms depending on MP concentration, shape, size, and type (Ingraffia et al., 2022). However, changes in soil attributes will only be gradual and significant when MP concentrations in soil are high, ranging between 0.5% and 2% (Zhou et al., 2021).

Few studies describe any relationship between MP abundance and terrain parameters or vegetation cover. The topography, and slope can influence the movement and accumulation of MP in soil, related to areas with steeper slopes (Hu et al., 2022). In our study, a significant negative relationship was observed between MP abundance and parameters such as the convergence index (CONVERGENCE), plan curvature (HCURV), slope position (RSP), and channel network distance (CHNL_DIST), along with a significant positive correlation with the topographic wetness index (TWI) (Figure 7d). These variables are derived from the digital terrain model (Figure 2b). Thus, the TWI, which reflects the tendency of water to accumulate at lower positions of the landscape (Huang et al., 2024), positively correlates with MP abundance (Figure 7d). Indeed, surface runoff can increase soil erosion and MP mobilization (Rehm et al., 2021). However, in areas with vegetative cover, erosion is generally reduced, which may limit MP mobilization (Akca et al., 2024).

Additionally, parameters modeling terrain curvature (HCURV), slope position (RSP), and surface water dynamics (CONVERGENCE) account for terrain slope and shape (Huang et al., 2024). These parameters were highly correlated in the PCA (Figure 7b), indicating high susceptibility to soil erosion and, MP transport. The negative correlations observed for these terrain attributes (Figure 7d) indicated lower MP abundance on convex slopes and higher positions, such as in summits and shoulders.

Our study is among the first to establish a relationship between soil properties, the normalized difference vegetation index (NDVI), terrain characteristics, and land use (forest, grassland, and agriculture), with the abundance, distribution, and identification of MP in tropical soils. The characterization of MP, including shape, size, and polymer type, can provide insights into their migration mechanisms within the soil (Li et al., 2021). This migration is closely related to particle size, bulk density, and organic matter content, which affect the ability of MP to move through soil pores, thereby altering soil hydrophysical properties (Hu et al., 2022; Souza Machado et al., 2019). In addition, vegetation type and density can act as barriers that limit the surface mobility of MP (Liu et al., 2023).

4.5. Limitations and future research

In this study, we quantified, characterized, and identified MP in three tropical land uses. However, we found that the complexity of the analyzed soil matrix, where mineral components, organic matter, microfauna, and plastic residues interact, posed a significant challenge for MP extraction, quantification, and complete identification with Raman spectrometry. This complexity also affects their mobility and degradation (Zhang et al., 2024). In our study, three density separation solutions ranging from 1.0 to 1.5 g cm^{-3} were used, which means that MP with higher densities were not considered or analyzed.

In addition, seasonal variation in the study area is another factor affecting the distribution and abundance of MP in terms of land use and soil properties (Feng et al., 2023). However, this study did not evaluate seasonal changes, particularly temperature variations, wind direction, and speed, or soil erosion caused by rainfall, which can transport MP and alter their concentrations and spatial variability (Dogra et al., 2024; Li et al., 2021).

Future studies should focus on better understanding MP transport mechanisms via soil erosion and how different agricultural management practices might influence this process, requiring further evaluation of factors such as rainfall (Ling et al., 2023) and atmospheric deposition (Liu et al., 2023) to identify more relevant relationships explaining the influence of these characteristics on MP concentrations across different land uses.

5. CONCLUSION

Microplastic particles were detected in all soil samples collected from a watershed in a tropical zone, encompassing three land use types: forest, grassland, and agriculture. The average

MP abundances were 3,825.9, 2,552.6, and 3,406.6 pieces kg^{-1} for forest, grassland, and agriculture, respectively. A diverse range of MP colors, sizes, shapes, and polymer types were identified, with similar proportions across the different land uses.

The spatial distribution of MP on the watershed was rather heterogeneous, with somewhat higher concentrations in forest and agricultural. Significant correlations between MP abundance and soil and terrain attributes were observed, with positive correlations for topographic wetness index, and negative correlations for clay and soil organic matter content, chemical properties (tCEC, eCEC, SB, Ca, Mg), and convergence index, plan curvature, distance to channel network and relative slope position.

This study provides the first evidence of MP pollution in Brazilian soils under different land uses influenced by diverse agricultural activities, paving the way for future research on the effects of MP on these ecosystems and their relation to soil and terrain attributes.

Acknowledgments

This work was supported by the Federal University of Lavras (UFLA), the Surcolombiana University (USCO), the National Council for Scientific and Technological Development (CNPq) (processes: 307950/2021-2 and 307059/2022-7), the Foundation for Research Support of the State of Minas Gerais (FAPEMIG) (processes: APQ 00802-18), and the Coordination for the Improvement of Personnel (CAPES) (code 001) The authors would to thank the Laboratory of Electron Microscopy and Analysis of the Ultrastructural Federal University of Lavras.

REFERENCES

Akca, H., Albayrak, R., Onur, M., Gündo, S., 2024. An evaluation on microplastic accumulations in Turkish soils under different land uses. Sci. Total Environ. 911. https://doi.org/10.1016/j.scitotenv.2023.168609

Alvares, C.A., Stape, J.L., Sentelhas, P.C., De Moraes Gonçalves, J.L., Sparovek, G., 2013. Köppen's climate classification map for Brazil. Meteorol. Zeitschrift 22, 711–728. https://doi.org/10.1127/0941-2948/2013/0507

Amjad, M., Huang, Q., Khan, S., Wang, Q., Huang, J., Fahad, X., Sajjad, M., Liu, Y., Mašek, O., Li, X., Wang, J., Xiaomao, C., 2023. Abundance, spatial distribution, and characteristics of microplastics in agricultural soils and their relationship with contributing factors. Rev. Gestão Ambient. 328. https://doi.org/https://doi.org/10.1016/j.jenvman.2022.117006

Arevalo-Hernandez, J.J., Barrera, D.B.A., Avanzi, J.C., Cirillo, M.A., Silva, M.L.N., 2025a. Plastic Debris in Agroecosystems : Distribution and Abundance Patterns , and Relationship with Terrain Characteristics in Southeastern Brazil. ACS OMEGA. https://doi.org/10.1021/acsomega.4c10678

Arevalo-Hernandez, J.J., Barrera, D.B.D.A., Curi, N., Avanzi, J.C., Silva, N.L.M., 2025b. A Method for the Extraction and Analysis of Microplastics from Tropical Agricultural Soils in Southeastern Brazil. Soil Syst. 9, 1–20. https://doi.org/https://doi.org/10.3390/soilsystems9020034

Berenstein, G., Córdoba, P., Díaz, Y.B., González, N., Ponce, M.B., Montserrat, J.M., 2024. Macro, meso, micro and nanoplastics in horticultural soils in Argentina: Abundance, size distribution and fragmentation mechanism. Sci. Total Environ. 906. https://doi.org/10.1016/j.scitotenv.2023.167672

Brandes, E., Henseler, M., Kreins, P., 2021. Identifying hot-spots for microplastic contamination in agricultural soils - A spatial modelling approach for Germany. Environ. Res. Lett. 16. https://doi.org/10.1088/1748-9326/ac21e6

Büks, F., Kaupenjohann, M., 2020. Global concentrations of microplastics in soils - A review. Soil 6, 649–662. https://doi.org/10.5194/soil-6-649-2020

Campanale, C., Galafassi, S., Savino, I., Massarelli, C., Ancona, V., Volta, P., Felice, V., 2022. Microplastics pollution in the terrestrial environments : Poorly known diffuse sources and implications for plants. Sci. Total Environ. 805, 150431. https://doi.org/https://doi.org/10.1016/j.scitotenv.2021.150431

Castelvetro, V., Corti, A., Biale, G., Ceccarini, A., Degano, I., Nasa, J. La, 2021. New methodologies for the detection, identification, and quantification of microplastics and their environmental degradation by-products. Environ. Sci. Pollut. Res. 28, 46764–46780. https://doi.org/10.1007/s11356-021-12466-z

Conrad, O., Bechtel, B., Bock, M., Dietrich, H., Fischer, E., Gerlitz, L., Wehberg, J., Wichmann, V., Böhner, J., 2015. System for Automated Geoscientific Analyses (SAGA) v. 2.1.4. Goesei. Model Dev. 8, 1991–2007. https://doi.org/10.5194/gmd-8-1991-2015

Corradini, F., Casado, F., Leiva, V., Huerta-lwanga, E., Geissen, V., 2021. Microplastics occurrence and frequency in soils under different land uses on a regional scale. Sci. Total Environ. 752, 141917. https://doi.org/10.1016/j.scitotenv.2020.141917

Corradini, F., Meza, P., Eguiluz, R., Casado, F., Huerta-Lwanga, E., Geissen, V., 2019. Evidence of microplastic accumulation in agricultural soils from sewage sludge disposal. Sci. Total Environ. 671, 411–420. https://doi.org/10.1016/j.scitotenv.2019.03.368

Dane, J.H., Topp, G.C., 2002. Methods of soil analysis: Physical methods, Soil Scien. ed. Madison.

Dantas, A.A.A., Carvalho, L.G. de, Ferreira, E., 2007. Classificação e tendências climáticas em Lavras, MG. Ciência e Agrotecnologia 31, 1862–1866. https://doi.org/10.1590/s1413-70542007000600039

Ding, F., Jones, D.L., Chadwick, D.R., Kim, P.J., Jiang, R., Flury, M., 2022. Environmental impacts of agricultural plastic film mulch: Fate, consequences, and solutions. Sci. Total Environ. 836, 1–4. https://doi.org/10.1016/j.scitotenv.2022.155668

Dogra, K., Kumar, M., Deoli Bahukhandi, K., Zang, J., 2024. Traversing the prevalence of microplastics in soil-agro ecosystems: Origin, occurrence, and pollutants synergies. J. Contam. Hydrol. 266. https://doi.org/10.1016/j.jconhyd.2024.104398

Falakdin, P., Lopez-Rosales, A., Andrade, J., Terzaghi, E., Di Guardo, A., Muniategui-Lorenzo, S., 2024. Comparison of microplastic type, size, and composition in atmospheric and foliage samples in an urban scenario. Environ. Pollut. 349, 123911. https://doi.org/10.1016/j.envpol.2024.123911

Feng, S., Lu, H., Yao, T., 2023. Effects of multiple environmental factors and land use patterns on microplastic distribution in the topsoil of the Qinghai and Sichuan provinces of China. J. Environ. Chem. Eng. 11, 109657. https://doi.org/10.1016/j.jece.2023.109657

Gerolin, R.C., Pupim, N.F., Sawakuchi, O.A., Grohmann, H.C., Labuto, G., Semensatto, D., 2020. Microplastics in sediments from Amazon rivers, Brazil. Sci. Total Environ. 749, 2016–2021. https://doi.org/10.1016/j.scitotenv.2020.141604

González-Córdova, J.A., Ariza-flores, D., Pérez-huerta, J.S., Madrigal-melchor, J., 2023. Optical anisotropy Raman response of polyethylene terephthalate strained thin films. Phys. B Condens. Matter 654, 414693. https://doi.org/10.1016/j.physb.2023.414693

Grause, G., Kuniyasu, Y., Chien, M., Inoue, C., 2022. Separation of microplastic from soil by centrifugation and its application to agricultural soil. Chemosphere 288, 132654. https://doi.org/10.1016/j.chemosphere.2021.132654

Guimarães, A., Moraes, B.R. De, Ando, R.A., Perotti, G.F., Sampaio, B., Anna, S., Hattori, G.Y., Macrobrachium, O., 2024. Is the shrimp Macrobrachium amazonicum sold in an urban center in the central Brazilian Amazon contaminated with microplastics ? Acta Amaz. 54. https://doi.org/10.1590/1809-4392202402002

Guo, J., Huang, X., Xiang, L., Wang, Y., Li, Y., Li, H., Cai, Q., 2020. Source, migration, and toxicology of microplastics in soil. Environ. Int. 137, 105263. https://doi.org/10.1016/j.envint.2019.105263

Guo, S., Zhang, J., Liu, J., Guo, N., Zhang, L., Wang, S., Wang, X., Zhao, M., 2023. Organic fertilizer and irrigation water are the primary sources of microplastics in the facility soil, Beijing. Sci. Total Environ. 895, 165005. https://doi.org/10.1016/j.scitotenv.2023.165005

He, D., Luo, Y., Lu, S., Liu, M., Song, Y., Lei, L., 2018. Microplastics in soils: Analytical methods, pollution characteristics, and ecological risks. TrAC Trends Anal. Chem. 109, 163–172. https://doi.org/10.1016/j.trac.2018.10.006

Hossain, M.N., Rahman, M.M., Afrin, S., Akbor, M.A., Bakar, S.A., Malafaia, G., 2023. Identification and quantification of microplastics in agricultural farmland soil and textile sludge in Bangladesh. Sci. Total Environ. 858. https://doi.org/10.1016/j.scitotenv.2022.160118

Hu, J., He, D., Zhang, X., Li, X., Chen, Y., Gao, W., 2022a. National-scale distribution of micro (meso) plastics in farmland soils across China : Implications for environmental impacts. J. Hazard. Mater. 424, 127283. https://doi.org/https://doi.org/10.1016/j.jhazmat.2021.127283

Huang, D., Wang, X., Yin, L., Chen, S., Tao, J., Zhou, W., Chen, H., Zhang, G., Xiao, R., 2022. Research progress of microplastics in soil-plant system : Ecological effects and potential risks. Sci. Total Environ. 812. https://doi.org/10.1016/j.scitotenv.2021.151487

Huang, D., Zhao, X., Yin, Z., Qin, W., 2024. Utilizing geodetectors to identify conditioning factors for gully erosion risk in the black soil region of northeast China. Int. Soil Water Conserv. Res. 12, 808–827. https://doi.org/10.1016/j.iswcr.2024.07.004

Ingraffia, R., Amato, G., Bagarello, V., Carollo, F.G., Giambalvo, D., Iovino, M., Lehmann, A., Rillig, M.C., Frenda, A.S., 2022. Polyester microplastic fibers affect soil physical properties and erosion as a function of soil type. SOIL 8, 421–435. https://doi.org/10.5194/soil-8-421-2022, 2022.

IUSS Working Group WRB, 2022. World reference base for soil resources. International soil classification system for naming soils and creating legends for soil maps., 4th ed. International Union of Soil Sciences (IUSS), Vienna, Austria.

Kemper, W.D., Rosenau, R.C., 1986. Aggregate Stability and Size Distribution, Klute, A. ed, Methods of Soil Analysis: Part 1 Physical and Mineralogical Methods. Second Edition.

Klaus, J., Seeger, M., Bigalke, M., Weber, C.J., 2024. Microplastics in vineyard soils: First insights from plastic-intensive viticulture systems. Sci. Total Environ. 947, 174699. https://doi.org/10.1016/j.scitotenv.2024.174699

La, Y., Zhang, L., Zhao, N., Ye, H., Zeng, Q., Zhao, L., Wang, Z., Lin, D., Wang, R., 2024. The microplastics distribution characteristics and their impact on soil physicochemical properties and bacterial communities in food legumes farmland in northern China. J. Hazard. Mater. 471, 134282. https://doi.org/10.1016/j.jhazmat.2024.134282

Li, H., Lu, X., Wang, S., Zheng, B., Xu, Y., 2021. Vertical migration of microplastics along soil profile under different crop root systems. Environ. Pollut. 278. https://doi.org/10.1016/j.envpol.2021.116833

Li, J., Song, Y., Cai, Y., 2020. Focus topics on microplastics in soil: Analytical methods, occurrence, transport, and ecological risks. Environ. Pollut. 257, 113570. https://doi.org/10.1016/j.envpol.2019.113570

Li, P., Li, Q., Hao, Z., Yu, S., Liu, J., 2020. Analytical methods and environmental processes of nanoplastics. J. Environ. Sci. (China) 94, 88–99. https://doi.org/10.1016/j.jes.2020.03.057

Li, R., Xi, B., Tan, W., Yuan, Y., 2022. Spatiotemporal heterogeneous effects of microplastics input on soil dissolved organic matter (DOM) under field conditions. Sci. Total Environ. 847. https://doi.org/10.1016/j.scitotenv.2022.157605

Li, S., Ding, F., Flury, M., Wang, Z., Xu, L., Li, Shuangyi, Jones, D.L., Wang, J., 2022. Macro- and microplastic accumulation in soil after 32 years of plastic film mulching. Environ. Pollut. 300. https://doi.org/10.1016/j.envpol.2022.118945

Li, W., Wufuer, R., Duo, J., Wang, S., Luo, Y., Zhang, D., Pan, X., 2020. Microplastics in agricultural soils: Extraction and characterization after different periods of polythene film mulching in an arid region. Sci. Total Environ. 749, 141420. https://doi.org/10.1016/j.scitotenv.2020.141420

Li, Y., Yao, J., Nie, P., Feng, X., Liu, J., 2021. An effective method for the rapid detection of microplastics in soil. Chemosphere 276, 128696. https://doi.org/https://doi.org/10.1016/j.chemosphere.2020.128696

Ling, Q., Yang, B., Jiao, J., Ma, X., Zhao, W., Zhang, X., 2023. Response of microplastic occurrence and migration to heavy rainstorm in agricultural catchment on the Loess plateau. J. Hazard. Mater. 460, 132416. https://doi.org/10.1016/j.jhazmat.2023.132416

Liu, H., Sun, K., Liu, X., Yao, R., Cao, W., Zhang, L., Wang, X., 2022. Spatial and temporal distributions of microplastics and their macroscopic relationship with algal blooms in Chaohu Lake, China. J. Contam. Hydrol. 248. https://doi.org/10.1016/j.jconhyd.2022.104028

Liu, M., Song, Y., Lu, S., Qiu, R., Hu, J., Li, X., Bigalke, M., Shi, H., He, D., 2019. A method for extracting soil microplastics through circulation of sodium bromide solutions. Sci. Total Environ. 691, 341–347. https://doi.org/https://doi.org/10.1016/j.scitotenv.2019.07.144

Liu, Yixuan, Liu, Yaxing, Li, Y., Bian, P., Hu, Y., Zhang, J., Shen, W., 2023. Effects of irrigation on the fate of microplastics in typical agricultural soil and freshwater environments in the upper irrigation area of the Yellow River. J. Hazard. Mater. 447, 130766. https://doi.org/10.1016/j.jhazmat.2023.130766

Liu, Z., Cai, L., Dong, Q., Zhao, X., Han, J., 2022. Effects of microplastics on water infiltration in agricultural soil on the Loess Plateau, China. Agric. Water Manag. 271. https://doi.org/10.1016/j.agwat.2022.107818

Lwanga, E.H., Beriot, N., Corradini, F., Silva, V., Yang, X., Baartman, J., Rezaei, M., van Schaik, L., Riksen, M., Geissen, V., 2022. Review of microplastic sources, transport pathways and correlations with other soil stressors: a journey from agricultural sites into the environment. Chem. Biol. Technol. Agric. 9, 1–20. https://doi.org/10.1186/s40538-021-00278-9

Munno, K., De Frond, H., O'Donnell, B., Rochman, C.M., 2020. Increasing the accessibility for characterizing microplastics: introducing new application-based and spectral libraries of plastic particles (SLoPP and SLoPP-E). Anal. Chem. 92, 2443–2451. https://doi.org/10.1021/acs.analchem.9b03626

Nizzetto, LuABNT, 2022ca, Futter, M., Langaas, S., 2016. Are Agricultural Soils Dumps for Microplastics of Urban Origin? Environ. Sci. Technol. 50, 10777–10779. https://doi.org/10.1021/acs.est.6b04140

OriginPro Lab Corporation, 2024. OriginPro.

Orona, N.C., García, M.R., Loge, F.J., Mahlknecht, J., Aguilar-Hernández, I., Ornelas-Soto, N., 2022. Microplastics in Latin America and the Caribbean: A review on current status and perspectives. J. Environ. Manage. 309. https://doi.org/10.1016/j.jenvman.2022.114698

Padha, S., Kumar, R., Dhar, A., Sharma, P., 2022. Microplastic pollution in mountain terrains and foothills: A review on source, extraction, and distribution of microplastics in remote areas. Environ. Res. 207, 112232. https://doi.org/10.1016/j.envres.2021.112232

Paes, E. da S., Gloaguen, T.V., Silva, H. dos A. da C., Duarte, T.S., de Almeida, M. da C., Costa, O.D.A.V., Bomfim, M.R., Santos, J.A.G., 2022. Widespread microplastic pollution in mangrove soils of Todos os Santos Bay, northern Brazil. Environ. Res. 210. https://doi.org/10.1016/j.envres.2022.112952

Pérez, R.R., Álvarez, M.S.J., Kropp, R.M., Perdomo, G, A., Hernandez, B.J., Díaz, F.J., 2022. Microplastics in Agricultural Systems : Analytical Methodologies and Effects on Soil Quality and Crop Yield. Agriculture 12, 1162. https://doi.org/10.3390/agriculture12081162

Phan, S., Padilla-Gamiño, J.L., Luscombe, C.K., 2022. The effect of weathering environments on microplastic chemical identification with Raman and IR spectroscopy: Part I. polyethylene and polypropylene. Polym. Test. 116. https://doi.org/10.1016/j.polymertesting.2022.107752

Piehl, S., Leibner, A., Löder, M.G.J., Dris, R., Bogner, C., Laforsch, C., 2018. Identification and quantification of macro- and microplastics on an agricultural farmland. Sci. Rep. 8, 1–9. https://doi.org/10.1038/s41598-018-36172-y

Prajapati, A., Jadhao, P.S., Khare, A., Vaidya, A.N., Kumar, A.R., Das, S., 2023. Characterization of Microplastics and Associated Heavy Metals in Urban Soils Affected by Anthropogenic Littering: Distribution, Spatial Variation, and Influence of Soil Properties. Soil Sediment Contam. 00, 1–29. https://doi.org/10.1080/15320383.2023.2286524

Praveena, S.M., Aiman, M.I.F., Nafisyah, A.L., 2023. Microplastics pollution in agricultural farms soils : preliminary findings from tropical environment (Klang. Environ. Monit. Assess. 195. https://doi.org/10.1007/s10661-023-11250-5

QGIS Development Team, 2024. QGIS Geographic Information System versão 3.28.2 Firenze.

Quinn, B., Murphy, F., Ewins, C., 2016. Validation of density separation for the rapid recovery of microplastics from sediment. Anal. Methods 9, 1491–1498. https://doi.org/https://doi.org/10.1039/C6AY02542K

R Core Team, 2024. R: A language and environment for statistical computing. R Foundation for Statistical Computing.

Radford, F., Zapata-Restrepo, L.M., Horton, A.A., Hudson, M.D., Shaw, P.J., Williams, I.D., 2021. Developing a systematic method for extraction of microplastics in soils. Anal. Methods 13, 1695–1705. https://doi.org/10.1039/d0ay02086a

Rafique, A., Irfan, M., Mumtaz, M., Qadir, A., 2020. Spatial distribution of microplastics in soil with context to human activities: a case study from the urban center. Environ. Monit. Assess. 192. https://doi.org/10.1007/s10661-020-08641-3

Rehm, R., Zeyer, T., Schmidt, A., Fiener, P., 2021. Soil erosion as transport pathway of microplastic from agriculture soils to aquatic ecosystems. Sci. Total Environ. 795. https://doi.org/10.1016/j.scitotenv.2021.148774

Rillig, M.C., Kim, S.W., Zhu, Y.G., 2023. The soil plastisphere. Nat. Rev. Microbiol. 1–11. https://doi.org/10.1038/s41579-023-00967-2

Samanta, P., Dey, S., Kundu, D., Dutta, D., Jambulkar, R., Mishra, R., Ghosh, A.R., Kumar, S., 2022. An insight on sampling, identification, quantification and characteristics of microplastics in solid wastes. Trends Environ. Anal. Chem. 36. https://doi.org/10.1016/j.teac.2022.e00181

Sarkar, A., Deb, S., Ghosh, S., Mandal, S., Quazi, S.A., Kushwaha, A., Hoque, A., Choudhury, A., 2022. Impact of anthropogenic pollution on soil properties in and around a town in Eastern India. Geoderma Reg. 28, e00462. https://doi.org/10.1016/j.geodrs.2021.e00462

Sarti, F.M.E., De Souza, G.A., da Silva, B.R., dos Santos, R.D., 2022. Municipal Park Grounds and Microplastics Contamination. J. Polym. Environ. 30, 5202–5210. https://doi.org/https://doi.org/10.1007/s10924-022-02580-5

Silva, B.M., Santos, W.J.R., Marques, J.J., 2014. Detailed Soil Survey of Muquém Farm / UFLA, Lavras- MG, Boletim Té. ed. Lavras MG, Brazil.

Silva, A.E. da, Fontana, A., Melo, A. da S., Martins, A.L. da S., Inda, A.V., Santi, A., Madari, B.E., Mattos, B.B., Almeida, B.G. de, Alves, B.J.R., Jantalia, C.P., Pérez, D.V., Campos, D.V.B. de, Villani, E.M. de A., Martins, E. de S., Oliveira, E.M. de, 2017. Manual de métodos de análise de solo, Empresa Br. ed. Rio de Janeiro.

Sobhani, Z., Amin, A., Naidu, R., Megharaj, M., Fang, C., 2019. Identification and visualisation of microplastics by Raman mapping. Anal. Chim. Acta 1077, 191–199. https://doi.org/10.1016/j.aca.2019.05.021

Souza Machado, Abel, A., Hempel, S., Rillig, M.C., Kloas, W., Zarfl, C., 2017. Microplastics as an emerging threat to terrestrial ecosystems. Glob. Chang. Biol. 24, 1405–1416. https://doi.org/10.1111/gcb.14020

Souza Machado, Abel, A., Lau, C.W., Kloas, W., Bergmann, J., 2019. Microplastics Can Change Soil Properties and A ff ect Plant Performance. Environ. Sci. Technol. 53, 6044–6052. https://doi.org/10.1021/acs.est.9b01339

Souza Machado, Abel, A., Lau, C.W., Till, J., Kloas, W., Lehmann, A., Becker, R., Rillig, M.C., 2018. Impacts of Microplastics on the Soil Biophysical Environment. Environ. Sci. Technol. 52, 9656–9665. https://doi.org/10.1021/acs.est.8b02212

Sunaga, N., Okochi, H., Niida, Y., Miyazaki, A., 2024. Alkaline extraction yields a higher number of microplastics in forest canopy leaves : implication for microplastic storage. Environ. Chem. Lett. 22, 1599–1606. https://doi.org/10.1007/s10311-024-01725-3

Teixeira, C.P., Donagemma, G.K., Fontana, A., Teixeira, G.W., 2017. Manual de métodos de análise de solo, 3 ed revis. ed. EMBRAPA, Brasilia DF.

Thomas, D., Schutze, B., Heinze, W.M., Steinmetz, Z., 2020. Sample Preparation Techniques for the Analysis of Microplastics in soil- A Review. Sustainability 12, 9074. https://doi.org/10.3390/su12219074

Wang, J., Li, J., Liu, S., Li, H., Chen, X., Peng, C., Zhang, P., Liu, X., 2021. Distinct microplastic distributions in soils of different land-use types : A case study of Chinese farmlands *. Environ. Pollut. 269, 116199. https://doi.org/https://doi.org/10.1016/j.envpol.2020.116199

Wang, J., Liu, X., Li, Y., Powell, T., Wang, X., Wang, G., Zhang, P., 2019. Microplastics as contaminants in the soil environment : A mini-review. Sci. Total Environ. 691, 848–857. https://doi.org/10.1016/j.scitotenv.2019.07.209

Wang, K., Chen, W., Tian, J., Niu, F., Xing, Y., Wu, Y., Zhang, R., Zheng, J., Xu, L., 2022. Accumulation of microplastics in greenhouse soil after long-term plastic film mulching in Beijing, China. Sci. Total Environ. 828. https://doi.org/10.1016/j.scitotenv.2022.154544

Wang, W., Ge, J., Yu, X., Li, H., 2020. Environmental fate and impacts of microplastics in soil ecosystems : Progress and perspective. Sci. Total Environ. 708, 134841. https://doi.org/10.1016/j.scitotenv.2019.134841

Wang, X., Feng, Q., Yang, L., Li, M., Zhao, F., Tang, J., Bu, Q., Zhang, Y., Chen, L., 2025. Effect of land use on occurrence and spatial variability of soil microplastics in agricultural watershed. Ecol. Front. https://doi.org/10.1016/j.ecofro.2024.12.005

Weber, C.J., Opp, C., Prume, J.A., Koch, M., Andersen, T.J., Chifflard, P., 2021. Deposition and in-situ translocation of microplastics in floodplain soils. Sci. Total Environ. 152039. https://doi.org/10.1016/j.scitotenv.2021.152039

Weber, C.J., Santowski, A., Chifflard, P., 2022. Investigating the dispersal of macro- and microplastics on agricultural fields 30 years after sewage sludge application. Sci. Rep. 12, 1–13. https://doi.org/10.1038/s41598-022-10294-w

Wen, X., Yin, L., Zhou, Z., Kang, Z., Sun, Q., Zhang, Y., 2022. Microplastics can affect soil properties and chemical speciation of metals in yellow-brown soil. Ecotoxicol. Environ. Saf. 243, 113958. https://doi.org/10.1016/j.ecoenv.2022.113958

Xiang, Y., Jiang, L., Zhou, Y., Luo, Z., Zhi, D., Yang, J., Lam, S.S., 2022. Microplastics and environmental pollutants: Key interaction and toxicology in aquatic and soil environments. J. Hazard. Mater. 422. https://doi.org/10.1016/j.jhazmat.2021.126843

Xiaoting, Z., Yingxin, C., Xinyu, L., Yalin, Z., Wei, G., Jie, J., Aoyun, M., Defu, H., 2022. Size_shape-dependent migration of microplastics in agricultural soil under simulative and natural rainfall. Sci. Total Environ. 815, 152507. https://doi.org/https://doi.org/10.1016/j.scitotenv.2021.152507.

Yang, J., Li, L., Li, R., Xu, L., Shen, Y., Li, S., Tu, C., Wu, L., Christie, P., Luo, Y., 2021a. Microplastics in an agricultural soil following repeated application of three types of sewage sludge : A field study ☆. Environ. Pollut. 289, 117943. https://doi.org/https://doi.org/10.1016/j.envpol.2021.117943

Yang, J., Li, R., Zhou, Q., Li, L., Li, Y., Tu, C., Zhao, X., 2021b. Abundance and morphology of microplastics in an agricultural soil following long-term repeated application of pig manure *. Environ. Pollut. 272, 116028. https://doi.org/https://doi.org/10.1016/j.envpol.2020.116028

Yoon, J.H., Kim, B.H., Kim, K.H., 2024. Distribution of microplastics in soil by types of land use in metropolitan area of Seoul. Appl. Biol. Chem. 67. https://doi.org/10.1186/s13765-024-00869-8

Yu, L., Zhang, J. Di, Liu, Y., Chen, L.Y., Tao, S., Liu, W.X., 2021. Distribution characteristics of microplastics in agricultural soils from the largest vegetable production base in China. Sci. Total Environ. 756, 1–9. https://doi.org/10.1016/j.scitotenv.2020.143860

Zhang, F., Yang, X., Zhang, Z., 2024. Effects of soil properties and land use patterns on the distribution of microplastics: A case study in southwest China. J. Environ. Manage. 356, 120598. https://doi.org/10.1016/j.jenvman.2024.120598

Zhang, G.S., Liu, Y.F., 2018. The distribution of microplastics in soil aggregate fractions in southwestern China. Sci. Total Environ. 642, 12–20. https://doi.org/10.1016/j.scitotenv.2018.06.004

Zhang, Y., Wang, K., Chen, Weizhi, Ba, Y., Khan, K., Chen, Wei, Tu, C., 2022. Effects of land use and landscape on the occurrence and distribution of microplastics in soil , China. Sci. Total Environ. 847. https://doi.org/10.1016/j.scitotenv.2022.157598

Zhou, J., Gui, H., Banfield, C.C., Wen, Y., Zang, H., Dippold, M.A., Charlton, A., Jones, D.L., 2021. The microplastisphere: Biodegradable microplastics addition alters soil microbial community structure and function. Soil Biol. Biochem. 156. https://doi.org/10.1016/j.soilbio.2021.108211

Zhou, Yujie, Jia, Z., Zheng, G., Chen, L., Zhang, Q., Su, B., Zhou, S., 2023. Microplastics in agricultural soils on the coastal plain : Spatial characteristics , influencing factors and sources. Sci. Total Environ. 901, 1–12. https://doi.org/https://doi.org/10.1016/j.scitotenv.2023.165948

Zhou, Yang, Jing, J., Yu, R., Zhao, Y., Gou, Y., Zhang, Z., Tang, H., Zhang, H., Huang, Y., 2023. Microplastics in plateau agricultural areas: Spatial changes reveal their source and distribution characteristics. Environ. Pollut. 319, 121006. https://doi.org/10.1016/j.envpol.2023.121006

Zhou, Y., Liu, X., Wang, J., 2019. Characterization of microplastics and the association of heavy metals with microplastics in suburban soil of central China. Sci. Total Environ. 694, 133798. https://doi.org/10.1016/j.scitotenv.2019.133798

This paper was submitted and is under review in the journal Geoderma regional

PAPER 4 – SPATIAL DISTRIBUTION AND GEOSTATISTICAL PREDICTION OF MICROPLASTIC ABUNDANCE IN TROPICAL SOILS IN SOUTHEASTERN BRAZIL

ABSTRACT

Research on microplastics (MP) in agricultural soils has received increasing attention due to their potential ecological risks and adverse effects on the food chain. Recently, geostatistical approaches have been increasingly used to assess the spatial distribution of MP in soils. Therefore, this study aims to predict the abundance of MP in the soil of an agricultural watershed using geostatistical methods and to produce a continuous map of the interpolated MP. Soil samples were collected, and MP abundance was determined using the density separation method. Subsequently, an exploratory data analysis was conducted, followed by the construction of the empirical semivariogram, theoretical variogram model fitting, ordinary kriging interpolation, and cross-validation. MP were detected in all samples, with average abundances of 3,826, 2,553, and 3,407 pieces kg^{-1} in forest, grassland, and agricultural land use systems, respectively. The experimental semivariogram showed that the spatial distribution of MP has a strong spatial dependence structure, which follows the Gaussian model. The Kriging map showed a distribution of MP in the range of 600 to 7,400 pieces kg^{-1}, with higher concentrations of MP for forest and agricultural areas. Additionally, the map reveals a high abundance of MP, with greater concentrations in depressions and areas near roads and urban centers, allowing for identifying critical points within the watershed. This study offers important insights into the presence of MP across various land uses, emphasizing the need for proactive measures to prevent and mitigate their accumulation in soils.

Keywords: Agricultural soil, Diffuse pollution, Geostatistics, Kriging, Polymers.

1. INTRODUCTION

Microplastics (MP) are pervasive pollutants in aquatic and terrestrial ecosystems (Li et al., 2023). They originate from plastic waste that degrades over time through ultraviolet radiation, mechanical wear, thermo-oxidative processes, and biological activity (Hossain et al., 2024; Zhou et al., 2020). With particle sizes ranging from <5 mm to 1 µm (Kumar et al., 2021; Shi et al., 2023; Weber et al., 2022), MP are highly persistent in the environment (Chamas et al., 2020) and can alter key properties of agricultural soils (Souza Machado et al., 2018; Yan et al., 2022). Additionally, they pose potential risks to soil fauna, microorganisms, and crop growth (Ding et al., 2022).

The identification and quantification of microplastics (MP) are crucial for evaluating their environmental impact. Despite growing research interest, there is still a lack of standardized methodologies for assessing MP abundance and spatial distribution in environmental matrices (Radford et al., 2021). Among the existing approaches, the most commonly employed method for isolating MPs from soil is density separation using high-density saline solutions (Grause et al., 2022; Li et al., 2020; Quinn et al., 2016), typically followed by filtration and retention of the particles on filter (Thomas et al., 2020).

Continuing with the identification and quantification process, stereoscopic microscopy is used to count and characterize MP based on their color, size, and shape, often assisted by professional imaging software (Samanta et al., 2022; Zhang and Liu, 2018). This is followed by identifying the polymer composition of the MP using non-destructive techniques such as Fourier-transform infrared spectroscopy (FTIR) and Raman spectroscopy (Munno et al., 2020; Souza Machado et al., 2019; Thomas et al., 2020).

Georeferencing techniques are commonly used to map the spatial distribution of MP isolated from soil, typically through point spatial analysis (Zhou et al., 2023b), which represents only the exact locations of the quantities or masses of MP. Leitão et al. (2023) spatially mapped the concentration of MP in Coimbra, a municipality in central Portugal.

Kriging interpolation can also be applied to map the spatial distribution of MP, as demonstrated by Liu et al. (2022) in a study of MP isolated from water and sediment samples in Chaohu Lake, China. Another method for mapping MP is the Inverse Distance Weighting (IDW) technique, as employed by Zhou et al. (2023) in surface agricultural soils in the Huangshui watershed, located in the northeastern Qinghai-Tibet Plateau. The results indicated that microplastic pollution is concentrated in densely populated and agricultural areas.

Recent studies highlight the urgent need to prioritize research on MP in agroecosystems (Zhou et al., 2023). However, the spatial distribution of MP in Brazilian agricultural soils remains largely unexplored (Sarti et al., 2022; Silva et al., 2022; Wrigley et al., 2024). The lack of studies on the spatial distribution of MP limits the understanding of their distribution patterns in tropical agricultural soils according to land use and potential environmental risks. It also hinders the development of effective mitigation strategies and the identification of critical hotspots where MP accumulates in tropical soils. Therefore, this study aims to analyze MP abundance in the soil based on land use and predict their spatial distribution within a watershed. MP was collected using a georeferenced sampling grid in the 0–20 cm soil layer, allowing the construction of a spatial distribution map through geostatistical methods for three land use types: forest, grassland, and agricultural land.

2. MATERIALS AND METHODS

2.1 Description of study area

The study area is located in a watershed within the Rio Grande basin, encompassing the Muquém Experimental Farm of the Federal University of Lavras (UFLA). This area covers approximately 165 hectares and features a diversified land use system comprising forest, grassland, and agricultural land (Figure 1). It is situated at a latitude of -21°12'037"S and a longitude of -44°59'3.77"W (WGS 84 UTM), with elevations ranging from 877 m to 1,040 m.

The characteristics of the study site have already been detailed in Arevalo-Hernandez et al. (2025). Soil classification in the study area indicates that the major soil orders in the sub-watershed, according to WRB-FAO (IUSS Working Group WRB, 2022) correspond to Cambisols (CX), which occupy 18.84 ha (11,41% of the area), Gleysols (GM) which occupy 1.92 ha (1.16% of the area), Ferrasols (LVA) occupy 63.60 ha (38.50%), Nitisols (NX) 8.30 ha (5.02%), Acrisols (PVA) 58.07 ha (35.15% of the area), and Leptsols (RL) 14.48 ha, representing 8.76% of the total area.

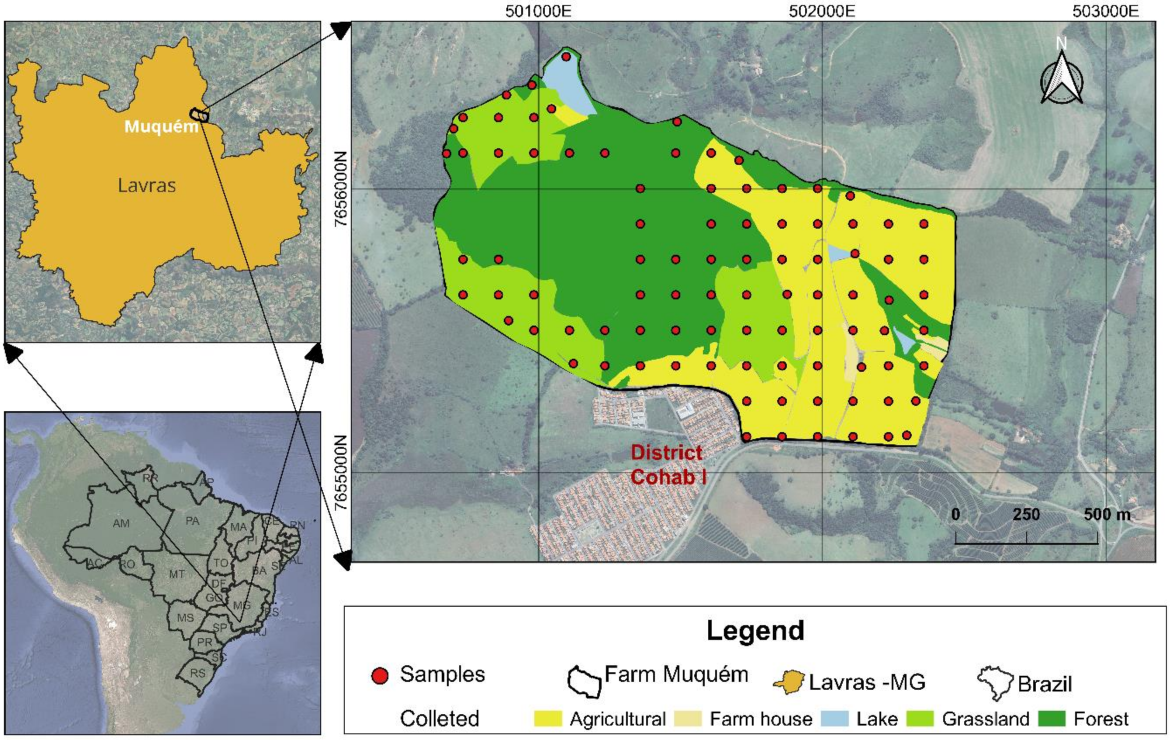

Figure 1. Map of the study area, land use, and geographic position of the sampled points at sub-basin from Muquém farm, municipality of Lavras, Brazil.

Land use in the watershed was classified into three main categories: agricultural, grasslands, and forests (Figure 1). Agricultural land accounts for 30.1% of the total area, with annual crops covering 29.2%, including corn (Zea mays L.), soybean (Glycine max (L.) Merrill), wheat (Triticum aestivum L.), common bean (Phaseolus vulgaris L.), sorghum (Sorghum bicolor (L.) Moench), and rice (Oryza sativa L.). Perennial crops, primarily coffee (Coffea arabica), occupy 0.9% of the area.

Grasslands represent the most extensive land use, covering 44% of the watershed. This includes 39.3% planted pastures (Brachiaria sp.) and 4.7% native grasslands. Forests occupy 24.4% of the area, comprising both planted eucalyptus (Eucalyptus sp.) and native forests. The remaining 1.5% of the area is allocated to water reservoirs and built-up areas.

2.2 Soil collection and sampling

Soil sampling was conducted between August 2022 and April 2023, following a predefined regular grid of 91 georeferenced points across a total area of 165 hectares. This resulted in a sampling density of 1.77 ha per sample, with a spatial resolution of 125 m × 125 m (Figure 1). Each sample consisted of three subsamples collected approximately 70 cm apart to ensure representativity. In terms of land use distribution, the regular grid enabled the collection of 19 samples from the forest area, 27 from the grassland area, and 45 from the agricultural area.

Some areas of the watershed were not sampled (Figure 1) due to steep slopes and high-density forest vegetation, which made access and sampling considerably challenging. Samples were collected from the 0–20 cm soil layer, with 100 g of soil taken from each point and stored in glass jars labeled with the corresponding grid point code. These samples were then transported to the laboratory for further analysis.

Each sampling point was georeferenced using a Garmin Oregon® 750 GPS device with 3-meter accuracy. Additionally, the altitude, surrounding vegetation type, and current land use were recorded at each location.

2.3 Separation and extraction of microplastics from the soil

Soil samples collected in the field were initially pretreated through air-drying and sieving using a 2.00 mm mesh. From each sampling point, 10 g of soil were used to conduct the microplastic (MP) extraction and analysis protocol, following the methodology adapted from (Zhou et al., 2019). The process comprised three main stages: (1) organic matter digestion, (2) density-based separation and filtration, and (3) quantification of MPs via optical microscopy.

The first stage involved digesting the organic matter in the soil samples using 10 g of soil and 20 mL of an alkaline solution of KOH: NaClO 30%. This mixture was dispersed in an ultrasonic bath at 35 W and 40 kHz for 5 minutes. After dispersion, the samples were placed in an oven at 50–60°C and manually stirred for 30 seconds every 4 hours until reaching a constant mass.

During the second stage, the separation procedure followed the sequential density gradient protocol detailed in Arevalo-Hernandez et al. (2025b), , the samples were centrifuged in solutions of sequentially increasing density (ρ): distilled water ($\rho = 1.00$ g cm^{-3}), saturated NaCl solution (5.33 mol L^{-1}, $\rho = 1.19$ g cm^{-3}), and $ZnCl_2$ solution (5.06 mol L^{-1}, $\rho = 1.5$ g cm^{-3}). Soil samples treated with distilled water underwent ultrasound dispersion for 5 minutes to separate MP from soil aggregates. Subsequently, the solution was centrifuged at 2500 rpm for

5 minutes. The high speed allowed MP to float in the supernatant, which was then collected with a pipette and filtered using a vacuum pump and a 2 µm membrane filter.

The residual soil was then treated with 20 mL of saturated NaCl solution, dispersed again with ultrasound, and centrifuged at 2,700 rpm for 5 minutes. The supernatant was recovered and filtered as in the previous step. Finally, the same procedure was repeated using the $ZnCl_2$ solution. Each separation step was reiterated until no additional particles were observed in the supernatant. All filters were left to air-dry at ambient temperature (≈23 °C) and subsequently stored in glass containers.

For the third and final stage, MP quantification was carried out using a Nikon Eclipse Ni optical microscope at 10× magnification. Images of the filters were captured with a Nikon DS-Fi3 digital camera and processed using NIS Elements software (version 4.6). MP abundance was reported as the number of particles per kilogram of dry soil, based on manual counting across the total filter surface.

2.4 Laboratory Contamination Prevention and Recovery Tests

To ensure the quality and control of the described procedure, soil samples collected in the field were stored in glass jars, and all materials used in the analysis were made of glass and rinsed with a disinfectant solution (filtered distilled water and 30% ethanol) to prevent contamination. Additionally, researchers wore nitrile gloves and cotton clothing, and laboratory access was restricted to minimize external contamination.

As part of data quality control and to detect potential contamination, the MP extraction process was also applied to five control samples without soil, which were stored in petri dishes and inspected at the end of the analysis (Corradini et al., 2019; Weber et al., 2021).

To assess methodological accuracy, recovery tests were conducted using four clean soil samples from the study area, along with low-density polyethylene (LDPE) and polyvinyl chloride (PVC). The results showed LDPE recovery rates ranging from 81.0% to 98.8%, while PVC recovery rates varied between 59.7% and 75.2% (Arevalo-Hernandez et al., 2025b).

2.5 Abundance and spatial distribution of microplastics

As previously mentioned, a total of 91 soil samples were collected across the study area, each consisting of three sub-samples taken approximately 70 cm apart to ensure representativity. Regarding land use distribution, 19 samples were collected in the forest area, 27 in the grassland area, and 45 in the agricultural area.

Subsequently, the abundance of MP was determined and recorded as the number of pieces per kilogram of dry soil by counting isolated MP particles retained on filter paper. The counting was performed using a Nikon Eclipse Ni microscope with 10× magnification. Equation 1 presents the calculation in terms of kilograms of dry soil, where N_i represents the number of plastic particles in 10 g of dry soil, and f_1 is the conversion factor to hectares (1000 $g \cdot kg^{-1}$).

$$Abundance \ \left[\frac{pieces}{kg}\right] = \frac{N_i}{10\ g\ solo\ seco} \times f_1 \qquad \text{(Equation 1)}$$

2.6 Geostatistical analysis of microplastics

The geostatistical analysis of the data was conducted based on an adaptation proposed by Scalon (2024), comprising five stages. The first stage involved exploratory analysis using descriptive statistics to identify outliers, trends, data distribution shapes, and to assess normality through visual inspection of the plots. In the second stage, the spatial dependence of the data was analyzed as a function of distance. To achieve this, the robust empirical semivariogram by Cressie and Hawkins (1980) was applied, due to the presence of outliers.

This semivariogram can be estimated using Equation 2, where $\gamma(h)$ represents the empirical variogram estimator, h is the distance vector (magnitude and direction) between pairs of observations, $|N(h)|$ denotes the number of paired observations corresponding to the distances analyzed, and Z(Si) and Z(Sj) are the data values at the spatial locations Si and Sj, respectively. Empirical semivariograms were computed under the assumption of intrinsic stationarity in four different directions to assess the presence of anisotropy.

$$\gamma(h) = \frac{\left\{\frac{1}{2|N(h)|}\sum_{(i,j)\in N(h)}\left|Z(S_i)-Z(S_j)\right|^{0,5}\right\}^4}{0,914+\frac{0,988}{N(h)}} \qquad \text{(Equation 2)}$$

For the application of the geostatistical model, it is necessary to assume that it meets the intrinsic stationarity condition and does not exhibit anisotropy, as the theoretical semivariograms used to construct the Kriging maps are based on isotropic models.

The third stage involved fitting the theoretical semivariogram to the empirical semivariogram using a continuous function. The Gaussian, exponential, and spherical models were fitted to estimate the parameters, including nugget effect (C0), contribution (C1), sill (C0 + C1), and range (a), as described by Ferraz et al. (2012) and Scalon (2024). To select the best model, the spatial dependence index (IDS) and the Akaike Information Criterion (AIC) were used (Ferraz et al., 2019; Scalon, 2024; Zanzarini et al., 2013).

In the fourth stage, data interpolation was performed using the ordinary kriging predictor to estimate MP values at unsampled locations. The result of this stage is a map depicting the spatial distribution of MP abundance across the study area. The ordinary kriging predictor is given by Equation 3.

$$Z(S_0) = m(S_0) + \sum_{i=1}^{n} \lambda_i [Z(S_i) - m(S_0)] \quad \text{(Equation 3)}$$

Where S0 is the vector with the prediction locations, m(S0) are the expected values for the prediction locations, and the observed values are denoted by E λ, which are the kriging weights assigned to each observed value of Z(Si) (Scalon, 2024). The interpolated maps can be converted into raster-type images and plotted in QGIS software for editing and analysis.

Finally, the fifth stage consists of performing cross-validation to assess the overall geostatistical prediction process. The comparison of predicted values with actual data can be done using the coefficient of determination (R^2) and square root of mean squared residuals (RQMR).

The statistical and geostatistical analyses were performed using the R computational system (R Core Team, 2024) and the gstat and geoR libraries (Pebesma, 2004; Ribeiro et al., 2024). The maps were obtained using QGIS software (QGIS Development Team, 2024). The maps were generated in flat coordinates (Universal Transverse Mercator UTM) in zone 23S, which encompasses the Lavras region in Minas Gerais, Brazil. For figure plotting, Origin Pro software (OriginPro Lab Corporation, 2024) was used.

3. RESULTS AND DISCUSSION

3.1 Abundance of microplastics in the soil

In most research on microplastics (MP) in soil, average abundance was reported as the number of particles per unit mass of soil (e.g., pieces kg^{-1} soil). Their spatial distribution is typically represented on a point-by-point basis for each sampled site, as illustrated in the maps by Rafique et al. (2020), and Akca et al. (2024). On the other hand, Zhou et al. (2023) and Hossain et al. (2024) developed maps to locate sampling sites and depict the spatial distribution of MP within the study area, without specifying the interpolation method used.

In our study, MP smaller than 2 mm were extracted using the density separation method and detected in all 91 georeferenced soil samples collected within the 0–20 cm soil profile. Subsequently, an interpolated map was generated to predict the spatial distribution of MP in a typical agricultural environment in southeastern Brazil.

The results showed an average abundance of MP of 3,826 and variation between (1,000 to 7,400), 2,553 (1,000 to 4,700), and 3,407 (600 to 7,300) pieces kg^{-1} for the land uses in forest, grassland, and agricultural, respectively, without showing significant differences between the different uses (Figure 2).

However, MP abundance was higher in forest and agricultural soils compared to grassland soils. Zhang et al. (2022) reported a similar pattern, with a higher concentration of MP in agricultural soils than in grassland soils. In contrast, Wang et al. (2025) found that MP abundance in agricultural soils was twice as high as in grassland soils and three times higher than in forest soils, attributing this difference to intensive agricultural activities such.

These findings suggest that agricultural areas tend to exhibit the highest MP concentrations compared to forests and grasslands, indicating greater soil contamination by MP due to the use of plastic products in agricultural practices.

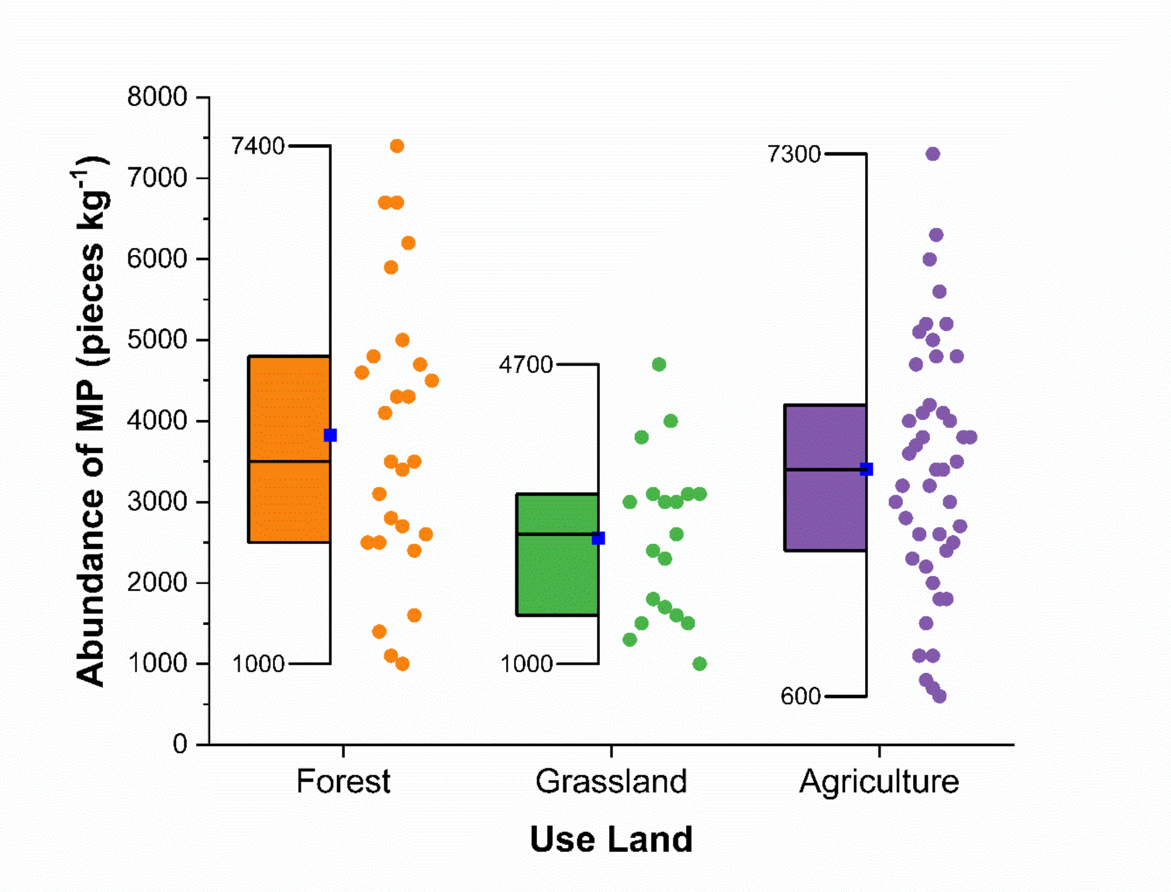

Figure 2. Analysis of the variation in the abundance of microplastics isolated by land use, from the 0 - 20 cm layer. Shown as violin graphs (pieces. kg^{-1}), values at the extremes of each box are the minimum and maximum MP abundance for each land use. The diagrams display data distribution, with the whiskers indicating the extreme values, while the lower and upper edges of the boxes represent the first and third quartiles, respectively. The line inside the boxes corresponds to the median, and the mean is highlighted by a blue box.

To contextualize our results, a review of scientific articles on MP abundance in soils was conducted, compiling reported average values from various studies (Table 1). This table includes the country or region of the study, land use type, and the minimum and maximum ranges of MP abundance. During this analysis, significant heterogeneity in the reports was observed, a challenge previously highlighted by Wrigley et al., (2024), who emphasized the need to standardize sampling protocols and MP separation methods in soils to enhance data comparability and accuracy.

This finding underscores the importance of establishing a classification system to compare MP concentrations in soil, categorizing them into low, medium, and high concentration levels. Wrigley et al., (2024) proposed a preliminary approach to this classification, analyzed 89 studies on MP in soils covering 553 sampling sites, and reported a minimum concentration of 0 pieces kg^{-1} and a maximum of 72,200 pieces kg^{-1}. Additionally, the study mentions that the global average is 2,900 ± 7,600 pieces kg^{-1}, a value that falls within the range of our results (Table 1).

Table 2. Locations, land uses, ranges, and averages of the values of the abundance of MP in the soil as reported by different authors.

Country, city, and region	Land use*	Abundance (pieces kg^{-1}) Range	Average **	Source
Shanghai, China	vegetable farmlands	N.A.	78	(Liu et al., 2018)
Mellipilla county Chile	Agricultural soil	18 to 41	34	(Corradini et al., 2019)
Lahore, Pakistan	Agricultural Public Parks house lawns industrial áreas drains, roadsides	1,750 to 12,200	4,483	(Rafique et al., 2020)
Suburbs of Wuhan China	Vegetable farmlands	320 to 12,560	2,020	(Chen et al., 2020)
Shandong Province China	Vegetable agricultural soils	310 to 5,698	1,444	(Yu et al., 2021)
Suburb of Beijing China	Greenhouse Agricultural soils	500 to 1,240	891	(Wang et al., 2022)
Zhuanglang County, China	Woodland Potato Orchard Wheat	N.A.	1,383.3 2,127.2 1,335.9 1,324.6	(H. Zhang et al., 2022)
Bangladesh	Agricultural land	N.A.	2.13×10^{4}	(Hossain et al., 2023)
Qinghai-Tibet	Agricultural soils	6 to 444	86	(Zhou et al., 2023)
Buenos Aires Argentina	Horticultural soil	27 to 69	43	(Berenstein et al., 2024)
Rhineland-Palatinate, Germany	Viticulture farmland soil	400 to 13,000	4,200	(Klaus et al., 2024)
Northern China	Legumes Farmland soil	1,600 to 36,200	11,058	(La et al., 2024)
Lavras MG Brazil	Forest Grassland Farmland	600 to 7,400	3,826 2,553 3,407	Authors (2025)

Note: NA = Not Available, * Microplastics extracted using the density separation method. ** Microplastics collected from the 0–20 cm soil profile

Analyzing the results in Table 1, the presence of MP was evident in all study areas, influenced by human activities in both rural and urban environments. The heterogeneity of MP abundance across studies is also notable, suggesting that agricultural activities may be a significant source of soil MP contamination (Rafique et al., 2020).

For example, Zhou et al. (2023) reported a range of MP from 6.0 to 444 pieces kg^{-1}, with an average of 86 pieces kg^{-1} in agricultural soils. In contrast, La et al. (2024) found that MP abundance in agricultural soils specifically used for legume cultivation ranged from 1,600 to 36,200 pieces kg^{-1}, with an average of 11,058 pieces kg^{-1}. Similarly, Zhang et al. (2022) reported that the amount of MP found in soils used for potato cultivation was significantly higher (2,127 pieces kg^{-1}) compared to other land uses studied.

A related review by Cai et al., (2024) proposed a preliminary classification of MP contamination in agricultural soils into four categories: micro contamination (<400 pieces kg^{-1}), light contamination (400 to 4,000 pieces kg^{-1}), moderate contamination (4,000 to 40,000 pieces kg^{-1}) and heavy contamination (≥40,000 pieces kg^{-1}). Based on this classification, our results indicate an average level of light MP pollution, providing a useful reference for comparison in future studies.

The heterogeneity in the concentration of MP in agricultural soils is due to different agricultural activities, including sewage sludge application, fertilizer use, mulch film use, atmospheric deposition, and irrigation with water from wastewater treatment plants (Wang et al., 2020). These practices can introduce MP of different sizes and compositions into the soil, resulting in varying concentrations (Li et al., 2021), with significant implications for soil health and food security (De Bhowmick et al., 2021), altering nutrient availability and soil structure, and affecting soil fertility (La et al., 2024).

Other explanations for the heterogeneity of MP concentrations in soils include environmental factors, terrain characteristics, and soil properties. For example, soil texture, structure, and porosity can affect MP retention and migration (Yang et al., 2022). Topography, vegetation, bulk density, and biological activity (such as bioturbation by soil organisms) play important roles in the distribution of MP (Corradini et al., 2019; Li et al., 2021). Finally, the variability in the spatial distribution of MP can be influenced by factors such as the topographic conditions of the site or specific locations characterized by practices with higher plastic use. These "hot spots" can significantly increase the concentrations of MP in soil, as will be analyzed below.

3.2 Spatial distribution of microplastics

The spatial distribution of the 91 sampling points is illustrated in Figure 3, where different shapes and colors represent four ranges of MP abundance. Blue circles correspond to the first quartile (600–2,300 pieces kg^{-1}), indicating the lowest MP concentrations. Green triangles represent the second quartile (2,300–3,100 pieces kg^{-1}). Crosses denote the third quartile, with values ranging from 3,100 to 4,250 pieces kg^{-1}. Finally, 'x' marks indicate the highest MP abundance values, corresponding to the fourth quartile (4,250–7,400 pieces kg^{-1}). Figures 3b and 3c show the spatial trend of the data in a north-south and east-west direction, respectively, where it can be seen that neither figure has a linear trend, indicating that the stochastic process may be stationary (Scalon, 2024). Finally, the histogram in Figure 3d shows that the abundance of MP in the region approximately follows a normal distribution.

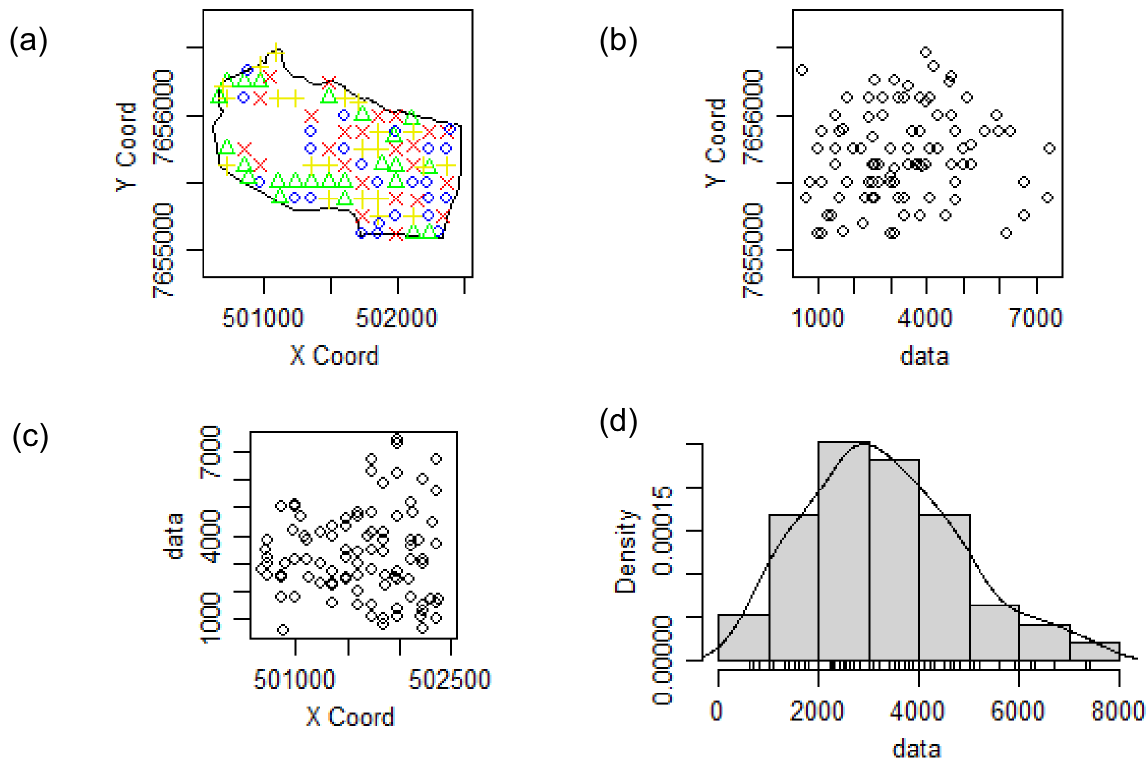

Figure 3. Spatial distribution of microplastic abundance by quartiles: (a) quartile classification, (b) trend along the y-axis, (c) trend along the x-axis, and (d) histogram. Blue circles indicate the first quartile (600–2,300 pieces·kg^{-1}), green triangles the second (2,300–3,100), crosses the third (3,100–4,250), and 'x' marks the fourth quartile (4,250–7,400), representing the highest concentrations.

The theoretical semivariogram model was first determined and then fitted to the empirical omnidirectional robust semivariogram (Figure 4), represented by dots, along with the fitted models, shown as solid lines. The fitting was performed using the weighted least squares estimator (WLS2) proposed by Cressie, (1985). The results indicate spatial dependence up to a maximum distance of approximately 350 m. The estimated parameters for each fitted model, along with the selection criteria for the best model, are presented in Table 2.

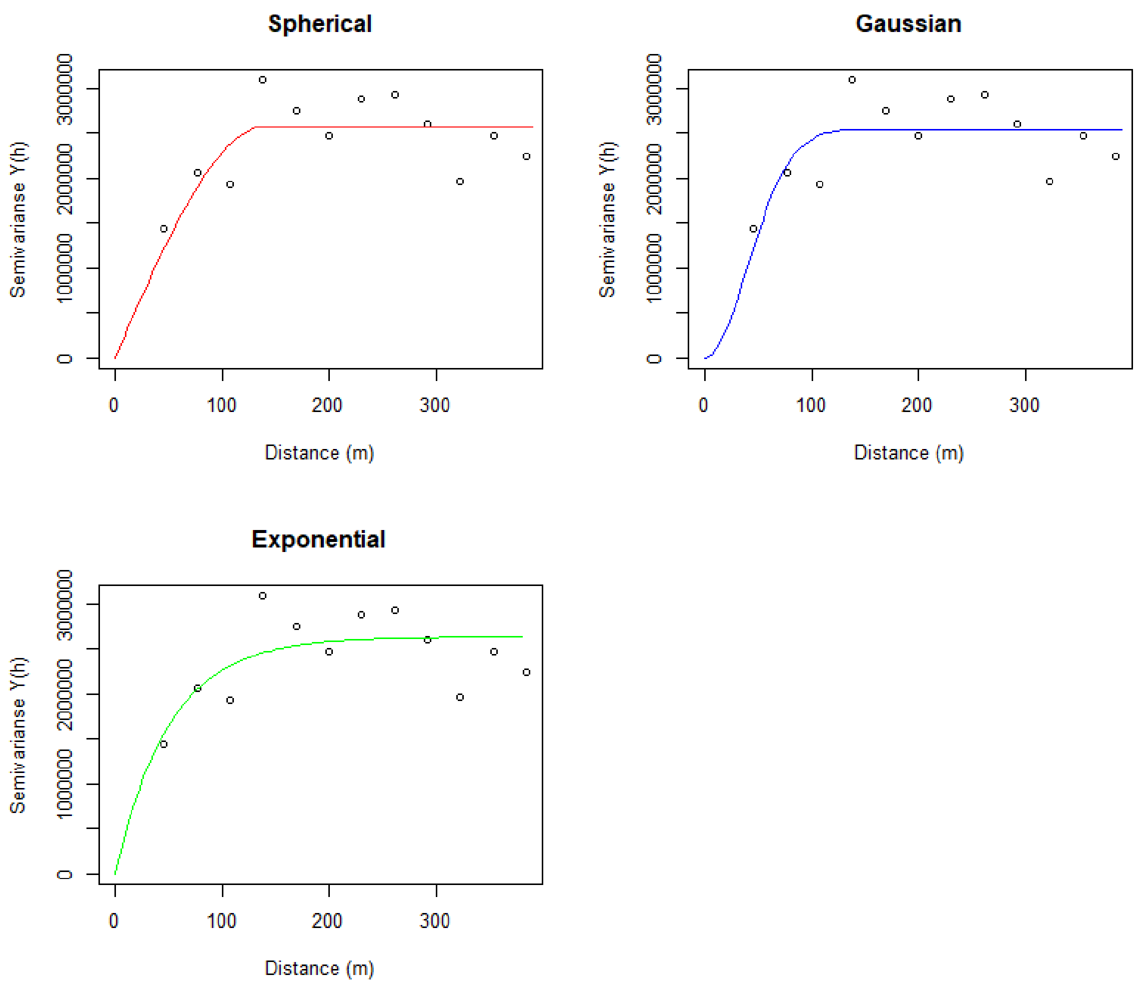

Figure 4. Empirical semivariograms (dots) and model fit (solid lines) Spherical, Gaussian, and Exponential of MP abundance data (pieces kg-1) at soil depth 0-20 cm in the micro-watershed.

The best model is the one with the lowest values of Akaike's information criterion (AIC), root mean square residuals (RQRM), and spatial dependence index (SDI) (Scalon, 2024). Thus, according to the results shown in Table 2, the Gaussian model has the lowest AIC and RQMR values, so it seems to be the best model to explain the spatial dependence of the data, and therefore its estimated parameters will be used to obtain the ordinary kriging weights.

Table 3. Models and parameter estimate of the experimental semivariograms for MP abundance in the 0-20 cm layer.

Parameter	Model		
	Gaussian	Exponential	Spherical
Nugget effect (C_0)	0.0	0.0	0.0
Contribution (C_1)	2546970	2637916	2581012
Sill ($C_0 + C_1$)	2546970	2637916	2581012
Range (a)	56.51	51.03	140.88
AIC	-55.93	- 56.17	- 68.13
SDI	0.0	0.0	0.0
R^2	0.123	0.125	0.122
RQMR	341573	362828	805292

Note: Akaike information criterion (AIC), spatial dependence index (SDI), coefficient of determination (R^2), Square root of mean squared residuals (RQMR).

Continuing with the geostatistical procedure, Figure 5 shows the Ordinary Kriging map of the spatial distribution of MP in the 0 to 20 cm layer. The predicted minimum and maximum values of MP are 600 to 7,400 pieces kg^{-1}, respectively, and show great variability in the abundance of MP in the study region. It is important to emphasize that this research presents a methodology for predicting the spatial abundance of MP in soil, with results different from the typical point distribution of MP. Figure 5 shows that the areas with the highest abundance of MP are located in forest and agricultural areas, especially near urban areas and highways, and in low-lying areas where precipitation runoff converges.

Local agricultural practices, such as the application of polymer-coated fertilizers, the handling of plastic covers, and the improper disposal of plastic materials, contribute to the accumulation of MP in agricultural soils. These materials gradually degrade through biotic and abiotic processes, releasing significant amounts of MP into the environment (Hossain et al., 2024; La et al., 2024).

Furthermore, several studies have indicated that urbanization and anthropogenic activities increase soil contamination by MP (Amjad et al., 2023). In this regard, the study by Prajapati et al. (2023) demonstrates that MP abundance in agricultural soils is significantly higher in areas near residential zones compared to commercial or industrial areas, as nearby population density directly influences contamination levels.

In addition, Ling et al. (2023) studied the occurrence and migration of MP during high-intensity rainfall in an agricultural watershed in Shaanxi Province, China. 3,710 pieces kg^{-1} were detected in the sediments, and the number of MP trapped by the check dam was estimated to be $6,140 \times 10^{10}$ pieces. Their conclusions indicated that high-intensity rainfall can significantly affect the migration of MP, transporting them to lower areas of the watershed where they tend to accumulate with the sediments. The evidence above-mentioned supports the identification of "hot spots" of the abundance of MP, as shown on the map in Figure 5.

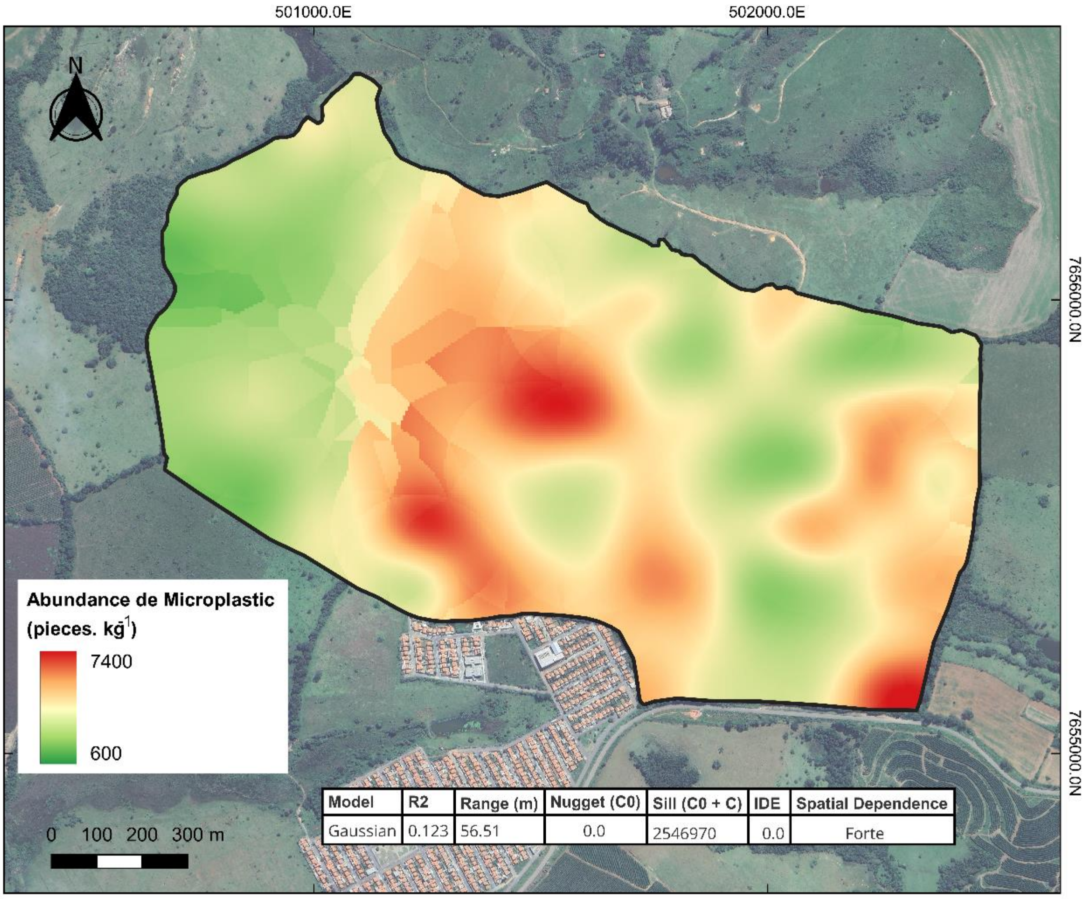

Figure 5. Map of the spatial distribution of microplastics (pieces kg^{-1}) in the study area, obtained from the Gaussian model and interpolation by ordinary Kriging.

In this study, MP particles were found throughout the farm regardless of land use (forest, grassland, and agricultural). It should be noted that due to the lack of standardized methods, the abundance of MP can be influenced by various factors, as shown in Table 1, such as sampling methods, locations, the way MP is isolated from the soil, agricultural activities (Berenstein et al., 2024), and other natural or anthropogenic factors as described by Zhou et al. (2023b).

For example, studies by Brandes et al. (2021) found high levels of MP in the northwestern region of Germany due to the high use of sewage sludge, compost, and plasticulture waste. Some authors suggest that MP in agricultural soils originate from packaging bags, plastic bottles, and mulch film and that atmospheric deposition of MP is more relevant for agricultural soils such as grasslands and forests (Zhang et al., 2022). Therefore, it is suggested that future research should investigate the origin of sources that generate MP in agricultural soils, and the effect of terrain and rainfall on the migration of MP, especially in regions with high soil erosion.

To complete the geostatistical analysis of microplastics, the final step was to cross-validate the entire geostatistical analysis using the Gaussian model and ordinary kriging. R^2 values close to 1 and RMSE values close to zero are expected. Table 2, which shows an R^2 of 0.125 and an RMSE of 16.3×10^6, indicates that there are opportunities to improve the predictions. Therefore, for future research, we suggest using other models to fit the theoretical semivariogram, such as maternal, cubic, power, etc. As well as implementing other interpolation methods, such as universal kriging or co-kriging (Scalon, 2024).

These approaches can improve modeling by incorporating information from data location coordinates (universal kriging) or information from an external variable correlated with MP abundance (Scalon, 2024), such as terrain morphology, pH, soil organic matter (SOM), or physical properties such as bulk density (Souza Machado et al., 2019; Zhang et al., 2022).

3.3 Limitations and Future Research

The analysis of the shape, color, size, and polymer type of microplastics found in the soil was presented in a separate study, as the primary focus of this research is on MP abundance and their spatial distribution within the watershed. Our study covered an area of 165 ha, identifying three land use types representative of tropical regions in southeastern Brazil: agricultural land, grasslands, and forests.

Expanding research to other representative ecosystems is essential, as well as assessing the influence of adjacent urban, industrial, and transportation areas on MP concentration and spatial distribution in the soil. Additionally, the methodology employed in this study only detected MP smaller than 2 mm, highlighting the need for standardized methods in MP extraction and classification across the entire size spectrum to enable data comparison across different regions.

Another important consideration is that this study did not address seasonal and temporal variations, preventing the assessment of MP contamination dynamics over time, particularly regarding transport processes driven by wind or water erosion.

Finally, the interpolation methodology applied in this study, which utilized semivariograms and a kriging predictor to generate spatial distribution maps and predict MP abundance in the soil, represents an innovative approach and was described in detail to facilitate replication by other researchers. However, implementing additional interpolation models, such as co-kriging, is recommended to enhance the validation of the geostatistical analysis.

4. CONCLUSIONS

Microplastic particles (MP) were detected in all soil samples across the three land uses (forest, grassland, and agricultural). Although no significant differences were observed in the average abundance of MP among the land uses, the average abundance of MP in grassland soils was lower compared to forest and agricultural areas.

The spatial variability of MP abundance in the 0-20 cm soil depth was also characterized. The spatial distribution of MP exhibited moderate spatial dependence, which allowed the construction of the experimental semivariogram fitted with the Gaussian model. This enabled the mapping of MP abundance using ordinary kriging.

Thus, the application of geostatistics facilitated the creation of a map depicting the MP abundance across the study area. High MP concentrations were found near highways, in urban areas, and in low-lying regions where rainwater accumulates. Future research should explore the relationship between land use, landscape patterns, soil properties, and microplastic characteristics.

Acknowledgments
The authors would like to thank the Federal University of Lavras (UFLA), the Surcolombiana University (USCO), and the National Council for Scientific and Technological Development (CNPq) (processes: 307950/2021-2 and 307059/2022-7), the Foundation for Research Support of the State of Minas Gerais (FAPEMIG) (processes: APQ 00802-18), and the Coordination for the Improvement of Personnel (CAPES) (code 001) The authors would to thank the Laboratory of Electron Microscopy and Analysis of the Ultrastructural Federal University of Lavras.

REFERENCES

Akca, H., Albayrak, R., Onur, M., Gündo, S., 2024. An evaluation on microplastic accumulations in Turkish soils under different land uses. Sci. Total Environ. 911. https://doi.org/10.1016/j.scitotenv.2023.168609

Amjad, M., Huang, Q., Khan, S., Wang, Q., Huang, J., Fahad, X., Sajjad, M., Liu, Y., Mašek, O., Li, X., Wang, J., Xiaomao, C., 2023. Abundance, spatial distribution, and characteristics of microplastics in agricultural soils and their relationship with contributing factors. Rev. Gestão Ambient. 328. https://doi.org/https://doi.org/10.1016/j.jenvman.2022.117006

Arevalo-Hernandez, J.J., Barrera, D.B.A., Avanzi, J.C., Cirillo, M.A., Silva, M.L.N., 2025a. Plastic Debris in Agroecosystems : Distribution and Abundance Patterns , and Relationship with Terrain Characteristics in Southeastern Brazil. ACS OMEGA. https://doi.org/10.1021/acsomega.4c10678

Arevalo-Hernandez, J.J., Barrera, D.B.D.A., Curi, N., Avanzi, J.C., Silva, N.L.M., 2025b. A Method for the Extraction and Analysis of Microplastics from Tropical Agricultural Soils in Southeastern Brazil. Soil Syst. 9, 1–20. https://doi.org/https://doi.org/10.3390/soilsystems9020034

Berenstein, G., Córdoba, P., Díaz, Y.B., González, N., Ponce, M.B., Montserrat, J.M., 2024. Macro, meso, micro and nanoplastics in horticultural soils in Argentina: Abundance, size distribution and fragmentation mechanism. Sci. Total Environ. 906. https://doi.org/10.1016/j.scitotenv.2023.167672

Brandes, E., Henseler, M., Kreins, P., 2021. Identifying hot-spots for microplastic contamination in agricultural soils - A spatial modelling approach for Germany. Environ. Res. Lett. 16. https://doi.org/10.1088/1748-9326/ac21e6

Cai, L., Zhang, L., Liu, Z., Zhao, X., Han, J., 2024. The factors affecting microplastic pollution in farmland soil for different agricultural uses : A case study of China. Catena 239, 107972. https://doi.org/10.1016/j.catena.2024.107972

Chamas, A., Moon, H., Zheng, J., Qiu, Y., Tabassum, T., Jang, J.H., Abu-omar, M., Scott, S.L., Suh, S., 2020. Degradation Rates of Plastics in the Environment. ACS Sustain. Chem. Eng. 8, 3494–3511. https://doi.org/DOI: 10.1021/acssuschemeng.9b06635

Chen, Y., Leng, Y., Liu, X., Wang, J., 2020. Microplastic pollution in vegetable farmlands of suburb Wuhan, central China. Environ. Pollut. 257, 113449. https://doi.org/10.1016/j.envpol.2019.113449

Corradini, F., Meza, P., Eguiluz, R., Casado, F., Huerta-Lwanga, E., Geissen, V., 2019. Evidence of microplastic accumulation in agricultural soils from sewage sludge disposal. Sci. Total Environ. 671, 411–420. https://doi.org/10.1016/j.scitotenv.2019.03.368

Cressie, N., 1985. Fitting variogram models by weighted least squares. J. Int. Assoc. Math. Geol. 17, 563–586.

De Bhowmick, G., Sarmah, A.K., Dubey, B., 2021. Microplastics in the NZ environment: Current status and future directions. Case Stud. Chem. Environ. Eng. 3. https://doi.org/10.1016/j.cscee.2020.100076

Ding, F., Jones, D.L., Chadwick, D.R., Kim, P.J., Jiang, R., Flury, M., 2022. Environmental impacts of agricultural plastic film mulch: Fate, consequences, and solutions. Sci. Total Environ. 836, 1–4. https://doi.org/10.1016/j.scitotenv.2022.155668

Ferraz, A.G., Moreira, F., Augusto, P., Silva, A.C., Carvalho, F.D.M., 2012. Precision agriculture to study soil chemical properties and the yield of a coffee field. Coffee Sci. 7, 59–67.

Ferraz, G.A.S., Ferraz, P.F.P., Martins, F.B., Silva, F.M., Damasceno, F.A., 2019. Principal components in the study of soil and plant properties in precision coffee farming. Agron. Res. 17, 418–429. https://doi.org/https://doi.org/10.15159/AR.19.114

Grause, G., Kuniyasu, Y., Chien, M., Inoue, C., 2022. Separation of microplastic from soil by centrifugation and its application to agricultural soil. Chemosphere 288, 132654. https://doi.org/10.1016/j.chemosphere.2021.132654

Hossain, A., Adham, I., Hasan, M., Mohammad, M., Siddique, B., Senapathi, V., Reza, A., Islam, T., 2024. Regional Studies in Marine Science Analysis and risk evaluation of soil microplastics in the Rohingya refugee camp area , Bangladesh : A comprehensive study. Reg. Stud. Mar. Sci. 76, 103578. https://doi.org/10.1016/j.rsma.2024.103578

Hossain, M.N., Rahman, M.M., Afrin, S., Akbor, M.A., Bakar, S.A., Malafaia, G., 2023. Identification and quantification of microplastics in agricultural farmland soil and textile sludge in Bangladesh. Sci. Total Environ. 858. https://doi.org/10.1016/j.scitotenv.2022.160118

IUSS Working Group WRB, 2022. World reference base for soil resources. International soil classification system for naming soils and creating legends for soil maps., 4th ed. International Union of Soil Sciences (IUSS), Vienna, Austria.

Klaus, J., Seeger, M., Bigalke, M., Weber, C.J., 2024. Microplastics in vineyard soils: First insights from plastic-intensive viticulture systems. Sci. Total Environ. 947, 174699. https://doi.org/10.1016/j.scitotenv.2024.174699

Kumar, P., Lee, J., Brown, R.J.C., Kim, K., 2021. Micro- and nano-plastic pollution : Behavior, microbial ecology, and remediation technologies. J. Clean. Prod. 291, 1–22. https://doi.org/https://doi.org/10.1016/j.jclepro.2020.125240

La, Y., Zhang, L., Zhao, N., Ye, H., Zeng, Q., Zhao, L., Wang, Z., Lin, D., Wang, R., 2024. The microplastics distribution characteristics and their impact on soil physicochemical properties and bacterial communities in food legumes farmland in northern China. J. Hazard. Mater. 471, 134282. https://doi.org/10.1016/j.jhazmat.2024.134282

Leitão, I.A., van Schaik, L., Ferreira, A.J.D., Alexandre, N., Geissen, V., 2023. The spatial distribution of microplastics in topsoils of an urban environment - Coimbra city case-study. Environ. Res. 218. https://doi.org/10.1016/j.envres.2022.114961

Li, H., Lu, X., Wang, S., Zheng, B., Xu, Y., 2021. Vertical migration of microplastics along soil profile under different crop root systems. Environ. Pollut. 278. https://doi.org/10.1016/j.envpol.2021.116833

Li, J., Zhu, B., Huang, B., Ma, J., Lu, C., Chi, G., Guo, W., Chen, X., 2023. Vertical distribution and characteristics of soil microplastics under different land use patterns: A case study of Shouguang City, China. Sci. Total Environ. 903. https://doi.org/10.1016/j.scitotenv.2023.166154

Li, W., Wufuer, R., Duo, J., Wang, S., Luo, Y., Zhang, D., Pan, X., 2020. Microplastics in agricultural soils: Extraction and characterization after different periods of polythene film mulching in an arid region. Sci. Total Environ. 749, 141420. https://doi.org/10.1016/j.scitotenv.2020.141420

Ling, Q., Yang, B., Jiao, J., Ma, X., Zhao, W., Zhang, X., 2023. Response of microplastic occurrence and migration to heavy rainstorm in agricultural catchment on the Loess plateau. J. Hazard. Mater. 460, 132416. https://doi.org/10.1016/j.jhazmat.2023.132416

Liu, H., Sun, K., Liu, X., Yao, R., Cao, W., Zhang, L., Wang, X., 2022. Spatial and temporal distributions of microplastics and their macroscopic relationship with algal blooms in Chaohu Lake, China. J. Contam. Hydrol. 248. https://doi.org/10.1016/j.jconhyd.2022.104028

Liu, M., Lu, S., Song, Y., Lei, L., Hu, J., Lv, W., Zhou, W., Cao, C., Shi, H., Yang, X., He, D., 2018. Microplastic and mesoplastic pollution in farmland soils in suburbs of Shanghai, China. Environ. Pollut. 242, 855–862. https://doi.org/10.1016/j.envpol.2018.07.051

Munno, K., De Frond, H., O'Donnell, B., Rochman, C.M., 2020. Increasing the accessibility for characterizing microplastics: introducing new application-based and spectral libraries of plastic particles (SLoPP and SLoPP-E). Anal. Chem. 92, 2443–2451. https://doi.org/10.1021/acs.analchem.9b03626

OriginPro Lab Corporation, 2024. OriginPro.

Pebesma, E.J., 2004. Multivariable geostatistics in S: the gstat package. Comput. Geosci. 30, 683-691.

Prajapati, A., Jadhao, P.S., Khare, A., Vaidya, A.N., Kumar, A.R., Das, S., 2023. Characterization of Microplastics and Associated Heavy Metals in Urban Soils Affected by Anthropogenic Littering: Distribution, Spatial Variation, and Influence of Soil Properties. Soil Sediment Contam. 00, 1–29. https://doi.org/10.1080/15320383.2023.2286524

QGIS Development Team, 2024. QGIS Geographic Information System versão 3.28.2 Firenze.

Quinn, B., Murphy, F., Ewins, C., 2016. Validation of density separation for the rapid recovery of microplastics from sediment. Anal. Methods 9, 1491–1498. https://doi.org/https://doi.org/10.1039/C6AY02542K

R Core Team, 2024. R: A language and environment for statistical computing. R Foundation for Statistical Computing.

Radford, F., Zapata-Restrepo, L.M., Horton, A.A., Hudson, M.D., Shaw, P.J., Williams, I.D., 2021. Developing a systematic method for extraction of microplastics in soils. Anal. Methods 13, 1695–1705. https://doi.org/10.1039/d0ay02086a

Rafique, A., Irfan, M., Mumtaz, M., Qadir, A., 2020. Spatial distribution of microplastics in soil with context to human activities: a case study from the urban center. Environ. Monit. Assess. 192. https://doi.org/10.1007/s10661-020-08641-3

Ribeiro, J.P., Diggle, P., Christensen, O., Schlather, M., Bivand, R., 2024. Analysis of Geostatistical Data. https://doi.org/doi:10.1007/978-0-387-48536-2

Samanta, P., Dey, S., Kundu, D., Dutta, D., Jambulkar, R., Mishra, R., Ghosh, A.R., Kumar, S., 2022. An insight on sampling, identification, quantification and characteristics of microplastics in solid wastes. Trends Environ. Anal. Chem. 36. https://doi.org/10.1016/j.teac.2022.e00181

Sarti, F.M.E., De Souza, G.A., da Silva, B.R., dos Santos, R.D., 2022. Municipal Park Grounds and Microplastics Contamination. J. Polym. Environ. 30, 5202–5210. https://doi.org/https://doi.org/10.1007/s10924-022-02580-5

Scalon, J.., 2024. Análise de dados espaciais com aplicações em R, UFLA. ed. Lavras MG, Brazil.

Shi, X., Chen, Z., Wei, W., Chen, J., Ni, B.-J., 2023. Toxicity of micro/nanoplastics in the environment: Roles of plastisphere and eco-corona. Soil Environ. Heal. 1, 100002. https://doi.org/10.1016/j.seh.2023.100002

Silva, P.E., Vincent, T., da Conceição, H., Santos, T., de Almeida, M., Vinhas Costa, O., Rebouças, M., Gonzaca, J., 2022. Widespread microplastic pollution in mangrove soils of Todos os Santos. Environ. Res. 210, 112952. https://doi.org/https://doi.org/10.1016/j.envres.2022.112952

Souza Machado, Abel, A., Lau, C.W., Kloas, W., Bergmann, J., 2019. Microplastics Can Change Soil Properties and A ff ect Plant Performance. Environ. Sci. Technol. 53, 6044–6052. https://doi.org/10.1021/acs.est.9b01339

Souza Machado, Abel, A., Lau, C.W., Till, J., Kloas, W., Lehmann, A., Becker, R., Rillig, M.C., 2018. Impacts of Microplastics on the Soil Biophysical Environment. Environ. Sci. Technol. 52, 9656–9665. https://doi.org/10.1021/acs.est.8b02212

Thomas, D., Schutze, B., Heinze, W.M., Steinmetz, Z., 2020. Sample Preparation Techniques for the Analysis of Microplastics in soil- A Review. Sustainability 12, 9074. https://doi.org/10.3390/su12219074

Wang, K., Chen, W., Tian, J., Niu, F., Xing, Y., Wu, Y., Zhang, R., Zheng, J., Xu, L., 2022. Accumulation of microplastics in greenhouse soil after long-term plastic film mulching in Beijing, China. Sci. Total Environ. 828. https://doi.org/10.1016/j.scitotenv.2022.154544

Wang, W., Ge, J., Yu, X., Li, H., 2020. Environmental fate and impacts of microplastics in soil ecosystems : Progress and perspective. Sci. Total Environ. 708, 134841. https://doi.org/10.1016/j.scitotenv.2019.134841

Wang, X., Feng, Q., Yang, L., Li, M., Zhao, F., Tang, J., Bu, Q., Zhang, Y., Chen, L., 2025. Effect of land use on occurrence and spatial variability of soil microplastics in agricultural watershed. Ecol. Front. https://doi.org/10.1016/j.ecofro.2024.12.005

Weber, C.J., Opp, C., Prume, J.A., Koch, M., Andersen, T.J., Chifflard, P., 2021. Deposition and in-situ translocation of microplastics in floodplain soils. Sci. Total Environ. 152039. https://doi.org/10.1016/j.scitotenv.2021.152039

Weber, C.J., Santowski, A., Chifflard, P., 2022. Investigating the dispersal of macro- and microplastics on agricultural fields 30 years after sewage sludge application. Sci. Rep. 12, 1–13. https://doi.org/10.1038/s41598-022-10294-w

Wrigley, O., Braun, M., Amelung, W., 2024. Global soil microplastic assessment in different land-use systems is largely determined by the method of analysis: A meta-analysis, Science of the Total Environment. Elsevier B.V. https://doi.org/10.1016/j.scitotenv.2024.177226

Yan, P., Zhang, S., Wang, J., Wang, W., Xu, B., Hao, X., Aurangzeib, M., 2022. Field management changes the distribution of mesoplastic and macroplastic in Mollisols of Northeast China. Chemosphere 308. https://doi.org/10.1016/j.chemosphere.2022.136282

Yang, L., Kang, S., Wang, Z., Luo, X., Guo, J., Gao, T., Chen, P., 2022. Microplastic characteristic in the soil across the Tibetan Plateau. Sci. Total Environ. 828, 154518. https://doi.org/http://dx.doi.org/10.1016/j.scitotenv.2022.154518

Yu, L., Zhang, J. Di, Liu, Y., Chen, L.Y., Tao, S., Liu, W.X., 2021. Distribution characteristics of microplastics in agricultural soils from the largest vegetable production base in China. Sci. Total Environ. 756, 1–9. https://doi.org/10.1016/j.scitotenv.2020.143860

Zanzarini, F. V., Pissarra, T.C.T., Brandão, F.J.C., Teixeira, D.D.B., 2013. Spatial correlation of the vegetation index (NDVI) of a Landsat/ETM+ images with soil attributes. Rev. Bras. Eng. Agrícola e Ambient. 17, 608–614. https://doi.org/10.1590/s1415-43662013000600006

Zhang, G.S., Liu, Y.F., 2018. The distribution of microplastics in soil aggregate fractions in southwestern China. Sci. Total Environ. 642, 12–20. https://doi.org/10.1016/j.scitotenv.2018.06.004

Zhang, H., Huang, Y., An, S., Zhao, J., Xiao, L., Li, H., Huang, Q., 2022. Microplastics trapped in soil aggregates of different land-use types: A case study of Loess Plateau terraces, China. Environ. Pollut. 310, 119880. https://doi.org/10.1016/j.envpol.2022.119880

Zhang, Y., Wang, K., Chen, Weizhi, Ba, Y., Khan, K., Chen, Wei, Tu, C., 2022. Effects of land use and landscape on the occurrence and distribution of microplastics in soil , China. Sci. Total Environ. 847. https://doi.org/10.1016/j.scitotenv.2022.157598

Zhou, Yang, Jing, J., Yu, R., Zhao, Y., Gou, Y., Zhang, Z., Tang, H., Zhang, H., Huang, Y., 2023. Microplastics in plateau agricultural areas: Spatial changes reveal their source and distribution characteristics. Environ. Pollut. 319, 121006. https://doi.org/10.1016/j.envpol.2023.121006

Zhou, Y., Liu, X., Wang, J., 2019. Characterization of microplastics and the association of heavy metals with microplastics in suburban soil of central China. Sci. Total Environ. 694, 133798. https://doi.org/10.1016/j.scitotenv.2019.133798

Zhou, Y., Wang, J., Zou, M., Jia, Z., Zhou, S., Li, Y., 2020. Microplastics in soils: A review of methods, occurrence, fate, transport, ecological and environmental risks. Sci. Total Environ. 748, 141368. https://doi.org/10.1016/j.scitotenv.2020.141368

Zhou, Yujie, Wang, T., Zou, M., Yin, Q., Jia, Z., Su, B., Zhang, Q., Chen, L., Zhou, S., 2023. Trends in the occurrence and accumulation of microplastics in urban soil of Nanjing and their policy implications. Sci. Total Environ. 903. https://doi.org/10.1016/j.scitotenv.2023.166144